



BIOMEDICAL ENGINEERING
FACULTY OF SCIENCE AND TECHNOLOGY
APPLIED STEM CELL TECHNOLOGIES

Insertion of an inducible construct in
the genome of human pluripotent
stem cells by CRISPR-Cas9 mediated
homology directed repair

G.A. ten Hag
Master Graduation Thesis
June 2021

Examination Committee:
Prof. Dr. P.C.J.J. Passier
Prof. Dr. H.B.J Karperien
Dr. V. Schwach
R.H. Slaats, MSc

UNIVERSITY OF TWENTE. | TECHMED CENTRE



Acknowledgement

By finishing my master graduation assignment at the Applied Stem Cell Technologies (AST) research group at the University of Twente, my time as a student has come to an end. I really liked the project about CRISPR-Cas9 genome editing. I learned a lot of different principles and techniques involved in CRISPR-Cas9 genome editing technology, such as the design and construction of plasmids and strategies to achieve transgene insertion in the genome. I would like to take the time to thank a few people involved during my master assignment at AST.

First of all, I would like to thank Dr. Verena Schwach and Rolf Slaats for the supervision during my project, which allowed me to grow as a scientist. It has been a great pleasure working with both of you and I really appreciated the help in and outside the lab. Thank you for the insightful comments and suggestions during the “Tuesday afternoon meetings”. The feedback on my thesis really helped me to improve my scientific writing skills. Verena, I am also grateful that you give me the chance to guide the bachelor student Sem during his graduation project. It was much fun to help Sem with the practical work and I learned a lot of guiding a student.

I would like to thank Prof. Dr. Robert Passier for the opportunity to conduct my master assignment at his research group and for reading and evaluating my report. I would also like to thank Prof. Dr. Marcel Karperien for taking part in my examination committee as external member.

Additionally, I would like to thank my colleagues at the AST group. I enjoyed the meetings and discussions together with the other master students Chiara, Niels and Margreet. Furthermore, I would like to thank Simone ten Den, Kim Vermeul and Carla Cofiño Fabrés for their lab assistance during my project, such as preparing stem cells plates for the targeting experiments. I also want to thank the students in office ZH114 for the nice time. In particular, I would like to thank Margreet for the enjoyable discussions and nice conversations.

Abstract

Human pluripotent stem cells (hPSCs) have emerged as a promising cells source in cardiac research. The differentiation of hiPSCs towards cardiomyocytes (CMs) and the combination with CRISPR-Cas9 genome editing technology has provided new opportunities for disease modeling, drug screening and tissue engineering. In this research, it was attempted to insert a construct for doxycycline-inducible expression of channelrhodopsin 2 (ChR2) into the AAVS1 genomic safe harbor (GSH) locus of hPSCs by CRISPR-Cas9 mediated homology directed repair (HDR) to enable optogenetic pacing of hPSC-derived CMs (hPSC-CMs). In order to validate transgene expression in the AAVS1 locus of hPSCs and hPSC-CMs, this study showed successful synthetization and characterization of a doxycycline-inducible construct for the expression of the red florescent protein mRuby2. As a proof of concept, hPSCs were co-transfected with the inducible mRuby2 construct and sgRNA-Cas9 plasmid targeting the AAVS1 GSH locus. PCR screening showed successful insertion of the inducible construct in the AAVS1 locus. Surprisingly, doxycycline treatment did not result in mRuby2 signal, which requires further investigation. This study also successfully showed the exchange of the mRuby2 gene with ChR2 coupled to Enhanced Yellow Fluorescent Protein (EYFP) tag (ChR2-EYFP) by sticky-end PCR cloning. It is recommended to start directly with targeting of the inducible construct for ChR2-EYFP expression in hPSC to evaluate transgene insertion and expression, instead of using the mRuby2 construct. Taken together, this study describes the creation of a doxycycline-inducible construct which contains unique restriction sites facilitating the rapid creation a new hPSC line with any genetic alteration of interest involved in cardiac research.

Samenvatting

Humane pluripotente stamcellen (hPSCs) zijn een veelbelovende bron van cellen in onderzoek naar het hart. De differentiatie van pluripotente stamcellen naar hartspiercellen (cardiomyocyten) gecombineerd met CRISPR-Cas9 biedt nieuwe kansen voor het modelleren van hartspierziekten, het testen van medicijnen en weefselregeneratie. Dit onderzoek beoogde om een construct voor doxycycline-induceerbare expressie van channelrhodopsin 2 (ChR2) in de AAVS1 genomic safe harbor (GSH) locatie van hPSCs te plaatsen middels CRISPR-Cas9 gemedieerde homologe recombinatie. Het uiteindelijke doel is het bereiken van optogenetische manipulatie van hPSC afgeleide cardiomyocyten. Om de expressie van het transgen te valideren in de AAVS1 locatie laat deze studie de productie zien van een doxycycline-induceerbaar construct voor de expressie van het rood fluorescerende eiwit mRuby2. Als “proof of concept” werden hPSCs getransfecteerd met het doxycycline-induceerbare mRuby2 construct en de sgRNA-Cas9 plasmide gericht op de AAVS1 locatie. PCR analyse laat de insertie van het induceerbare construct in de AAVS1 locatie zien. Verassend genoeg leidde doxycycline behandeling van de getransfecteerde cellen niet tot mRuby2 expressie, wat verder onderzoek vereist. Deze studie laat ook de vervanging van het mRuby2 gen zien door ChR2 gekoppeld aan een geel fluorescerend eiwit zien middels “sticky-end PCR klonering”. Het wordt aanbevolen om direct te starten met de transfectie van het doxycycline-induceerbare ChR2 construct in hPSC om de expressie van het transgen te valideren in de AAVS1 locatie. Concluderend, deze studie beschrijft de creatie van een doxycycline-induceerbare construct dat unieke restrictie-enzym locaties bevat dat het mogelijk maakt om snel een nieuwe hPSC lijn te creëren met elke gewenste genetische aanpassing met als doel om onderzoek te doen naar het hart.

Table of contents

Acknowledgement.....	3
Abstract.....	5
Samenvatting.....	6
Abbreviations	9
1. Introduction.....	10
1.1 Pluripotent stem cells in cardiovascular research	10
1.2 CRISPR-Cas9 genome editing.....	11
1.3 Homology directed repair.....	13
1.4 Genomic safe harbor locations	14
1.5 Channelrhodopsin	15
1.6 Aims and objectives.....	15
2. Materials and methods	16
2.1 sgRNA-Cas9 plasmid.....	16
2.2 HDR template generation.....	16
2.3 Targeting of hPSCs with the HDR template	17
2.4 Transient transfection HDR (mRuby2) plasmid.....	18
2.5 Chr2 cloning	18
2.6 Transient transfection HDR (Chr2-EYFP) plasmid.....	19
3. Results	20
3.1 Sanger sequencing sgRNA-Cas9 plasmids	20
3.2 HDR template generation.....	20
3.2.1 HDR template generation step 1.....	22
3.2.2 HDR template generation step 2.....	24
3.3 Targeting of hPSCs with the inducible construct	26
3.3.1 Transient transfection	28
3.4 HDR template 2.0.....	29
3.4.1 Transient transfection HDR template 2.0	30
3.5 HDR (Chr2-EYFP) template.....	30
3.5.1 HDR (Chr2-EYFP) template generation	30
3.5.2 Transient transfection HDR (Chr2-EYFP) plasmid.....	34
4. Discussion	35
4.1 HDR template construction	35
4.2 CRISPR-Cas9-mediated targeting in PSCs	36
4.2.1 HiPSCs	36

4.2.2 HESCs	36
4.3 Poly(A) tail.....	37
4.4 Channelrhodopsin	38
4.5 AAVS1 GSH location	38
5. Experimental recommendations and future outlook	40
5.1 Towards successful targeting of hPSCs with the inducible construct	40
5.2 Increase HDR efficiency	40
5.3 Future outlook	41
6. Conclusion	42
References.....	43
Supplemental information	49
Supplementary figures	49
Supplementary experimental procedures.....	54
sgRNA-Cas9 plasmid.....	54
Generation of the HDR template fragments	54
In-Fusion cloning and transformation	57
Stem cell culture	58
Stem cell transfection, selection and sorting	58
Transient transfection HDR plasmid	59
HDR template 2.0.....	60
ChR2 cloning	60
Transient transfection HDR (ChR2-EYFP) plasmid.....	62
HDR (ChR2-EYFP) template 2.0.....	62
Supplementary references	64

Abbreviations

AAVS1	Adeno-associated virus site 1
Cas	CRISPR associated protein
CCR5	C-C Motif Chemokine Receptor 5
ChR2	Channelrhodopsin 2
CLYBL	Citrate lyase beta-like
CM	Cardiomyocyte
CMV	Cytomegalovirus
CRISPR	Clustered regularly interspaced short palindromic repeats
crRNA	CRISPR-RNA
CVD	Cardiovascular disease
DSB	Double strand break
EF1 α	Elongation factor 1 alpha
EYFP	Enhanced yellow fluorescent protein
FACS	Fluorescence-activated cell sorting
GFP	Green fluorescent protein
GSHs	Genomic safe harbors
HAL	Left homology arm
HAR	Right homology arm
HDR	Homology directed repair
hESC	Human embryonic stem cells
hPSC	Human pluripotent stem cells
hPSC-CMs	Human pluripotent stem cell-derived cardiomyocytes
iPSC	Induced pluripotent stem cells
MEF	Mouse embryonic fibroblasts
NHEJ	Nonhomologous end joining
PAM	Protospacer Adjacent Motif
PPP1R12C	Phosphatase 1 regulatory subunit 12C
sgRNA	Single-guide RNA
TALENs	Transcription activator-like effector nucleases
tracrRNA	Trans-activating crRNA
TRE	Tetracycline Response Elements
ZFNs	Zinc-finger nucleases

1. Introduction

1.1 Pluripotent stem cells in cardiovascular research

Cardiovascular disease (CVD) is the leading cause of death globally. The prevalence of CVD increased from 271 million in 1990 to 523 million people in 2019 [1]. CVD refers to a class of diseases that involves structure and function of the heart and blood vessels. Diseases affecting the heart are often related to cardiac remodelling, which is defined as a group of molecular, cellular and interstitial changes that clinically manifest as changes in size, shape and function of the heart after injury [2]. The understanding of pathophysiological mechanisms involved in cardiac remodeling is crucial in the development of new therapeutic strategies [3].

In order to investigate molecular mechanisms of cardiac disease, it is necessary to generate predictive human *in vitro* cell models that reflect human disease [4-6]. Since primary human cardiac cells are difficult to obtain from biopsies and to maintain in culture for extended periods of time due to their finite lifespan and limited proliferation properties [5,6], efforts have been conducted to find alternatives to this cell type. Human pluripotent stem cells (hPSCs) have emerged as a promising cells source in cardiac research [7-11]. HPSCs possess intrinsic properties of unlimited self-renewal and potential to differentiate into any somatic cell types in the body, which makes it possible to generate large numbers of cardiac cells from both healthy individuals and patients [6]. There are two types of PSCs: embryonic stem cells (ESCs) and induced pluripotent stem cells (iPSC). ESCs are derived from the inner cell mass of developing embryos and are used in a wide range of applications. However, the strong ethical concerns and immunological rejection are main limitations [12,13]. In 2006, it was discovered that human somatic cells could be reprogrammed to a pluripotent state by a cocktail of four transcription factors: OCT4, SOX2, KLF4 and MYC [13,14]. These reprogrammed cells are called iPSC. Advantages of iPSCs are their human origin, easy accessibility, avoidance of ethical issues and the potential to use patient-specific iPSCs [13].

Both ESCs and iPSCs have been extensively used in disease modeling, drug testing and regenerative medicine in cardiac research [15-17]. The combination of PSCs with genome editing technology have been used to increase the understanding of molecular mechanisms of cardiac diseases and to investigate new treatment options (**Figure 1**) [18]. One of the rising technologies to genetically modify PSCs is CRISPR-Cas9. The next paragraph describes the basic principles of CRISPR-Cas9 genome editing in PSCs technology.

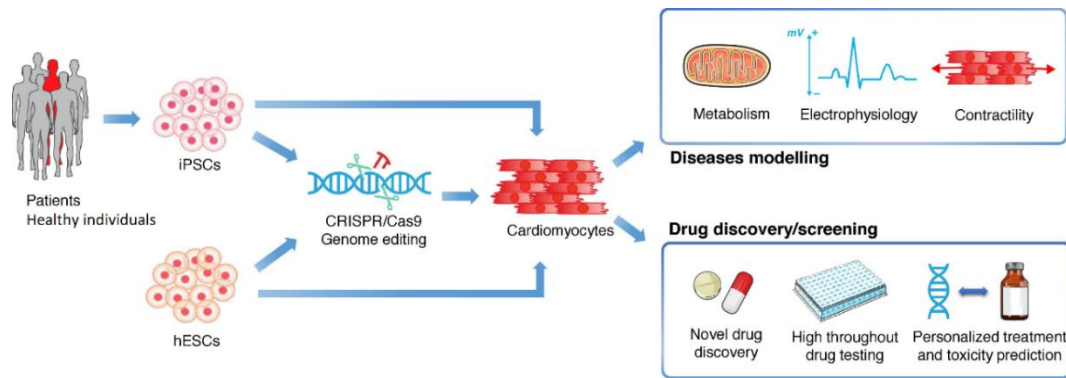


Figure 1: Pluripotent stem cells (PSCs) include induced pluripotent stem cells (iPSC) and embryonic stem cells (ESCs). iPSCs are reprogrammed from somatic cells of healthy individuals or patients. Both iPSCs and ESCs are differentiated towards cardiomyocytes (CMs) and used for disease modeling or drug discovery and screening. The possibilities of PSCs are increased by genome editing technologies, such as CRISPR-Cas9, either to induce disease-associated mutations or to make fluorescent PSC-derived CMs reporter lines. Figure reproduced from [18].

1.2 CRISPR-Cas9 genome editing

Genome editing or gene editing is a technology to manipulate the DNA in a diverse range of cell types and organisms. Zinc-finger nucleases (ZFNs) and transcription activator-like effector nucleases (TALENs) are two well-known genome editing platforms [19,20]. Both techniques use a sequence-specific DNA-binding protein fused to an endonuclease, facilitating targeted double-strand breaks (DSBs) within the DNA [20]. In addition to these techniques, the genome editing technique CRISPR-Cas has been gaining much attention in biotechnology in the last decade [19-21]. It is a simple but powerful technique to alter DNA sequences and modify gene functions. CRISPR-Cas has several advantages compared to ZFNs and TALENs, including the higher targeting efficiency and ability to facilitate multiplex genome editing [21]. Furthermore, the design and production of CRISPR-Cas is relatively simple, cheap and fast. The CRISPR-Cas genome editing technique is based on the adaptive immune system of prokaryotic organisms. In those organisms, CRISPR (clustered regularly interspaced short palindromic repeats) is a DNA sequence array containing short variable sequences and continuously repeating DNA sequences. The variable sequences, called protospacers, are derived from previously invading organisms [21]. The CRISPR array is transcribed into a precursor RNA transcript that is further processed into smaller units, called CRISPR-RNA (crRNA). The crRNAs are combined with one or more CRISPR-associated (Cas) proteins to form the active Cas-crRNA complex [22]. Three types of CRISPR systems have been identified from which type II CRISPR system is one of the best characterized [21,22]. Type II CRISPR system uses a structural non-coding RNA sequence known as trans-activating crRNA (tracrRNA) that assists in the maturation of crRNA [21-23]. The tracrRNA forms a complex with each individual crRNA and the Cas9 nuclease and this complex target foreign nucleic acids (**Figure 2A**). The crRNA unit contains a 20-nucleotide guide sequence which is responsible for recognition and binding to the target sequences. This results in cleavage and degradation of the target DNA sequence by the

Cas9 nuclease. However, it is important that the target sequence contains a Protospacer Adjacent Motif (PAM) directly after the targeted DNA region. This short, conserved sequence of 2-5 nucleotides is required to discriminate between self and foreign DNA [24]. PAMs differ between variants of the CRISPR–Cas system. The Cas9 nuclease for example, recognize only a PAM sequence of 5'-NGG-3' (where "N" can be any nucleotide base) [21].

CRISPR-Cas9 genome editing uses a simplified version of the biological version. The RNA components of the CRISPR-Cas9 system can be fused together to create chimeric, single-guide RNA (sgRNA). This chimeric RNA strand is generated by fusing the 3' end of crRNA to the 5' end of tracrRNA (**Figure 2B**) [25]. This simple, rational design of sgRNA is robust and allows rapid implementation of CRISPR-Cas9 system for genome editing. By changing the 20-nucleotide guide sequence within the synthetic sgRNA, the Cas9 nuclease can be directed toward any target to make a DSB. There are two main considerations in the design of the 20-nucleotide guide sequence [21]: 1) The target sequence must immediately precede the PAM sequence of 5'-NGG-3' which allows cleavage by the Cas9 enzyme and 2) the guide sequence should be specific to minimize off-target activity. After designing the sgRNA, the sequence can be delivered by several methods depending on the desired application. The most straightforward approach is to construct an expression plasmid encoding the Cas9 protein and the sgRNA (**Figure 2C**) [26]. In this method, two single stranded oligonucleotides (encoding the 20-nucleotide guide sequence) are annealed and ligated into a plasmid containing both Cas9 and the remainder of the sgRNA. This plasmid can be transfected into cells to induce cleavage at a specific location.

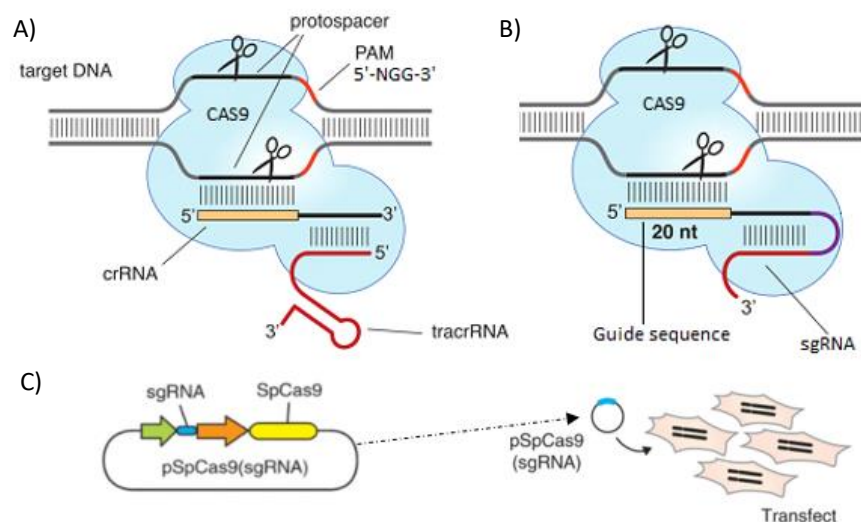


Figure 2: The mechanism of introducing a double-strand break (DSB) by CRISPR-Cas9. **A)** Base-pairing between CRISPR-RNA (crRNA) with trans-activating crRNA (tracrRNA) guides the Cas9 nuclease (in blue) to cleave the target DNA. **B)** The chimeric single-guide RNA (sgRNA) sequence is generated by fusing the 3' end of crRNA to the 5' end of tracrRNA mimicking the dual-RNA structure. This sgRNA consist of a 20-nucleotide guide sequence at the 5' site followed by a hairpin structure retaining the interactions between crRNA and tracrRNA. Figure reproduced from [25]. **C)** The expression plasmid containing both sgRNA and Cas9. The expression plasmid can be transfected into cells to mediate targeted cleavage. Figure adapted from [21].

1.3 Homology directed repair

The Cas9 nuclease creates a DSB at a specific location (between the 17th and 18th bases in the target sequence) determined by the sgRNA sequence [21]. The cell recognizes DNA damage and the DSB-repair machinery is activated. There are two mechanisms for DNA damage repair in mammalian cells: Nonhomologous end joining (NHEJ) and homology directed repair (HDR). NHEJ is the most predominant pathway to repair DSBs [27], in which broken DNA strands are ligated. This is a rapid and efficient procedure, but often results in insertion and deletion mutations [28]. On the other hand, HDR requires an undamaged homologous DNA template to repair the DSB. CRISPR-Cas9 mediated HDR can be utilized by introducing an exogenous repair template into the cell to make defined modifications at the target locus [21]. The repair template contains the desired insertion or modification with homology arms flanking the insertion sequence (**Figure 3A**). Using the natural DNA-repair mechanism, the desired modification is made with high precision.

The HDR template containing the desired insertion can be constructed in several ways. Most of the methods require ligation at restriction enzyme sites present in the backbone vector and the insert. However, the options are limited by the available restriction sites. In contrast, In-Fusion[®] cloning is a ligation-independent cloning method based on the annealing of complementary ends of the insert and the backbone vector (**Figure 3B**) [29]. The different parts of the template contain at least a 15-base-pair overlap at their ends, which can be engineered in PCR primers used to amplify the intended DNA fragment. One of the advantages of In-Fusion[®] cloning is the option of cloning more fragments at the same time in a single reaction, making it a fast and simple cloning procedure [30].

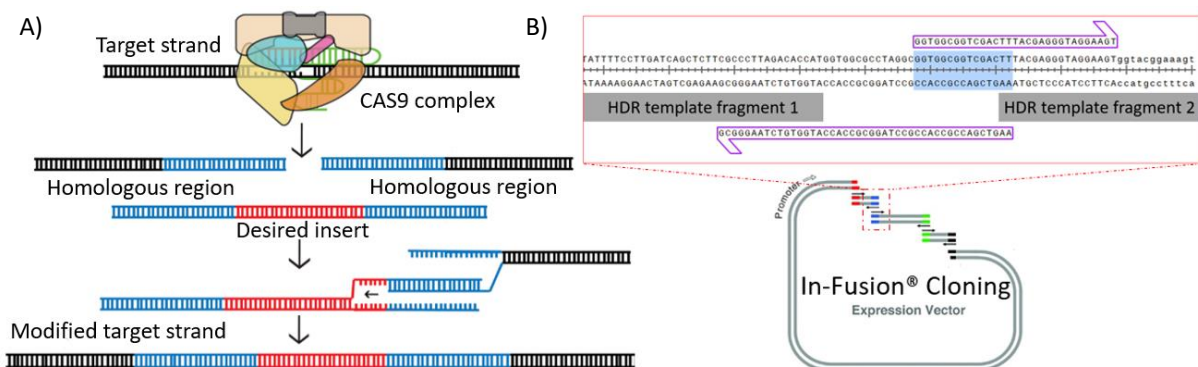


Figure 3: A) The mechanism of homology directed repair (HDR): Cleavage of the target DNA by the sgRNA guided Cas9 nuclease results in a double-strand break (DSB). Addition of an exogenous repair template, with two regions homologous to each side of the DSB, results in HDR. The desired gene is inserted in the target DNA. Figure adapted from [31]. **B)** HDR template containing different DNA fragments inserted in an expression vector using the In-Fusion[®] cloning reaction mechanism. The coloured regions represent overlap region between the different parts of the HDR template. Each part is generated by PCR with primers that include the 15-base-pair overlap (marked in blue). Figure adapted from [29].

1.4 Genomic safe harbor locations

The previous paragraphs discussed the principles of CRISPR-Cas9 genome editing and insertion of foreign DNA by HDR. The question is: Where to insert the transgene to maximize efficacy and safety? The so-called “genomic safe harbors” (GSHs) are suitable locations for the stable integration of transgenes to achieve predictable expression without adverse effects on the host cell [32,33]. There are five GSH criteria proposed in order to avoid activation of adjacent genes and gene disruption: 1) The distance should be at least 50 kb from the 5’ end of any gene, 2) the distance should be at least 300 kb from any cancer-related gene, 3) the distance should be at least 300 kb from any microRNA, 4) the location should be outside a transcription unit and 5) the location should be outside the ultra-conserved region of the human genome [34]. Although no GSH has yet been fully validated for reliable and safe therapeutic transgene addition, there are a few sites which have been extensively tested. 1) the adeno-associated virus site 1 (AAVS1), 2) the C-C Motif Chemokine Receptor 5 (*CCR5*) gene and 3) the human ortholog of the mouse *Rosa26* locus [32,33]. There is some functional data available on robustness and expression of the integrated transgenes and their effects on surrounding genome.

AAVS1 is a naturally occurring site of integration of the Adeno-associated virus (AAV) on chromosome 19 (position 19q13.42). The AAVS1 target site lies in the first intron of the gene phosphatase 1 regulatory subunit 12C (*PPP1R12C*) (**Figure 4, red arrow**) and disruption of *PPP1R12C* is not associated with adverse effects [35,36]. This GSH has gained a lot of interest, because this locus allows stable, long term transgene expression in many cell types, including ESCs and iPSCs [36,37]. Smith et al. showed that transgene expression from the AAVS1 locus in hESCs was maintained and the transgene expression was shown to be stable during hESC differentiation into the three primary germ layers [37]. In the study of Ocegüera-Yanez, a green fluorescent protein (GFP) reporter gene was introduced into the AAVS1 locus of iPSCs. It was reported that the GFP expression levels in iPSCs are maintained upon differentiation into cardiomyocytes (CMs) [36]. These studies indicate that the AAVS1 GSH location is suitable for the insertion of transgenes. The next paragraph describes an example of transgene expression in cardiac research.

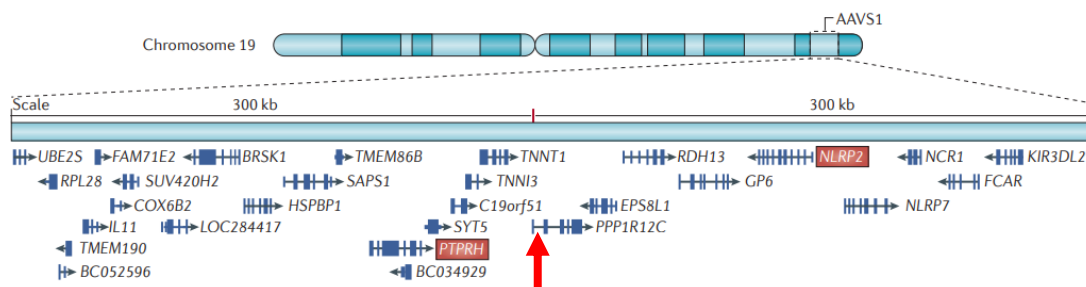


Figure 4: The adeno-associated virus site 1 (AAVS1) on chromosome 19. The transgene integration site is present in the first intron of the gene phosphatase 1 regulatory subunit 12C (*PPP1R12C*) (red arrow). Figure adapted from [32].

1.5 Channelrhodopsin

The utilization of genetic engineering with optical technology has led to the development of cardiac optogenetics, in which light sensitive proteins are introduced in CMs making them responsive to certain wavelength light pulses [38,39]. In this way, it is possible to manipulate and control cardiac cells and tissue using light. Optogenetics has several advantages compared to electrical stimulation: The traditional electrical stimulation carries disadvantages such as toxicity to the tissues, lack of cellular specificity of the stimulation and limited duration of stimulation, whereas optogenetics allow temporal and spatial precise modulation of cellular activity [40,41]. Optogenetic pacing of cardiac tissues can be achieved through the genetic insertion of light-sensitive ion channels in CM or hPSC-CMs. Channelrhodopsin 2 (ChR2) is one of the key molecules used for light-induced stimulation of CMs [42-45]. ChR2 consists of seven transmembrane proteins and is activated by absorption of blue light (470 nm), causing photochemical isomerization of the all-trans retinal to 13-cis retinal. This results in opening of the channel and cations (sodium, potassium and calcium ions) enter the cells, inducing an action potential (**Figure 5**) [46].

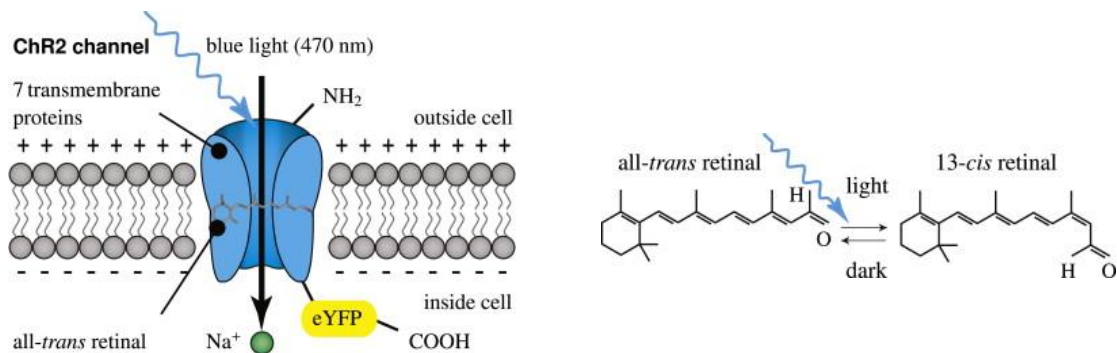


Figure 5: Channelrhodopsin 2 (ChR2) is a light-gated cation channel, consisting of 7 transmembrane proteins. The photochemical isomerization from all-trans retinal to 13-cis retinal occurs when illuminated by blue light (470 nm). This change introduces an influx of cations (mainly Na⁺), causing depolarization and generation of action potentials. The Enhanced Yellow Fluorescent Protein (eYFP) is connected to the C-terminus of ChR2 to provide a fluorescent tag for visualization of the fusion construct. Figures reproduced from [46].

1.6 Aims and objectives

This research aims to insert a doxycycline-inducible ChR2 gene into the AAVS1 GSH locus of hPSCs by CRISPR-Cas9 mediated HDR to enable optogenetic pacing of hPSC-derived CMs (hPSC-CMs). To achieve this aim, several objectives are defined: The first objective is to design and construct a HDR template for doxycycline-inducible expression of the red fluorescent protein mRuby2 to validate transgene expression in the AAVS1 locus of hPSCs and hPSCs-CMs. The second objective is to target doxycycline-inducible mRuby2 in the AAVS1 locus of hiPSCs or hESCs. The third objective is to replace the mRuby2 gene by the ChR2 gene coupled to Enhanced Yellow Fluorescent Protein (eYFP) tag in the HDR construct and insert the ChR2 into the AAVS1 locus of PSCs.

2. Materials and methods

2.1 sgRNA-Cas9 plasmid

To achieve HDR at the AAVS1 GSH location, a DNA repair template containing the desired sequence should be delivered into the human PSCs together with the sgRNA-Cas9 plasmid. Previously, Van den Bos designed three different guide sequences targeting the AAVS1 region [47], based on the article of Smith et al. [37]). The guide sequences were inserted in the pSp-Cas9(BB)-2A-puro plasmid as described by Ran et al. (2013) [21]. The presence of the 20-nucleotide guide sequence within the pSp-Cas9(BB)-2A-puro plasmid was tested with Sanger sequencing (Eurofins Genomics). See **Supplementary experimental procedures** for extended description and sequencing primer.

2.2 HDR template generation

The HDR template consists of a pENTR1A backbone plasmid carrying two homology arms (matching the AAVS1 locus), the gene encoding for the red fluorescent protein mRuby2 ($\lambda_{ex} = 559$ nm, $\lambda_{em} = 600$ nm), the minimal promoter Tetracycline Response Elements (TRE) and a constitutively active promoter elongation factor 1 alpha (EF1 α) before the gene encoding for the TetOn3G transactivator protein. The HDR template fragments were amplified with the Phusion High-Fidelity PCR Kit (Thermo Fisher Scientific™). The genomic DNA of hiPSCs (LUMC0020iCTRL-06) was used to obtain the right homology arm (HAR) and left homology arm (HAL). The fragments mRuby2, TRE3G promoter and EF1 α -TetOn3G were amplified from commercially available plasmids (Addgene #54614, #96964 and #104543, respectively). The primers used for amplification of HDR template fragments were designed with the In-Fusion® cloning tool in SnapGene (SnapGene® software from GSL Biotech; available at snapgene.com). The PCR products were loaded on an agarose gel and the desired DNA fragments were isolated and purified with the NucleoSpin Gel and PCR Clean-up kit (Macherey-Nagel), according to the manufacturer's protocol (**Figure 6**).

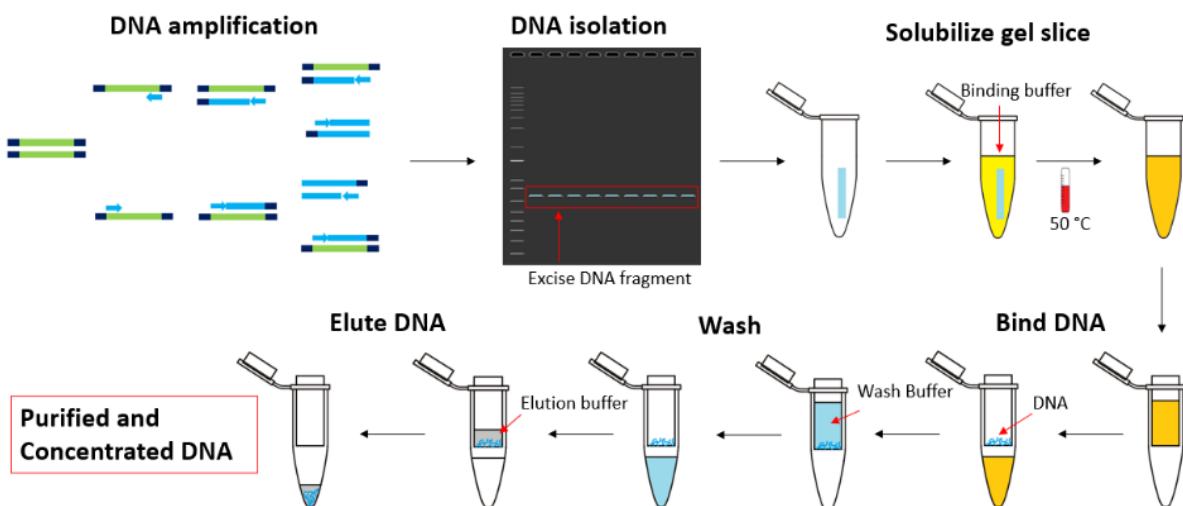


Figure 6: Schematic overview of the amplification and isolation of HDR template fragments.

The different fragments of the HDR template were inserted in the pENTR1A by a two-step In-Fusion® cloning mechanism. The pENTR1A plasmid (Addgene #2525) was linearized at the AjiI (BmgBI) restriction site and mRuby2, the TRE3G promoter and HAR were inserted using the In-Fusion® HD Cloning Kit (Takara Bio). The plasmid was transformed and expanded in One Shot® TOP10 Competent *E. coli* Cells (Invitrogen™). Subsequently, plasmids were isolated and purified with the PureLink™ Quick Plasmid Miniprep Kit (Invitrogen™) or PureYield™ Plasmid Midiprep System (Promega Corporation) according to the manufacturer’s protocol (**Figure 7**). The isolated plasmids were analysed by restriction enzyme digestion and sent for Sanger sequencing. After confirmation of the insertion of mRuby2, TRE3G and HAR into the pENTR1A plasmid, the plasmid was opened at the BcuI (SpeI) restriction site present between mRuby2 and pENTR1A vector. The HAL and EF1α-TetOn3G fragments were inserted in the linearized pENTR1A plasmid by In-Fusion® cloning. After bacterial transformation, expansion and isolation, the plasmids were analysed by restriction enzyme digestion, sent for Sanger sequencing and stored for transfection in hPSCs. See **Supplementary experimental procedures** for extended description, vector maps, In-Fusion® cloning primers and sequencing primers.

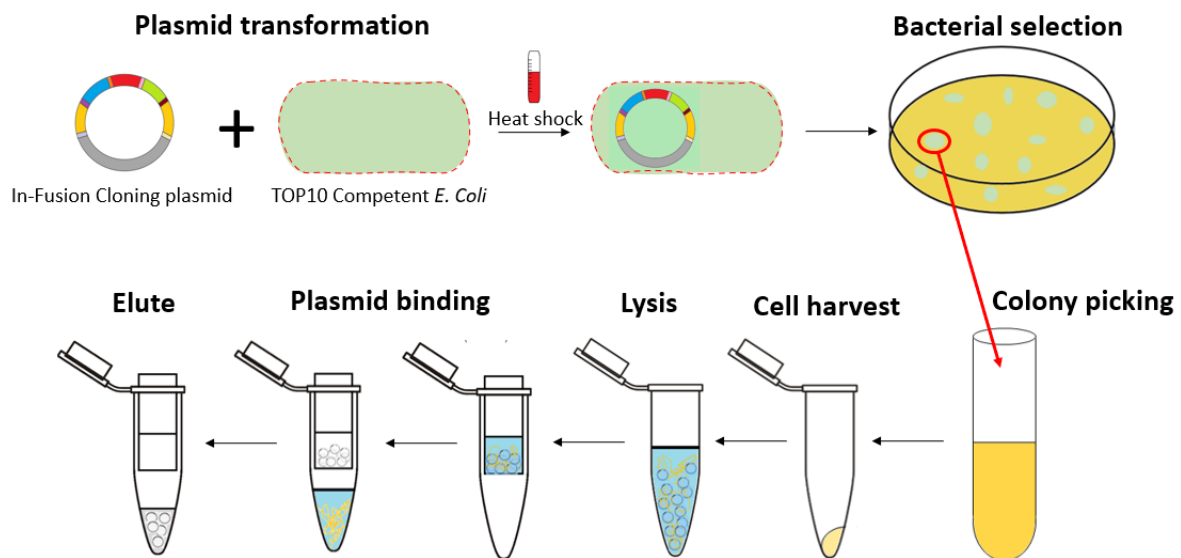


Figure 7: Schematic overview of plasmid transformation into TOP10 Competent *E. coli*, expansion of the selected bacterial clones and isolation of the plasmid.

2.3 Targeting of hPSCs with the HDR template

Stem cells (hESCs and hiPSCs) were maintained in Essential 8™ medium on 0.5 µg/cm² vitronectin (Gibco™, Thermo Fisher Scientific™) at 37°C, 5% CO₂ and were passaged twice a week. One day before transfection, hiPSCs and hESCs were seeded in a 6-well on irradiated mouse embryonic fibroblasts (MEFs) in hESC medium. The stem cells were transfected with 4 µg sgRNA-Cas9 plasmid and 3 – 4.5 µg of HDR plasmid using Lipofectamine™ Stem Transfection Reagent (Invitrogen™, Thermo Fisher

Scientific™) according to manufacturer's instructions. The cells were incubated in 37 °C and 5% CO₂ or 32 °C and 5% CO₂ for 24 h. The presence of the puromycin resistance gene in the sgRNA-Cas9 plasmid allowed selection of the transfected cells. After 24 h of puromycin exposure, the cells were recovered for several days on MEFs before passaging the cells to vitronectin coated wells in Essential 8™ medium. The cells were grown for several days and treated with doxycycline (Doxycycline Hydrochloride, Ready Made Solution, Sigma-Aldrich) 24 h or 48 h before fluorescence-activated cell sorting (FACS). Different doxycycline concentrations (ranging from 10 ng/ml to 10 µg/ml) were tested. The mRuby2 positive cells were sorted with a 488 nm laser and a 600/60 nm emission filter using the SH800S Cell Sorter (Sony Biotechnology) after exclusion of dead cells and debris according to side and forward scatter. The positive cell population was seeded on vitronectin coated wells for further analysis. The genomic DNA was analysed for the insertion of the HDR template into the AAVS1 locus by PCR and agarose gel electrophoresis. See **Supplementary experimental procedures** for extended description and primers.

2.4 Transient transfection HDR (mRuby2) plasmid

HESCs were seeded in vitronectin coated plates (24-well plate) one day before transfection. The stem cells were transfected with 250 – 500 ng plasmid using Lipofectamine™ Stem Transfection Reagent for 48 h at 30 °C. The plasmids that were used for transient transfection were mRubyII-N1 (Addgene #54614) and the HDR plasmid. The cells that were transfected with HDR template were treated with doxycycline (concentrations ranging from 10 ng/ml to 1000 ng/ml) 24 h after transfection. Cells were observed 24 h and 54 h post transfection using $\lambda_{\text{ex}} = 540$ nm with the Nikon Eclipse Ti2 Inverted Microscope. See **Supplementary experimental procedures** for extended description.

2.5 ChR2 cloning

The mRuby2 gene in the HDR template was replaced with human ChR2 coupled to EYFP ($\lambda_{\text{ex}} = 513$ nm, $\lambda_{\text{em}} = 527$ nm). The mRuby2 gene was removed from the HDR template by restriction enzyme digestion using the restriction sites Sgsl (Ascl) and XmaJI (AvrII). The ChR2-EYFP gene was amplified from the plasmid tol2-CAG::ChR2-YFP (Addgene #59740) with “sticky-end PCR” primers. Sticky-end PCR is based on the article of Zeng [48] and requires four PCR primers and reactions in two separate tubes. After mixing, denaturing and annealing both PCR products, circa 25% of the final products contains overhangs corresponding to the Sgsl (Ascl) and XmaJI (AvrII) restriction sites (**Figure 8**). The ChR2-EYFP fragment was ligated into the HDR template using the T4 DNA Ligase kit (Promega Corporation) according to the manufacturer's protocol. The plasmid was transformed in bacteria, expanded and isolated before restriction enzyme digestion analysis and Sanger sequencing. See **Supplementary experimental procedures** for extended description, sticky-end PCR primers and sequencing primers.

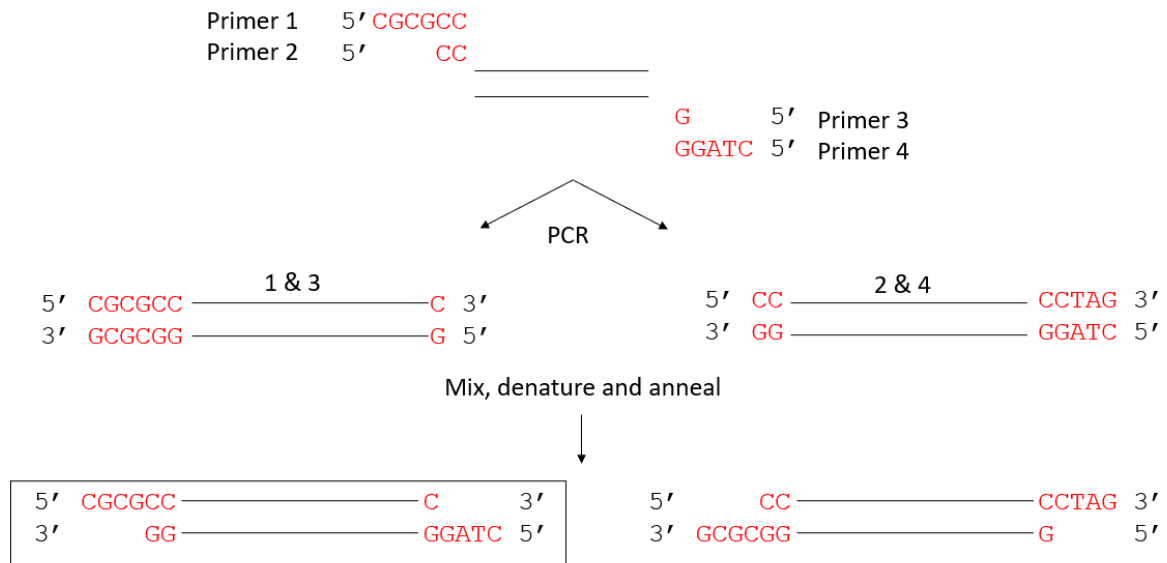


Figure 8: The principle of sticky-end PCR. The primers 1 and 2 differ in their 5' overhang corresponding to the *SgsI* (*Ascl*) restriction site. The primers 3 and 4 contain overhangs corresponding to the *XmaI* (*AvrII*) restriction site. The PCR reactions were performed in two separated tubes using primers 1 and 3, and primers 2 and 4, respectively. The PCR products were mixed, denatured and annealed, which means that 25% of the desired product can be used for ligation in the HDR template.

2.6 Transient transfection HDR (ChR2-EYFP) plasmid

The transfection of the HDR (ChR2-EYFP) plasmid was performed as described in paragraph 2.4. The plasmids that were used for transient transfection were tol2-CAG::*ChR2*-YFP (Addgene #59740) and the HDR (ChR2-EYFP) plasmid. The cells that were transfected with HDR (ChR2-EYFP) plasmid were treated with doxycycline (concentrations ranging from 10 ng/ml to 1000 ng/ml) 24 h after transfection. Cells were observed 24 h and 54 h post transfection using $\lambda_{\text{ex}} = 470 \text{ nm}$ with the Nikon Eclipse Ti2 Inverted Microscope. See **Supplementary experimental procedures** for extended description.

3. Results

3.1 Sanger sequencing sgRNA-Cas9 plasmids

The guide sequence was inserted at the Bpil (BbsI) restriction sites in the sgRNA-Cas9 plasmid between the U6 promoter and the gRNA scaffold (**Figure 9A**). Sanger sequencing confirmed the correct guide sequence within the sgRNA-Cas9 plasmid (**Figure 9C-D**). The location of the three different sgRNAs targeting the AAVS1 GSH locus with respect to each other is depicted in **Figure 9E**.

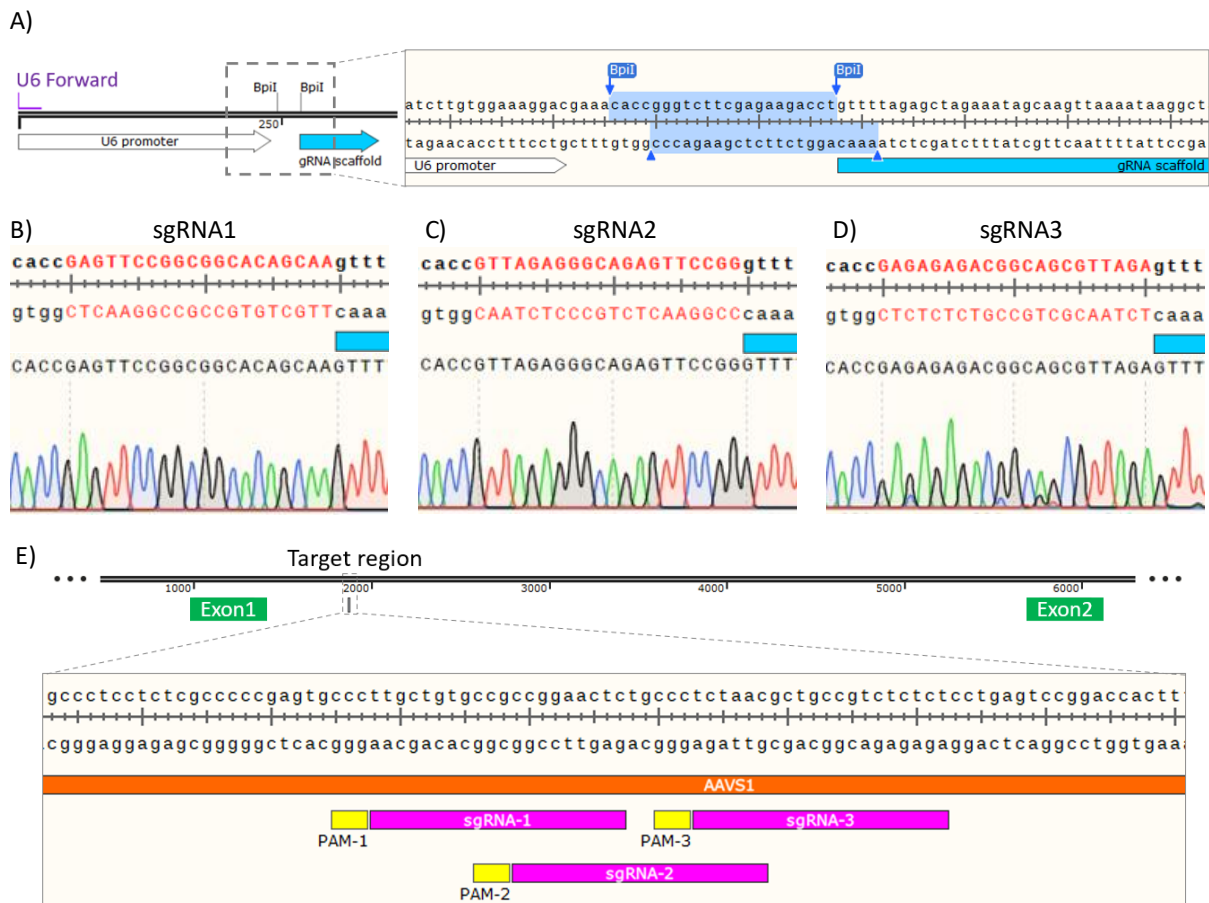


Figure 9: **A)** Part of the pSpCas9(BB)-2A-Puro plasmid containing Cas9 and the sgRNA scaffold. Digestion of the plasmid with the Bpil (BbsI) restriction enzymes (blue outline) allows the direct insertion of the 20-nucleotide guide sequence. **B-D)** Sequencing results of the insertion of the guide sequence of sgRNA1, sgRNA2 and sgRNA3, respectively. **E)** Location of the different 20-nucleotide guide sequences within the PPP1R12C gene.

3.2 HDR template generation

The sgRNA-Cas9 plasmids targets the first intron of the PPP1R12C gene to achieve insertion of doxycycline-inducible mRuby2 by HDR (**Figure 10**). The HDR template contains five different DNA fragments: EF1 α -TetOn3G, TRE3G promoter and mRuby2 flanked by two homology arms, which allows integration in the genomic AAVS1 locus. The HDR template for doxycycline-inducible expression of mRuby2 was constructed in a two-step In-Fusion[®] cloning mechanism (**Figure 11A**). In the first step, the HAR, TRE3G promoter and mRuby2 fragments were inserted in the linearized pENTR1A plasmid.

In the second step, the HAL and EF1 α -TetOn3G fragments were inserted in the pENTR1A plasmid containing the first three fragments. The protein TetOn3G can only bind to the TRE promoter when bound to the antibiotic tetracycline (or tetracycline derivatives like doxycycline). This means that the fluorescent protein mRuby2 is only expressed in the presence of doxycycline (**Figure 11B**).

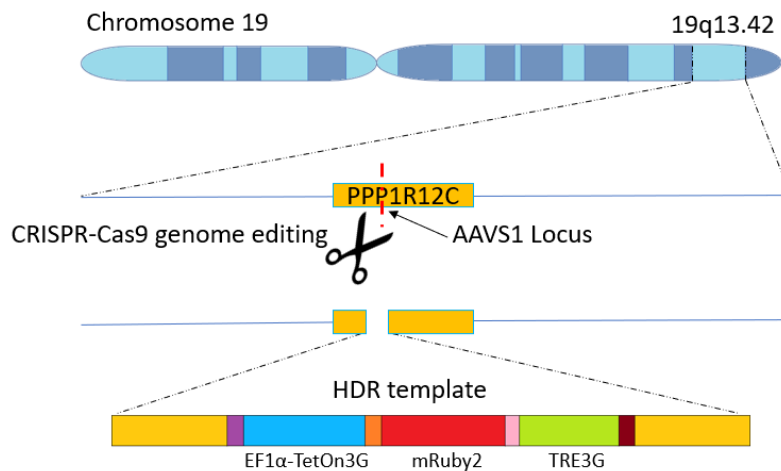


Figure 10: Schematic overview of CRISPR-Cas9 genome editing at the AAVS1 genomic safe harbor (GSH) location on chromosome 19 (position 19q13.42). The AAVS1 target site lies in the first intron of the gene phosphatase 1 regulatory subunit 12C (PPP1R12C). The Cas9 nuclease creates a double-strand break (DSB) determined by a 20-nucleotide guide sequence and the homology directed repair (HDR) machinery is activated in the presence of an exogenous repair template.

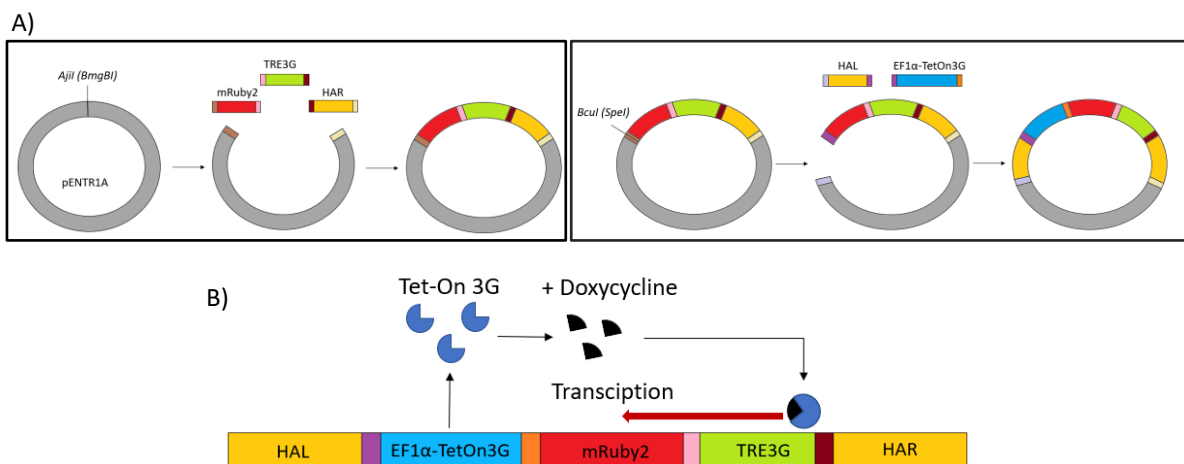


Figure 11: A) Schematic overview of the In-Fusion[®] cloning reaction mechanism. In-Fusion[®] cloning requires a 15-base-pair overlap between the different parts, indicated by the same colours at the termini of the vector or fragment. The different fragments of the HDR template are inserted in the backbone vector by a two-step In-Fusion[®] cloning mechanism: **Left panel)** The pENTR1A vector is linearized at the Ajil (BmgBI) restriction site and the mRuby2, TRE3G promoter and HAR are inserted in the backbone vector. **Right panel)** The vector is opened at the Bcul (SpeI) restriction site between the pENTR1A plasmid and mRuby2 and the HAL and EF1 α -TetOn3G are inserted. The HAL and HAR allow the insertion of the inducible mRuby2 gene at the AAVS1 GSH location. **B)** Working mechanism of the construct. The constitutively active promoter EF-1 α is located before the gene encoding for the TetOn3G transactivator protein. The protein TetOn3G can only bind to the TRE promoter in the presence of the antibiotic tetracycline (or tetracycline derivatives like doxycycline). This means that the fluorescent protein mRuby2 is only expressed in the presence of doxycycline.

3.2.1 HDR template generation step 1

The fragments HAR (532 bp), TRE3G (400 bp), mRuby2 (760 bp), EF1 α -TetOn3G (2146 bp) and the HAL (571 bp) were successfully amplified (**Figure 12, left panel**). Initially, the HAL fragment could not be produced. New HAL forward primers were designed, which resulted in HAL fragments of the correct size after PCR amplification (**Supplementary figure 1**). The PCR reaction of the fragments was performed in large amounts and the correct PCR product was extracted from the agarose gel. As an example, the amplification of the HAL is shown (**Figure 12, right panel**). The backbone plasmid pENTR1A (2717 bp) was linearized with the AjiI (BmgBI) restriction enzyme (**Figure 13, left panel**). The linearized plasmid was extracted from the agarose gel and it was shown that only the linearized plasmid was isolated (**Figure 13, middle panel**). The HAR, TRE3G promoter and mRuby2 were inserted into the linearized pENTR1A vector by In-Fusion[®] cloning (**Figure 13, right panel**).

The pENTR1A plasmid with the inserted HAR, TRE3G and mRuby2 were transformed in TOP10 competent *E. coli* cells. Ten bacterial colonies were selected and grown. Subsequently, the plasmids were isolated and analysed with restriction enzyme digestions (data shown for one plasmid). Digestion with the restriction enzymes XmaI (AvrII) and BclI (SpeI) should result in two fragments and digestion with the restriction enzyme BpiI (BbsI) should result in four fragments (**Figure 14**). The experimental data showed indeed two fragments after XmaI (AvrII) and BclI (SpeI) digestion and the three largest fragments after BpiI (BbsI) digestion (**Figure 14, right panel**). Sanger sequencing confirmed successful insertion of the first three fragments (**Figure 15**).

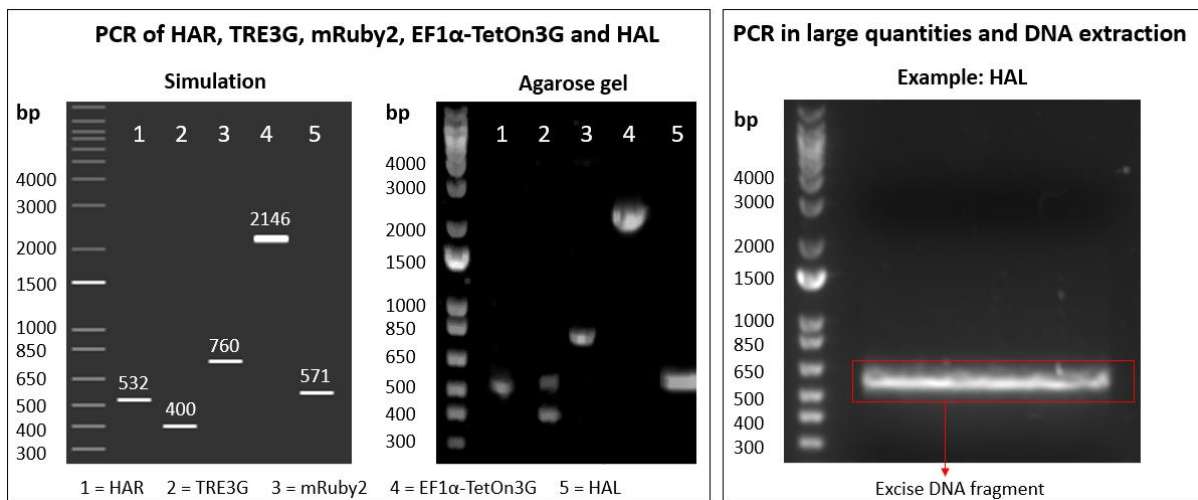


Figure 12: Left panel) Results of the PCR reaction on an agarose gel of the HAR (532 bp), TRE3G promoter (400 bp), mRuby2 (760 bp), EF1 α -TetOn3G (2146 bp) and HAL (571 bp). The TRE3G promoter also showed an amplified DNA fragment just above 500 bp. **Right panel)** The PCR reaction of the HAR, TRE3G, mRuby2, EF1 α -TetOn3G and HAL was performed in large quantities and the DNA fragments were extracted from the gel. As an example, the agarose gel of the HAL is shown.

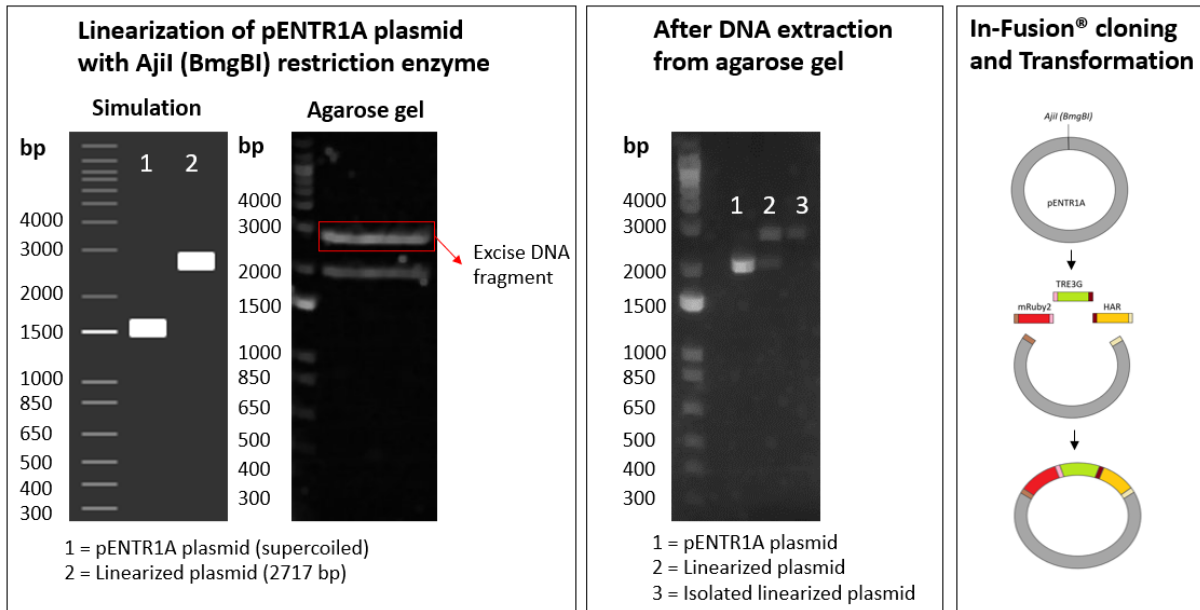


Figure 13: Left panel) The backbone vector pENTR1A was linearized with the Ajil (BmgBI) restriction enzyme. The intact supercoiled pENTR1A plasmid is indicated by number 1. The linearized plasmid (2717 bp) is indicated by number 2. The digestion was performed in large amounts and the plasmid was extracted from the agarose gel. There is also some intact pENTR1A plasmid visible. **Middle panel)** The isolated linearized plasmid was checked on gel (number 3). This indicates that only the linearized plasmid is isolated from gel. **Left panel)** The first three fragments can be inserted in the linearized pENTR1A vector by In-Fusion® cloning.

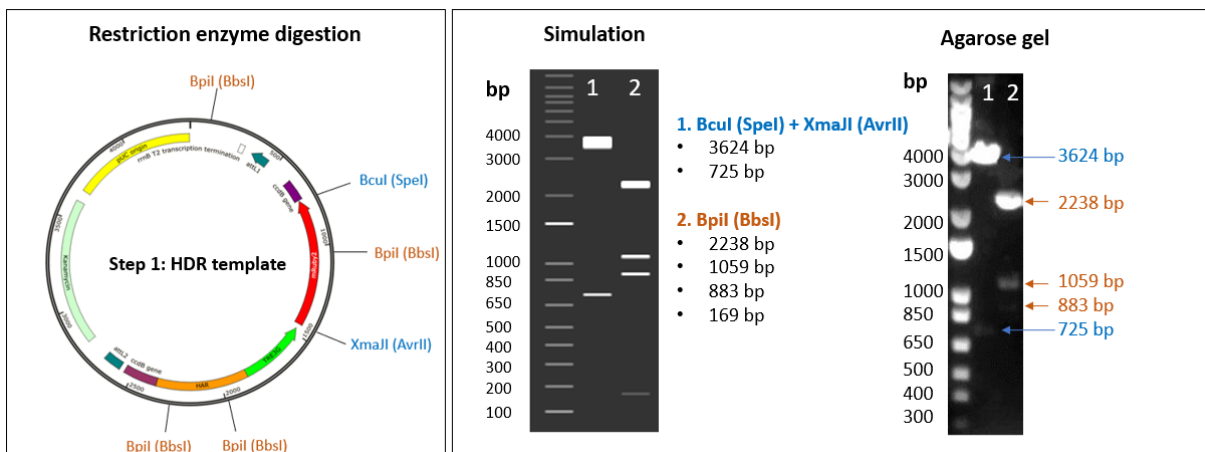


Figure 14: Left panel) The pENTR1A plasmid with the inserted HAR (orange), TRE3G (green) and mRuby2 (red). The restriction sites Bpil (BbsI), Bcul (SpeI) and XmaJI (AvaII) are shown. **Right panel)** The restriction enzymes Bcul (SpeI) and XmaJI (AvaII) cuts the plasmid into two fragments with the length of 3624 bp and 725 bp (number 1). The plasmid digested with Bpil (BbsI) results in four fragments (number 2) of which the three largest fragments are visible at the expected height. The intensity of the lane becomes lower if the size of the fragment decreases.



Figure 15: Top panel) Six different sequencing primers were designed covering the inserted HAR (orange), TRE3G (green) and mRuby2 (red). **Middle panel)** Schematic overview of the sequencing results. The brown bars represent a complete match with the simulated sequence. **Bottom panel)** Sequencing details of transition between mRuby2 and TRE3G. The simulated double-stranded DNA sequence is shown at the top. The results (graph at the bottom) are perfectly aligned with the simulated sequence, confirming successful insertion of the HAR, TRE3G and mRuby2 without any insertions, deletions or mutations.

3.2.2 HDR template generation step 2

The pENTR1A plasmid with the inserted HAR, TRE3G and mRuby2 was opened at the BcuI (SpeI) restriction site present between mRuby2 and pENTR1A. The linearized plasmid (4349 bp) was extracted from the agarose gel (**Figure 16, left panel**) and a small sample was used to check successful extraction of the linearized plasmid (**Figure 16, middle panel**). The EF1 α -TetOn3G and HAL were inserted in the linearized pENTR1A vector by In-Fusion[®] cloning (**Figure 16, right panel**) and amplified in bacteria.

Restriction enzyme digestion of the isolated plasmid with BpiI (BbsI) should result in five fragments and digestion with XmaI (AvrII) and BcuI (SpeI) should result in two fragments (**Figure 17**). The digested plasmids were loaded on agarose gel and the results resembled the simulated data, except for the 169 bp fragment after BpiI (BbsI) digestion (**Figure 17, right panel**). Sanger sequencing confirmed successful insertion of EF1 α -TetOn3G and HAL (**Figure 18**). It is worth mentioning that the PAM sequence in the HDR template was mutated to prevent Cas9 from cutting the template during transfection. The C \rightarrow G mutation in the HAL and the C \rightarrow T mutation in the HAR corresponds to PAM sequence inactivation of sgRNA1 and sgRNA3, respectively (**Figure 18, bottom panel**). The PAM sequence of sgRNA2 is disturbed by insertion of the TRE3G fragment.

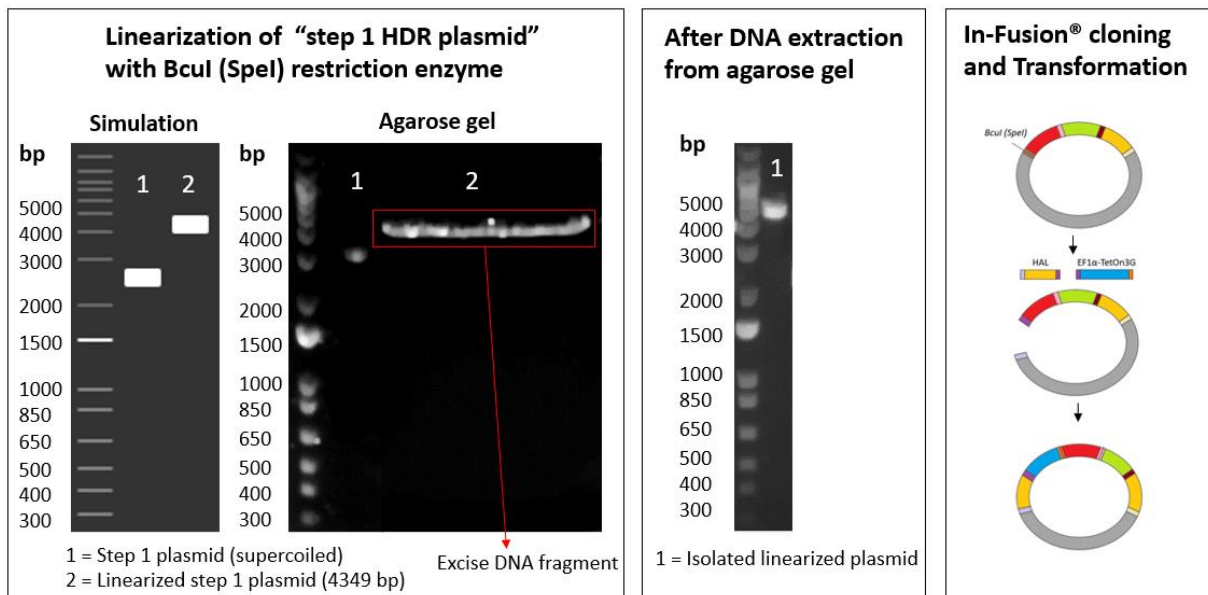


Figure 16: Left panel) The *pENTR1A* plasmid with the inserted *HAR*, *TRE3G* and *mRuby2* (“step 1 HDR plasmid”) was linearized with the *BcuI* (*SpeI*) restriction enzyme. The “non-linearized” plasmid is indicated by number 1. The linearized plasmid (4349 bp) is indicated by number 2 and extracted from the agarose gel. **Middle panel)** The linearized plasmid was successfully isolated. **Right panel)** The fragments *EF1α-TetOn3G* and *HAL* can be inserted in the “step 1 HDR plasmid” by *In-Fusion®* cloning.

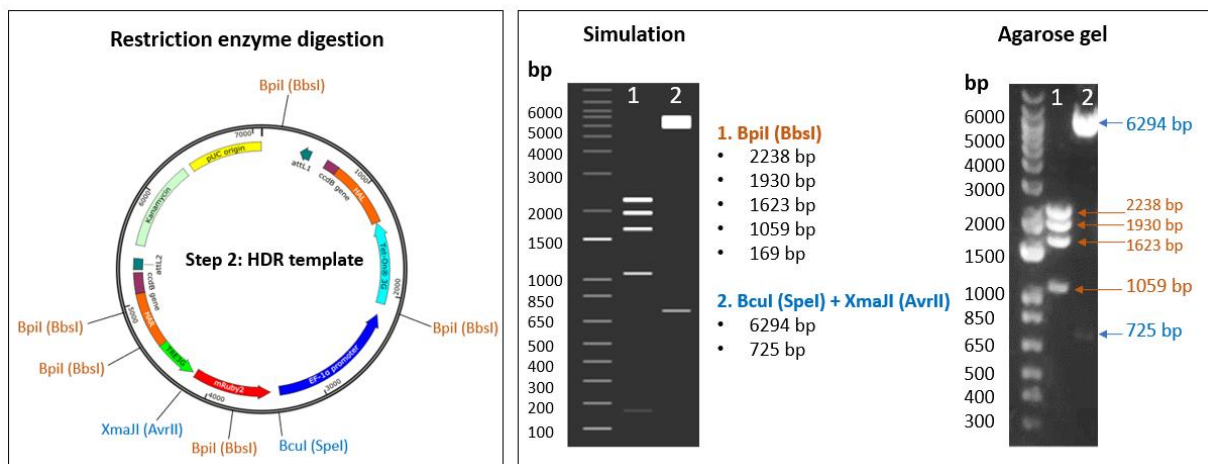


Figure 17: Left panel) The restriction sites *Bpil* (*BbsI*), *BcuI* (*SpeI*) and *XmaII* (*AvrII*) are shown in the *pENTR1A* plasmid with the inserted homology arms (orange), *TRE3G* (green), *mRuby2* (red) and *EF1α-TetOn3G* (Blue). **Right panel)** The results of the restriction enzyme digestion suggested that the *HAR*, *TRE3G*, *mRuby2*, *EF1α-TetOn3G* and *HAL* were inserted. The plasmid digested with *Bpil* results in five fragments, of which the four largest fragments are visible at the expected height (number 1). The restriction enzymes *BcuI* and *XmaII* cuts the plasmid into a 6294 bp fragment and 725 bp fragment (number 2).

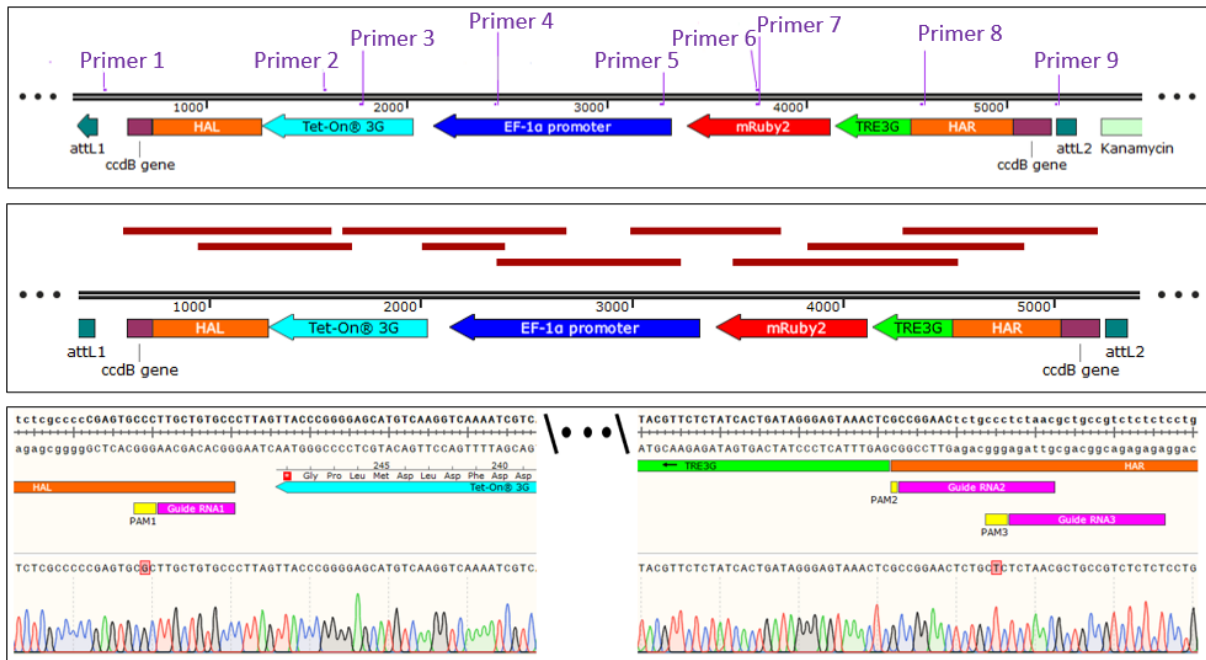


Figure 18: Top panel) Nine different sequencing primers were designed covering the inserted homology arms (orange), TRE3G (green), mRuby2 (red) and EF1 α -TetOn3G (Blue). **Middle panel)** Schematic overview of the sequencing results. The brown bars represent overlap with the simulated sequence, confirming successful insertion of homology arms, TRE3G, mRuby2 and EF1 α -TetOn3G. **Bottom panel)** Sequencing details of the transition between the HAL and TetOn3G gene. The simulated double-stranded DNA sequence is shown at the top. The results (graph at the bottom) are perfectly aligned with the simulated sequence, except for the PAM sequence of guide RNA1 and guide RNA3. The C \rightarrow G mutation in the HAL and the C \rightarrow T mutation in the HAR were deliberately made to prevent Cas9 re-cutting the target site.

3.3 Targeting of hPSCs with the inducible construct

Both hiPSCs and hESCs were co-transfected with the sgRNA-Cas9 plasmid and the inducible HDR template using the chemical transfection reagent lipofectamine (**Figure 19**). After puromycin antibiotic selection, the cells were treated with doxycycline and the positive mRuby2 cells were sorted.

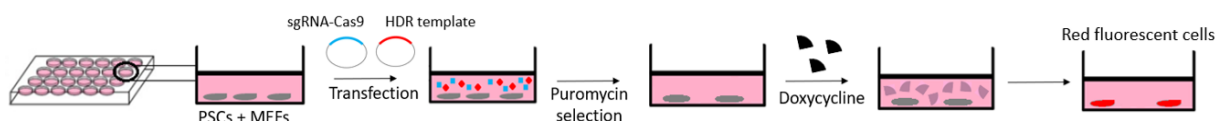


Figure 19: Schematic overview of the CRISPR-Cas9-mediated targeting of doxycycline-inducible mRuby2 in human induced pluripotent stem cells (hiPSCs) or human embryonic stem cells (hESCs) on mouse embryonic fibroblasts (MEFs). After transfection, the cells were treated with puromycin to select sgRNA-Cas9 transfected cells. Treatment with doxycycline should result in fluorescent mRuby2 expression.

HiPSC survival after puromycin selection was superior in the condition transfected with the HDR template and sgRNA3 compared to the other sgRNAs (sgRNA1 and sgRNA2). The hiPSC transfected with HDR template and sgRNA3 were treated with 2 μ g/ml doxycycline for 24 h and this seemed to result in a positive and negative mRuby2 population as detected by flow cytometry (**Figure 20A**). There was little difference in mRuby2 expression between transfection with 3 μ g (low)

and 4.5 μg (high) HDR template, 1.35% and 1.64% mRuby2-positive cells respectively. The gates that were set to exclude dead cells and debris are shown in **Supplementary figure 2**. The positive cell population was sorted and plated for further analysis. Unfortunately, the cells were lost due to bacterial contamination. PCR screening of the genomic DNA of the mRuby2-negative cell population suggested that a DSB was made at the sgRNA3 location (**Figure 20B-C**).

Targeting of hESCs was performed in parallel, since previous work showed successful insertion of genes in hESCs with CRISPR-Cas9 mediated HDR [49]. Surprisingly, the majority of the cells survived puromycin selection; especially the “cold shock” transfection at 32 °C showed around 80% confluency one day after puromycin selection compared to 0% confluency of hESCs in the control well (**Supplementary figure 3**). Treatment with doxycycline in various concentrations (10 ng/ml – 10 $\mu\text{g}/\text{ml}$) for 24 h to 48 h did not result in mRuby2 signal (**Figure 21A**). The flow cytometry data is shown for the “cold shock” transfections and the remaining plots of the other conditions are shown in **Supplementary figure 4**. However, a PCR screening showed insertion of EF1 α -TetOn3G, TRE3G and mRuby2 genes in the DNA (**Figure 21B**, data shown for the sgRNA3 condition). To test it if the doxycycline-inducible construct is properly working, a transient transfection was performed.

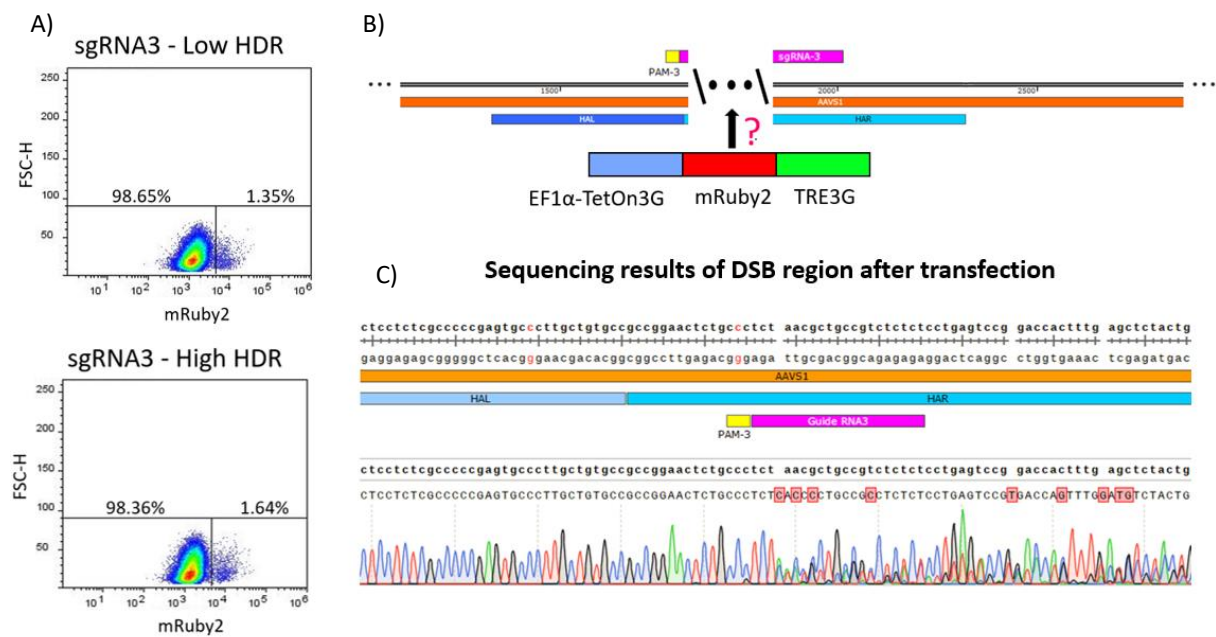


Figure 20: A) Flow cytometry plots depicting the percentage of mRuby2 positive hiPSC cells after doxycycline stimulation (2 $\mu\text{g}/\text{ml}$ for 24 h) of targeted cells with sgRNA3 and low HDR (3.0 μg) or high HDR (4.5 μg) template. **B)** Schematic representation of the location of the double-strand break (DSB) made by sgRNA3 (purple) within the AAVS1 locus (orange). **C)** PCR screening of the negative cell population after sorting of the hiPSCs suggest that a DSB was made at the sgRNA3 location. At the DSB location, the sequencing results showed multiple peaks indicating indels.

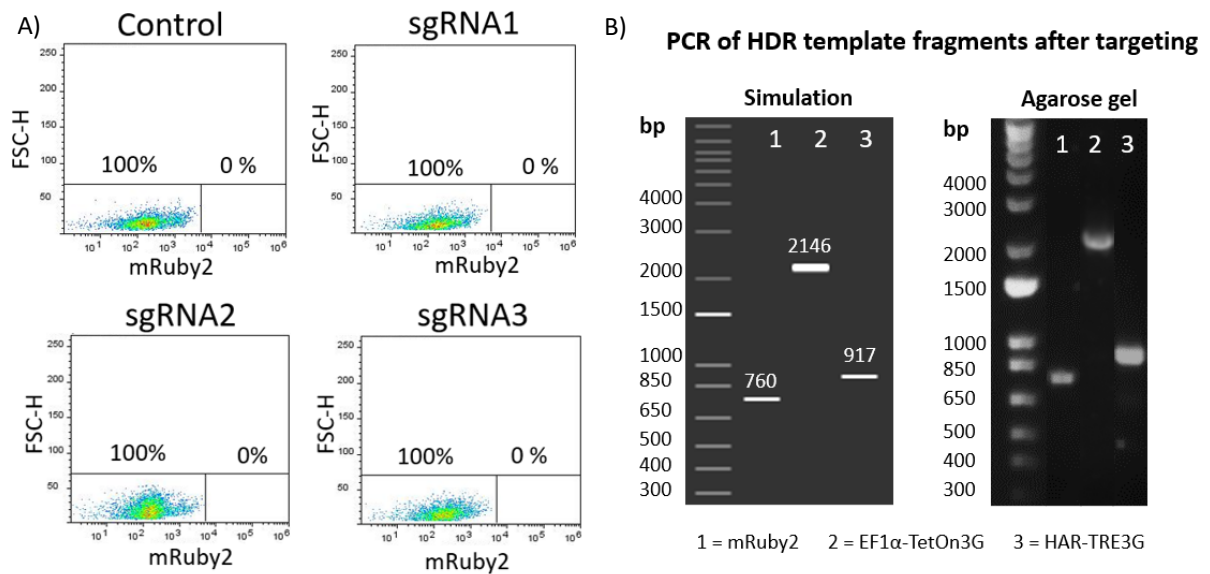
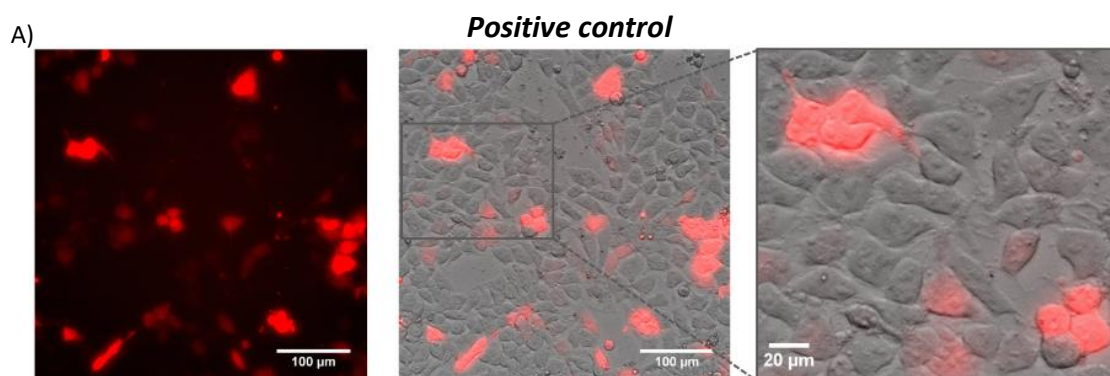


Figure 21: **A)** Flow cytometry plots showing the percentage of mRuby2 positive hESC cells after doxycycline stimulation (1 µg/ml for 48 h). The conditions that are shown in this figure are sgRNA1 – 3.0 µg HDR template, sgRNA2 – 3.0 µg HDR template and sgRNA3 – 3.0 µg HDR template, which were transfected in “cold shock”. The control was transfected, but not stimulated with doxycycline. **B)** PCR screening of the hESC cells after transfection showed the insertion of EF1α-TetOn3G, mRuby2 and TRE3G fragments in the AAVS1 locus. Results shown for sgRNA3.

3.3.1 Transient transfection

HESCs were transfected with the inducible HDR template and the mRubyII-N1 plasmid (as positive control). The mRuby2 gene in the mRubyII-N1 plasmid is under expression of a cytomegalovirus (CMV) promoter and mRuby2 expression was shown 48 h after transfection (**Figure 22A**). Compared to the positive control, the intensity of fluorescence and the number of mRuby2 positive cells is far lower in the inducible construct after doxycycline stimulation (1000 ng/ml for 30 h) and difficult to distinguish from autofluorescent dead cells and debris (**Figure 22B**).

It was hypothesized that the lack of signal in the stable transfection and the low signal in the transient transfection was caused by absence of the poly(A) tail after the TetOn3G gene. Therefore, a new HDR template was made in which the poly(A) tail after the TetOn3G fragment was incorporated.



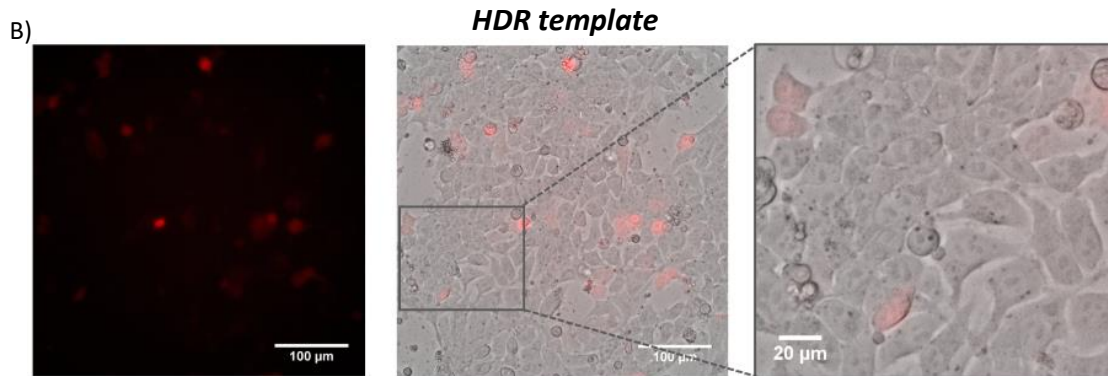


Figure 22: Fluorescent mRuby2 expression in hESCs 48 h after transfection with **A)** mRubyII-N1 plasmid (as positive control) and **B)** the doxycycline-inducible HDR template. The HDR template was stimulated with 1000 ng/ml doxycycline for 30 h. The intensity of mRuby2 signal and the number of mRuby2 positive cells is significantly lower in the HDR template and difficult to distinguish from background.

3.4 HDR template 2.0

The new HDR template, called HDR template 2.0, was produced as described in paragraph 3.2.2. Because the HDR template was generated in two steps, it was possible to reuse the “step 1 HDR plasmid” produced in 3.2.1. and the corrected EF1 α -TetOn3G fragment with SV40 poly(A) tail and the HAL were inserted via In-Fusion[®] cloning. New In-Fusion[®] cloning primers connecting the HAL with the EF1 α -TetOn3G fragments were designed, which resulted in fragments of the correct size after PCR amplification (**Supplementary figure 5**). The insertion of the HAL and EF1 α -TetOn3G (including poly(A) tail) was confirmed with Sanger sequencing (**Figure 23**).

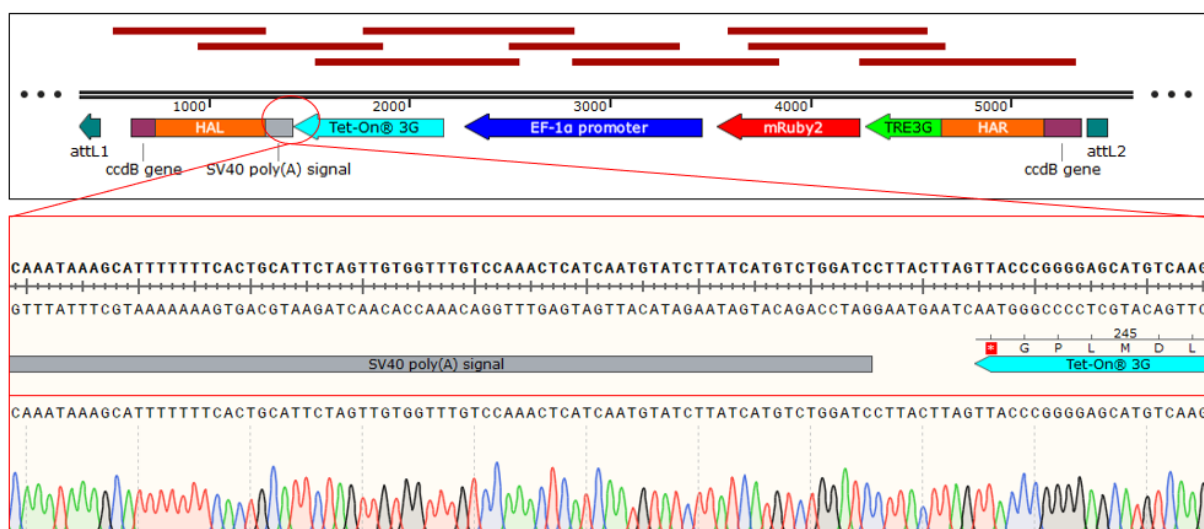


Figure 23: Sequencing results of the HDR template 2.0. The sequencing primers are the same primers used in figure 18. **Top panel)** Schematic overview of the sequencing results. The brown bars represent overlap with the simulated sequence, confirming successful insertion the HAL, EF1 α promoter and TetOn3G including the SV40 poly(A) tail. **Bottom panel)** Sequencing details of the transition between TetOn3G gene and the SV40 poly(A) tail. The simulated double-stranded DNA sequence is shown at the top. The results (graph at the bottom) are identical to simulated sequence.

3.4.1 Transient transfection HDR template 2.0

The HDR template 2.0 (including the poly(A) tail after the TetOn3G protein) was tested in a transient transfection. HESCs were transfected with the HDR template 2.0 and the mRubyII-N1 plasmid (as positive control). Expression of the mRubyII-N1 plasmid was shown both 24 h and 48 h after transfection (**Supplementary figure 6**). However, no fluorescence was observed in the inducible HDR template 2.0 after doxycycline stimulation (100 - 2000 ng/ml for 48 h), suggesting that the presence of the poly(A) tail after the TetOn3G does not improve mRuby2 expression in the inducible construct.

3.5 HDR (ChR2-EYFP) template

One of the main advantages of the designed HDR construct is that any gene can be inserted at the location of the mRuby2 gene. The restriction sites XmaJI (AvrII) and SgsI (Ascl) on both sites of the mRuby2 gene allow easy replacement of the mRuby2 gene. In this case, the ChR2-EYFP was inserted in the HDR template for doxycycline-inducible expression of ChR2 (**Figure 24**). The EYFP is connected to the C-terminus of ChR2 to provide a fluorescent tag for visualization of the fusion construct.

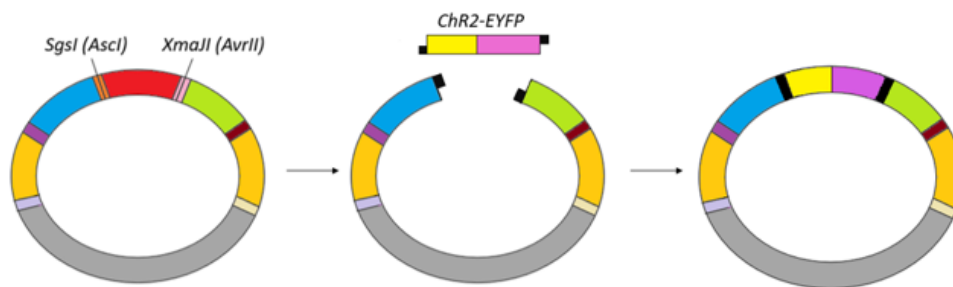


Figure 24: Schematic overview of the two restriction sites on both sites of mRuby2 in the HDR template. Restriction enzyme digestion creates a linear construct with sticky-ends. The ChR2-EYFP fragment is generated by sticky-end PCR, which generates PCR products containing cohesive ends compatible with the restriction sites XmaJI (AvrII) and SgsI (Ascl). This facilitates the insertion of the ChR2-EYFP fragment into the HDR template.

3.5.1 HDR (ChR2-EYFP) template generation

The HDR template¹ for doxycycline-inducible expression of mRuby2 was digested with the SgsI (Ascl) and XmaJI (AvrII) restriction enzymes, resulting in the removal of the mRuby2 gene (**Figure 25, left panel**). The digested plasmid was extracted, checked on gel and compared with the complete HDR template and linearized HDR template (**Figure 25, right panel**). The results suggested successful removal of mRuby2 from the HDR template.

The plasmid tol2-CAG::ChR2-YFP (Addgene #59740) was isolated from bacteria and sent for Sanger sequencing. This plasmid contains human CHR2(H134R) carrying a single point mutation at position 134 (histidine to arginine). This gain-of-function mutation generates larger photocurrents

¹ The HDR template used for the ligation of ChR2-EYFP in the HDR template does not contain the poly(A) tail behind the TetOn3G gene. Sticky-end PCR cloning was performed before the “HDR template 2.0” was produced.

than wild-type Chr2 [43,50]. The presence of Chr2-EYFP within the plasmid was confirmed with Sanger sequencing (**Figure 26, top and middle panel**). A small part of the sequence before the Chr2 could not be sequenced, but it was assumed that the sequence matches the sequencing results deposited on the Addgene website. Three different sets of sticky-end PCR primers were developed and tested. PCR with all primer sets resulted in a single sharp band of the correct size on agarose gel (results not shown). One set of sticky-end primers was chosen (**Figure 26, bottom panel**).

The Chr2-EYFP fragments were successfully amplified by PCR using primers 1 and 3, and primers 2 and 4 (**Figure 27, left panel**). The fragments were isolated from the agarose gel and were mixed in equimolar concentrations, followed by denaturation and annealing. This means that 25% of the final products carry cohesive ends compatible with the overhangs generated by the Sgsl (Ascl) and XmaJI (AvrII) restriction digestion of the HDR template (**Figure 27, right panel**). The Chr2-EYFP fragment was ligated into the HDR template without mRuby2. The plasmid with the inserted Chr2-EYFP fragment was transformed in TOP10 competent *E. coli* cells. Two bacterial colonies were selected and the plasmids were isolated and subsequently analysed with restriction enzyme digestion and PCR (**Figure 28, data shown for one plasmid**). Restriction enzyme digestion showed DNA fragments corresponding with the simulated digestions (**Figure 28, right panel number 1 and 2**). The presence of the Chr2-EYFP fragment was confirmed by PCR (**Figure 28, right panel number 3**) and Sanger sequencing (**Figure 29**).

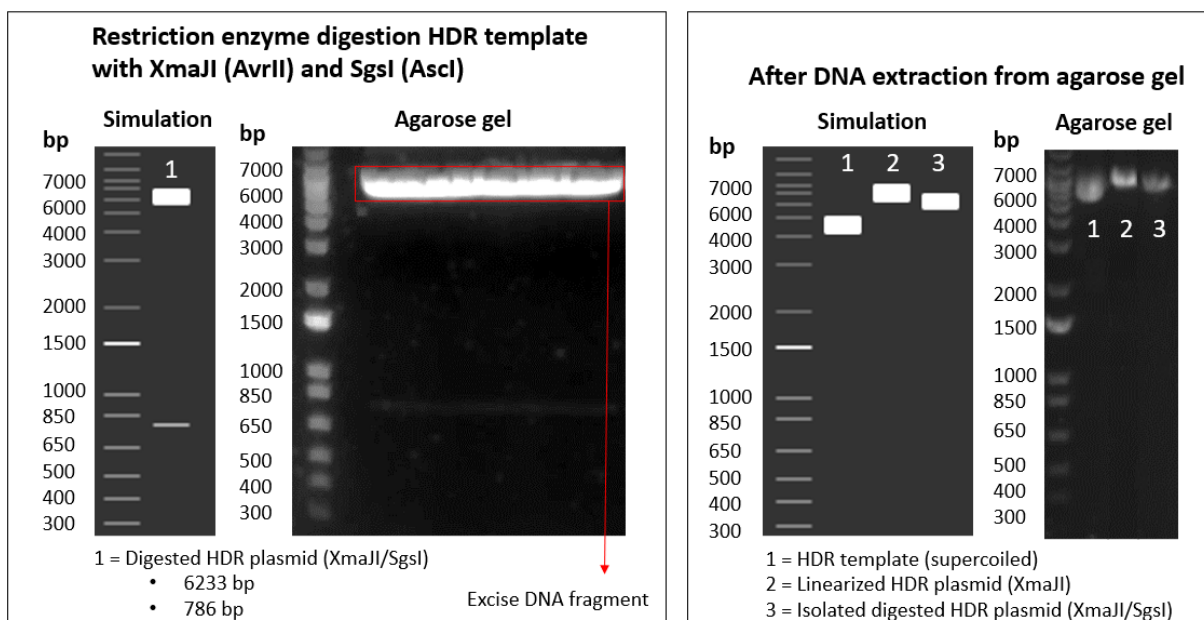


Figure 25: Left panel) The HDR plasmid with was digested with the restriction enzymes XmaJI (AvrII) and Sgsl (Ascl), resulting in the removal of mRuby2 from the HDR template. The digested plasmid (6233 bp) was extracted from the agarose gel. **Right panel)** Comparison between the complete HDR template (number 1), linearized plasmid with the XmaJI (AvrII) restriction enzyme (number 2) and isolated plasmid after XmaJI (AvrII) and Sgsl (Ascl) digestion (number 3).



Figure 26: Top panel) The Chr2-EYFP fusion fragment within the *tol2-CAG::Chr2-YFP* plasmid was sequenced with six different sequencing primers. **Middle panel)** Schematic overview of the sequencing results. The brown bars represent overlap with the simulated sequence, confirming correct sequence of Chr2-EYFP. **Bottom panel):** Sticky-end primers used for amplification of Chr2-EYFP². The primer overhangs are compatible with the overhangs generated by the *SgsI* (*Ascl*) and *XmaI* (*AvrII*) restriction digestion of the HDR template.

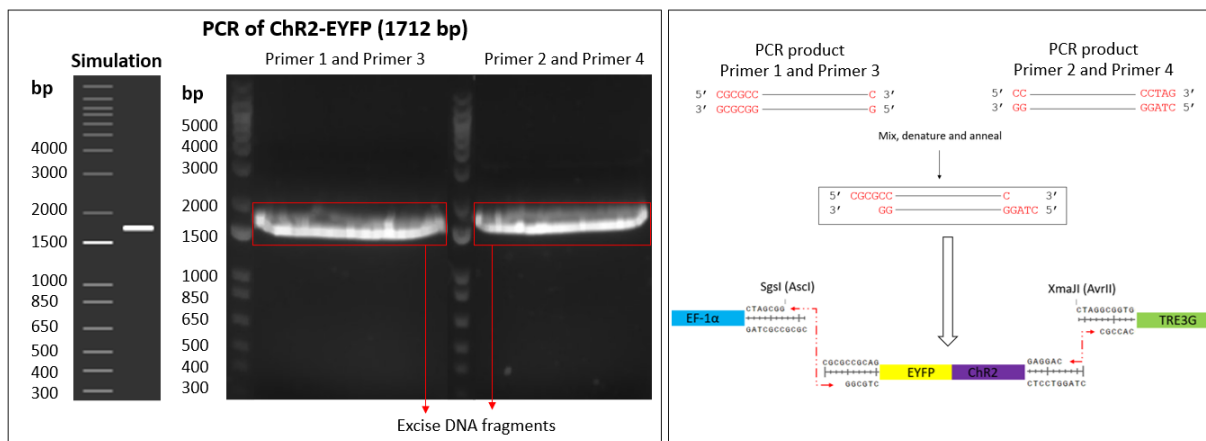


Figure 27: Left panel) Results of the PCR reaction of Chr2-EYFP using primers 1 and 3, and primers 2 and 4. The fragments (1712 bp) were extracted from the agarose gel. **Right panel)** The PCR products were mixed, denatured and annealed. One-quarter of the final product contains sticky-ends ends which can be ligated into the HDR template.

² The designed sticky-end primers did not amplify the bGH poly(A) tail behind the EYFP gene. New sticky-end PCR primers for amplification of Chr2-EYFP with poly(A) after EYFP were designed and ordered (**Supplementary experimental procedures**).

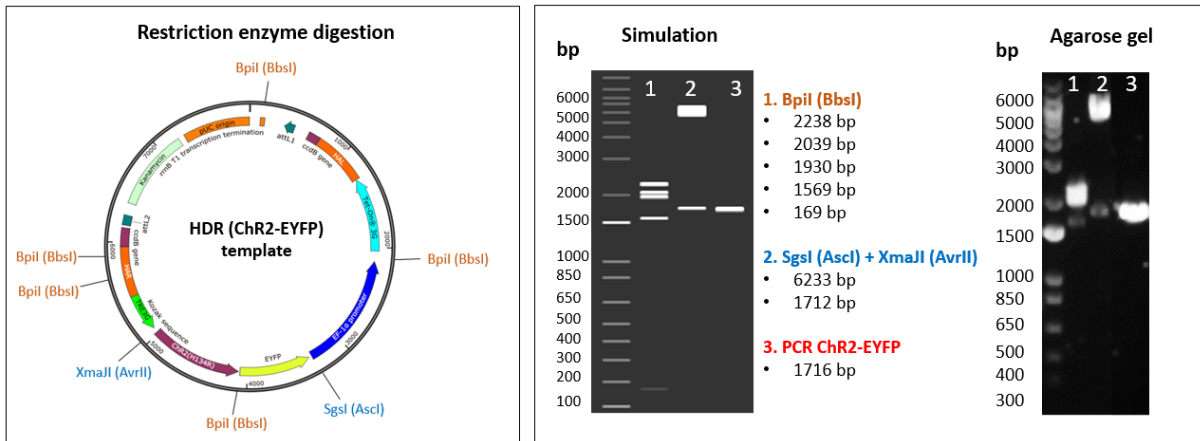


Figure 28: Right panel) The restriction sites *Bpil* (*BbsI*), *XmaII* (*AvrII*) and *SgsI* (*AscI*) are shown in the HDR template with *ChR2* (purple) and *EYFP* (yellow). **Right panel)** Results of the restriction enzyme digestion and PCR of *ChR2-EYFP*. The size of the fragments corresponds to the simulated data, suggesting that the *ChR2-EYFP* fragment is inserted in the HDR template.

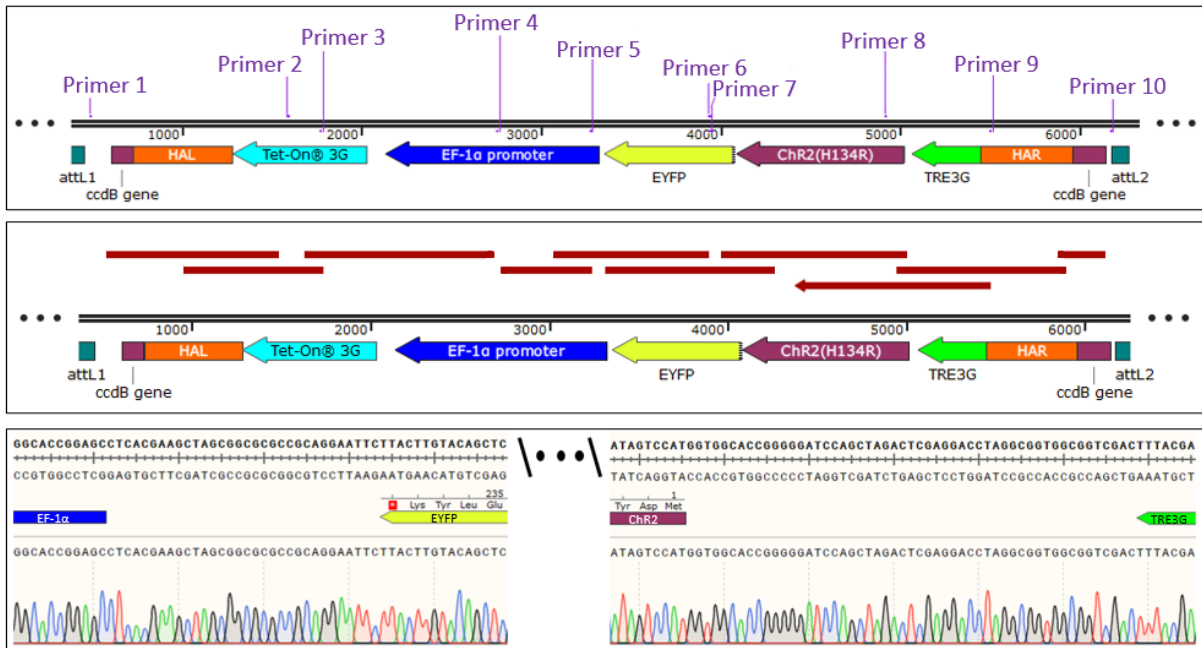


Figure 29: Top panel) The HDR (*ChR2-EYFP*) template was sequenced with ten primers. **Middle panel)** Schematic overview of the sequencing results. Insertion of *ChR2-EYFP* was confirmed (brown bars represent a match with the simulated sequence). **Bottom panel)** Sequencing details of the transition between *EF1α* promoter and *EYFP* and the transition between *TRE3G* and *ChR2*. The simulated double-stranded DNA sequence is shown at the top and the sequencing results are shown at the bottom.

3.5.2 Transient transfection HDR (ChR2-EYFP) plasmid

The tol2-CAG::ChR2-YFP plasmid (as a positive control) and HDR (ChR2-EYFP) plasmid were tested in a transient transfection to evaluate YFP expression. The tol2-CAG::ChR2-YFP plasmid showed bright YFP expression 48 h after transfection in hESC (**Figure 30**). The HDR (ChR2-EYFP) plasmid showed some YFP positive cells after doxycycline stimulation (100 ng/ml for 30 h). However, the intensity and number of positive cells in the HDR (ChR2-EYFP) plasmid after doxycycline stimulation (100 ng/ml for 30 h) is lower compared to the positive control (**Figure 30**).

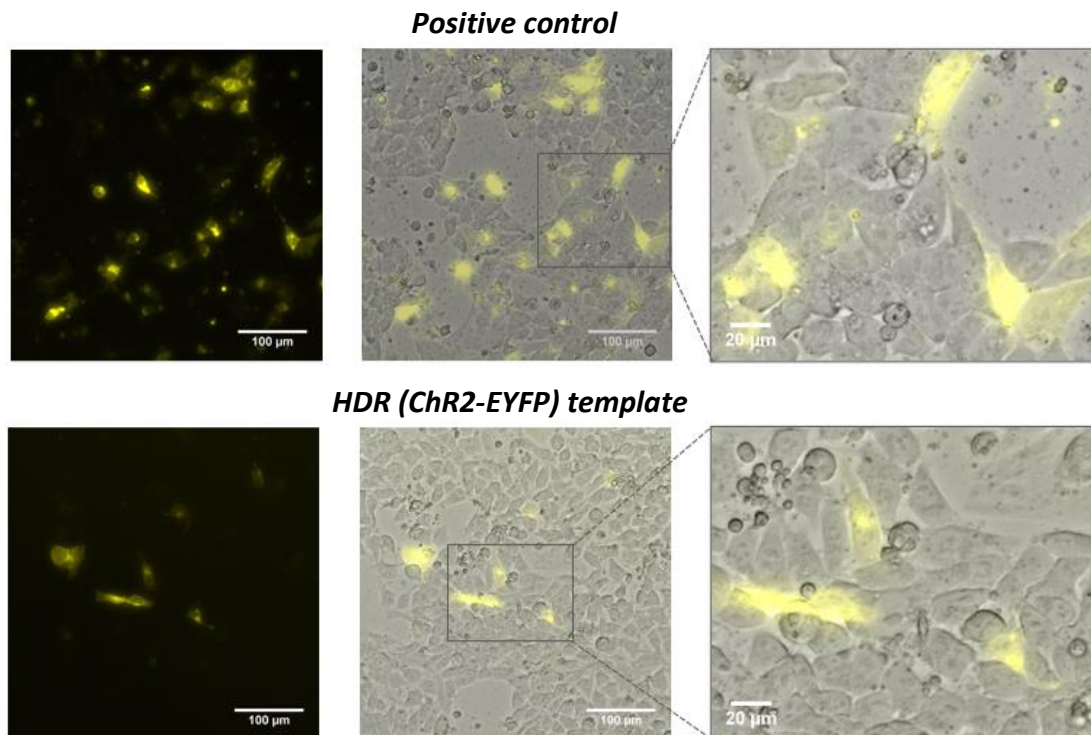


Figure 30: Enhanced yellow fluorescent protein (EYFP) expression in hESCs 48 h after transfection with **A)** tol2-CAG::ChR2-YFP plasmid (as a positive control) and **B)** the doxycycline-inducible HDR (ChR2-EYFP) template. The HDR template was stimulated with 100 ng/ml doxycycline for 30 h. The intensity of EYFP signal and the number of EYFP positive cells is lower in the HDR template compared to the positive control.

4. Discussion

HiPSCs-CMs represent a promising cell source in cardiac research [9,51,52] and the development of genome editing technologies such as CRISPR-Cas9 extended the possibilities even more [18]. CRISPR-Cas9 is rapidly becoming the most popular choice of site-specific gene editing. It has been shown that CRISPR-Cas9 genome editing is superior to TALENs and ZFNs in the targeted introduction of exogenous DNA [53,54]. In this study, it was attempted to insert a construct for doxycycline-inducible fluorescent protein expression in the AAVS1 GSH locus of hPSCs by CRISPR-Cas9 mediated HDR. The inducible construct can be utilized to rapidly create a new hPSC line with any genetic alteration of interest, such as fluorescent reporter constructs. Fluorescent PSC reporter lines play an important role in cardiac research. Fluorescent reporters have been shown to contribute to a better understanding of molecular mechanisms involved in differentiation of PSCs towards CMs and to their applications in cardiac diseases, such as cell-based therapies, drug discovery and toxicity screenings [55]. For example, it was shown that insertion of a fluorescent reporter coupled to the transcription factor COUP-TFII (using CRISPR-Cas9 gene editing) in hPSC-CMs allows identification and selection of atrial and ventricular CMs, since PSC differentiation to CMs yields heterogeneous CM populations [49]. Furthermore, reporter genes allow fast and straightforward visualization of exogenous genes, such as exogenously introduced Chr2 coupled to EYFP [56].

4.1 HDR template construction

In order to introduce the doxycycline-inducible construct in the genome of PSC, three different sgRNA-Cas9 plasmids targeting the AAVS1 locus were designed and characterized [47], increasing the chance of acquiring a successfully targeted stem cell line. The inducible construct consists of five different fragments, the HAL, EF1 α -TetOn3G, TRE3G, mRuby2 and HAR, which were inserted in the backbone vector by In-Fusion[®] cloning. Previous attempts to insert the five different parts of the template in one step failed, likely because of the large number of DNA fragments used in a single cloning reaction [47,57]. This study showed successful synthesis and characterization of the inducible construct by a two-step In-Fusion[®] cloning mechanism.

One of the major advantages of this construct is the use of a doxycycline-inducible promoter, which allows high quantitative and temporal control of gene expression [58]. Several studies reported the utilization of doxycycline-inducible gene expression in (PSC derived) CMs. For example, doxycycline-inducible systems were used to induce pluripotency in human ventricular CMs [59] or to enhance cardiac and pacemaker cell differentiation from stem cells [60]. Moreover, it proved a valuable genetic tool for the analysis of spatiotemporal gene function and CM lineage tracing during development [61], and was applied to study mechanisms of cardiac hypertrophy [62,63].

4.2 CRISPR-Cas9-mediated targeting in PSCs

In this study, both hESC and hiPSC were co-transfected with the inducible construct and sgRNA-Cas9 plasmid to validate mRuby2 expression after stable integration in the AAVS1 locus. The chemical transfection reagent lipofectamine was used to introduce the HDR template and Cas9 plasmid in PSCs. The transfection was performed with three different sgRNAs and different HDR template concentrations. Moreover, various doxycycline concentrations and stimulation times were tested to induce the expression of mRuby2.

4.2.1 HiPSCs

After puromycin selection, hiPSC survival was highest in the cells transfected with the inducible construct and sgRNA3, so it was decided to continue with this sgRNA condition. The targeted hiPSCs were treated with doxycycline, which appeared to result in a positive and negative mRuby2 population as shown by flow cytometry. However, there was no negative control (hiPSCs without doxycycline stimulation) incorporated in the flow cytometry measurement, which means that mRuby2 expression could not be confirmed. Nevertheless, the mRuby2-positive cells were sorted and plated for further analysis, but unfortunately these cells were lost due to a bacterial contamination.

Flow cytometry measurement showed that the size of the positive mRuby2 population is quite small, suggesting low transfection efficiency. The cells transfected with low (3 μ g) HDR template concentration resulted in 1.35% mRuby2-positive cells and high (4.5 μ g) HDR template concentration resulted in 1.64% mRuby2-positive cells. Some studies showed that increasing the distance between the insert and the cut site larger than 10 bp decreases HDR efficiency [64,65]. The distance from the insert to the DSB is 18 bp in case of sgRNA3, which may have caused a low HDR efficiency. Another factor that can contribute to HDR efficiency is the length of the homology arms. Byrne et al. reported that the optimal length of homology arms is around 2 kb in case of HDR-mediated gene targeting in hiPSCs [66]. However, the homology arms used in this study are much shorter, around ~550 bp in length. The length is based on the studies of Han Li et al. and Zhang et al., which reported that the optimal length of the homology arms ranges from 350-700 bp [67] and increasing the homology arm length only slightly enhances HDR [68]. Furthermore, it appears that the length of the homology arms is less important than quality control of the targeted cells [69], so therefore the length of homology arms was chosen to be ~550 bp in length. PCR screening showed the presence of the EF1 α -TetOn3G, TRE3G and mRuby2 fragments in the genomic DNA of hESC targeted cells, suggesting that ~550 bp homology arms are sufficient to achieve integration in the AAVS1 locus.

4.2.2 HESCs

In parallel to targeting the doxycycline-inducible construct in hiPSCs, targeting in hESCs was also performed, because previous work showed successful insertion of fluorescent reporter in hESCs with CRISPR-Cas9 mediated HDR [49]. Transfection with “cold shock” conditions (32 °C and 5% CO₂) was

compared to transfection at normal cell culture conditions (37 °C and 5% CO₂), since Guo et al. reported that “cold shock” transfection enhanced HDR rates two- to ten-fold in iPSCs [70]. This study showed that “cold shock” transfection was superior in cell survival compared to transfection at 37 °C after puromycin selection, suggesting that transfection efficiency was higher with “cold shock”. However, subsequent doxycycline treatment following CRISPR-Cas9-mediated insertion of the inducible mRuby2 in hESCs did not result in mRuby2 expression, as determined with flow cytometry. Surprisingly, PCR screening showed successful insertion of the EF1 α -TetOn3G, TRE3G and mRuby2 fragments in the genomic DNA. The cells were treated with doxycycline in a concentration range from 10 ng/ml to 2 μ g/ml for 24 h and 48 h. Numerous studies reported similar concentrations and stimulation times [71-74], so it is likely that doxycycline stimulation is not the limiting factor. Doxycycline concentration of 10 μ g/ml was also tested to induce mRuby2 expression, but this concentration led to cytotoxic effects which was also previously reported [75].

In order to evaluate fluorescent expression of the inducible construct, a transient transfection in hESCs (without integration in the AAVS1 locus) was performed. The doxycycline-inducible mRuby2 signal was very low compared to the positive control (a constitutively expressed mRuby2 plasmid) and difficult to distinguish from background signal. Concluding, this study successfully showed the insertion of a construct for doxycycline-inducible mRuby2 expression in the AAVS1 GSH locus of hPSCs by CRISPR-Cas9 mediated HDR. Unexpectedly, doxycycline treatment did not result in mRuby2 expression, suggesting that the inducible construct is not functioning.

4.3 Poly(A) tail

The construct was extensively screened and it was observed that the poly(A) tail after the TetOn3G gene was missing, which was possibly the cause of the absence of fluorescent signal. The poly(A) tail is important for stability of the mRNA, regulate mRNA transport from the nucleus [76] and promote translation initiation [77]. It has been shown that the poly(A) tail strongly influences transgene expression [78] and transgenes with poly(A) tail are up to 10 times more active than transgenes without polyadenylation [76]. The absence of the poly(A) tail after the TetOn3G gene might explain why the expression of mRuby2 is not (or in limited amount) induced by doxycycline. Therefore, a new construct (HDR template 2.0) was successfully made with a SV40 poly(A) tail after the TetOn3G gene.

The HDR template 2.0 (including the poly(A) tail after the TetOn3G protein) did still not result in fluorescent expression of mRuby2 in a transient transfection experiment after stimulation with various concentrations of doxycycline for 24 h - 72 h. Close observation of the inducible construct does not reveal any abnormalities in the sequences of the different fragments, although there is one residue (tyrosine) added at the C-terminal of the mRuby2 fragment before the stop codon (because of the In-Fusion[®] cloning primer design) compared to the mRuby2 sequence present in the commercially

available mRubyII-N1 plasmid (Addgene #54614). The effects of the addition of this amino acid are unknown, but is expected that it does not influence fluorescent expression. Furthermore, there is a SV40 poly(A) tail present 121 bp after the mRuby2 gene in the mRubyII-N1 plasmid, but mRuby2 expression without poly(A) tail is also reported (Addgene #59148) [79]. Another parameter is the distance between the TRE3G promoter and mRuby2 gene, which is 27 bp (and 21 bp including Kozak sequence). In literature distances of the TRE3G promoter to the functional gene are reported in the same range (from 6 bp [80] to 35 bp [81]), so this should not be a problem. Further investigation is required to determine the cause of the absence of fluorescent expression.

4.4 Channelrhodopsin

The inducible construct developed in this study has the unique capability to exchange the inducible transgene. The restriction sites on both sites of the inducible mRuby2 gene allows the incorporation of any intended gene in the construct, such as ChR2. Various studies reported the introduction of ChR2 into ESCs followed by differentiation into CMs [56,82,83], which can be used for different cardiac optogenetics applications [41]. One of the applications is the development of high-throughput assays that use light-based actuation to study electrophysiological properties of ChR2-expressing CMs *in vitro* and *in vivo* [45]. Furthermore, optogenetics has been used to disturb cardiac tissue rhythm to investigate the mechanism of arrhythmia [45]. These applications highlight the possibilities of the insertion of ChR2 into PSCs in cardiac research.

This study showed the exchange of the mRuby2 gene with the ChR2-EYFP fusion by sticky-end PCR cloning. Sticky-end PCR cloning is a simple and versatile approach to clone genes into plasmids without restriction enzyme digestions of the PCR products required for traditional restriction cloning [84]. The HDR (ChR2-EYFP) template were transiently transfected in hESCs to evaluate YFP expression. There were a few YFP positive cells visible after doxycycline stimulation. Surprisingly, compared to mRuby2 expression, the intensity of EYFP expression was much higher, even though the poly(A) tail after the TetOn3G protein and EYFP were missing. This suggests that the exchange with mRuby2 by EYFP in the inducible construct increased fluorescent protein expression.

4.5 AAVS1 GSH location

In this study the AAVS1 locus was chosen as location of transgene insertion because the AAVS1 locus is extensively studied as a GSH location [32,33]. Multiple studies showed stable, long term transgene expression in ESCs and iPSCs [36,37,85]. For example, Yu et al. reported that GFP expression levels were stable in ESC-derived CMs in which the DNA fragment containing GFP was inserted into the AAVS1 locus of the PPP1R12C gene of ESCs [85]. Despite the promising data of the AAVS1 GSH, unexpected and variable transgene expression inhibition was also observed in hESCs, indicating that the AAVS1 cannot be considered as a universally GSH location for faithful transgene expression [86]. Furthermore,

it was shown that robust AAVS1 targeted transgene expression in hiPSCs was silenced upon differentiation to hiPSC-CMs [87]. If it appears that the insertion of the inducible construct (with mRuby2 or Chr2-EYFP) in the AAVS1 location resulted in transgene silencing in hPSCs or hPSC-CMs, it might be better to choose a different GSH location.

Recently, the citrate lyase beta-like (CLYBL) locus was reported as a promising GSH [88]. CLYBL lies in a gene-deficient region on chromosome 13 (13q32.2) and was one of the identified random integration hot spots of the phage-derived phiC31 integrase [89]. CLYBL is a mitochondrial enzyme with unknown function with the highest expression in brown fat and kidney [90]. Although the CLYBL locus is less studied compared to the AAVS1 locus, it was reported that transgene expression in intron 2 of the CLYBL locus resulted in 5~10-times higher transgene expression than the AAVS1 locus in human hiPSCs and the transgene expression was maintained during self-renewal and differentiation into hiPSCs-CMs [88]. Transgene integration in the CLYBL locus has minimal effects on global and local gene expression, whereas the integration of the transgene in PPP1R12C resulted in upregulation of the oncogenes NLRP2 with 3.5-fold and PTPRH with 3.0-fold [88]. This indicate that the CLYBL locus might be more promising as GSH than the AAVS1 locus.

5. Experimental recommendations and future outlook

Unfortunately, multiple attempts of introducing a construct for doxycycline-inducible fluorescent protein expression in the AAVS1 GSH locus of hPSCs did not result in visible fluorescent protein expression. It was shown that EF1 α -TetOn3G, TRE3G and mRuby2 were inserted in the genome of PSCs by PCR, suggesting successful integration in the genome. Unexpectedly, no fluorescence was observed after stimulation with doxycycline. The addition of a SV40 poly(A) tail after the TetOn3G gene did still not result in an increase in fluorescent signal. Therefore, several recommendations to achieve successful inducible expression of mRuby2 in the AAVS1 locus are described below.

5.1 Towards successful targeting of hPSCs with the inducible construct

It is recommended to validate mRNA and protein expression levels of the different genes present in the inducible construct after transfection. The mRNA levels of the TRE3G promoter, the constitutively active promoter EF1 α , the TetOn3G protein and mRuby2 can be determined by qPCR. The TetOn3G protein expression can be detected and measured in a western blot, using the commercially available TetR monoclonal antibody (Takara Bio).

Furthermore, it could be useful to make a new construct amplifying the TRE promoter and fluorescent gene from the same plasmid. Commercially available plasmids such as pAAV-TRE-mRuby2 (Addgene #99114) and AAVS1-TRE3G-EGFP (Addgene #52343) showed successful doxycycline induced expression of mRuby2 and EGFP respectively [80,91]. Those plasmids contain a fluorescent protein behind the TRE promoter, so it is already established that the construct is working. Another option is to construct a HDR template without the doxycycline-inducible part to constitutively express a fluorescent protein. This can help in fast evaluation of transgene integration in the AAVS1 locus. Thereafter, the construct can be easily adapted to make it doxycycline-inducible.

The final and most straightforward option is to directly start with targeting of the inducible HDR (Chr2-EYFP) template in hPSCs, instead of using the doxycycline-inducible mRuby2 construct. Since the intensity of inducible EYFP expression was much higher than mRuby2 expression, it is recommended to use the HDR (Chr2-EYFP) template to evaluate transgene insertion and expression in the AAVS1 locus of hPSCs and hPSC-CMs.

5.2 Increase HDR efficiency

After co-transfection of this HDR construct with the sgRNA-Cas9 plasmid, HDR efficiency can be evaluated based on fluorescent signal. Because the HDR efficiency was not determined in this study, several recommendations are described to increase transgene insertion in case of low HDR efficiency (< 5%). Improving the HDR efficiency is currently a major topic in CRISPR-Cas9 genome editing and various strategies have been developed [92-95], including the addition of small molecules that promote HDR either directly or indirectly interfere with several steps of NHEJ. One of the

strategies that can be readily implemented to improve HDR efficiency is the use of a linearized HDR plasmid [96-98]. Another possibility is to use a HDR template selection marker besides the sgRNA-Cas9 plasmid puromycin selection marker to select dual-transfected cells, increasing the chance of selecting HDR modified cells. It might also be worthwhile to test an HDR template with increased homology arm sizes. The insert (EF1 α -TetOn3G, TRE3G and mRuby2) is quite large (~3.2 kb) and Li et al. reported that increasing homology arm size can compensate for increased insert size [99]. However, it should be kept in mind that the presence of long homology arms, while enhancing the targeting efficiency, also increases random integration [100].

5.3 Future outlook

After targeting hPSCs with the inducible ChR2-EYFP construct, the fluorescent cells will be sorted and clonally expanded. If the doxycycline-inducible ChR2 gene is successfully inserted into the AAVS1 GSH locus of hPSCs, the new clonal cell line will be differentiated towards hPSC-CMs to validate if inducible expression is also present in hPSC-CMs. This should enable optogenetic pacing of the hPSC-CMs. Laser light or LEDs are commonly used light sources for optical stimulation of ChR2, whereas monitoring of the response of hPSC-CMs can be done by both electrophysiological readouts and optical readouts [41]. One of the future applications is the combination of ChR2 expressing hiPSC-CMs with of engineered heart tissues (EHTs), which allows the optical stimulation of 3D advanced cardiac models. In those EHTs, PSCs-CMs are combined with fibroblast (or other cardiac related cells) in a hydrogel and transferred to a casting mold with elastic micropillars. EHTs can be used for studying basic features of cardiac muscle tissue, disease modeling, *in vitro* drug testing and regenerative medicine [101-105], because the EHTs resemble better the native heart. The enhanced maturation of CMs compared to a standard 2D culture may be one of the reasons [101,106,107]. As example, optical stimulation of ChR expressing CMs improved EHT maturity and increased electrophysiological properties [108]. Furthermore, chronic optical tachypacing of hiPSC-CMs in EHTs can be used to study the development and mechanism of arrhythmia and to test anti-arrhythmic drugs [109].

Besides ChR2, another example of an important target in cardiac research is the Myocyte Enhancer Factor 2 (MEF2) transcription factor. This transcription factor plays an important role in cardiac development and differentiation [110,111]. However, activation of MEF2 is also involved in cardiac hypertrophy and pathological cardiac remodelling, although the underlying mechanisms remain poorly understood [112,113]. Different studies measured the MEF2 transcriptional activity using a reporter gene under the control of copies of the desmin MEF2 DNA-binding site in cardiomyoblasts [114], CMs [115,116] and transgenic mice [117]. The MEF2 binding site can be inserted in the HDR construct before a fluorescent protein gene. In this way, activity of MEF2 can be measured using fluorescent signal after integration of the construct within the AAVS1 locus.

6. Conclusion

This study describes the production of a doxycycline-inducible construct intended for CRISPR-Cas9-mediated HDR, with the aim to create a new hPSC line with any gene of interest involved in cardiac research. The inducible construct was synthesized by a two-step In-Fusion® cloning mechanism. The EF1 α promoter provides consistent long-term expression of the TetOn3G transactivator protein. This TetOn3G protein can bind to the TRE3G promoter in the presence of doxycycline, which allows high quantitative and temporal control of mRuby2 gene expression. A main advantage of the inducible construct is that any gene can be inserted instead of the mRuby2 gene due to restriction sites on both sites of mRuby2. This study showed the replacement of mRuby2 by the gene encoding for Chr2 by sticky-end PCR cloning. PSCs were co-transfected with the inducible mRuby2 construct and sgRNA-Cas9 plasmid targeting the AAVS1 GSH locus, which is a suitable location for stable integration of transgenes. It was shown that the Cas9 nuclease made a DSB at the location determined by the 20-nucleotide guide sequence within the sgRNA and PCR screening suggested successful insertion of the EF1 α -TetOn3G, TRE3G and mRuby2 genes in the AAVS1 location. Surprisingly, doxycycline treatment did not result in fluorescent mRuby2 signal, with or without the presence of the poly(A) tail after the TetOn3G gene. Concluding, this study showed the development and insertion of a doxycycline-inducible construct in the AAVS1 GSH locus of hPSCs by CRISPR-Cas9 mediated HDR. Unexpectedly, doxycycline treatment did not result in mRuby2 expression and the reason of the absence of signal requires further investigation.

References

1. Roth, G.A.; Mensah, G.A.; Johnson, C.O.; Addolorato, G.; Ammirati, E.; Baddour, L.M.; Barengo, N.C.; Beaton, A.Z.; Benjamin, E.J.; Benziger, C.P.; et al. Global Burden of Cardiovascular Diseases and Risk Factors, 1990–2019: Update From the GBD 2019 Study. *Journal of the American College of Cardiology* **2020**, *76*, 2982–3021, doi:<https://doi.org/10.1016/j.jacc.2020.11.010>.
2. Cohn, J.N.; Ferrari, R.; Sharpe, N. Cardiac remodeling—concepts and clinical implications: a consensus paper from an international forum on cardiac remodeling. *Journal of the American College of Cardiology* **2000**, *35*, 569–582, doi:[https://doi.org/10.1016/S0735-1097\(99\)00630-0](https://doi.org/10.1016/S0735-1097(99)00630-0).
3. Azevedo, P.S.; Polegato, B.F.; Minicucci, M.F.; Paiva, S.A.R.; Zornoff, L.A.M. Cardiac Remodeling: Concepts, Clinical Impact, Pathophysiological Mechanisms and Pharmacologic Treatment. *Arq Bras Cardiol* **2016**, *106*, 62–69, doi:10.5935/abc.20160005.
4. Lippi, M.; Stadiotti, I.; Pompilio, G.; Sommariva, E. Human Cell Modeling for Cardiovascular Diseases. *Int J Mol Sci* **2020**, *21*, 6388, doi:10.3390/ijms21176388.
5. Jimenez-Tellez, N.; Greenway, S.C. Cellular models for human cardiomyopathy: What is the best option? *World J Cardiol* **2019**, *11*, 221–235, doi:10.4330/wjc.v11.i10.221.
6. Moretti, A.; Laugwitz, K.-L.; Dorn, T.; Sinnecker, D.; Mummery, C. Pluripotent stem cell models of human heart disease. *Cold Spring Harb Perspect Med* **2013**, *3*, a014027, doi:10.1101/cshperspect.a014027.
7. Fan, C.; Zhang, E.; Joshi, J.; Yang, J.; Zhang, J.; Zhu, W. Utilization of Human Induced Pluripotent Stem Cells for Cardiac Repair. *Frontiers in Cell and Developmental Biology* **2020**, *8*, doi:10.3389/fcell.2020.00036.
8. Guadix, J.A.; Orlova, V.V.; Giacomelli, E.; Bellin, M.; Ribeiro, M.C.; Mummery, C.L.; Pérez-Pomares, J.M.; Passier, R. Human Pluripotent Stem Cell Differentiation into Functional Epicardial Progenitor Cells. *Stem Cell Reports* **2017**, *9*, 1754–1764, doi:10.1016/j.stemcr.2017.10.023.
9. Musunuru, K.; Sheikh, F.; Gupta, R.M.; Houser, S.R.; Maher, K.O.; Milan, D.J.; Terzic, A.; Wu, J.C. Induced Pluripotent Stem Cells for Cardiovascular Disease Modeling and Precision Medicine: A Scientific Statement From the American Heart Association. *Circulation: Genomic and Precision Medicine* **2018**, *11*, e000043, doi:10.1161/HCG.0000000000000043.
10. Csöbönyeiová, M.; Polák, Š.; Danišovič, L. Perspectives of induced pluripotent stem cells for cardiovascular system regeneration. *Exp Biol Med (Maywood)* **2015**, *240*, 549–556, doi:10.1177/1535370214565976.
11. Rikhtegar, R.; Pezeshkian, M.; Dolati, S.; Safaie, N.; Afrasiabi Rad, A.; Mahdipour, M.; Nouri, M.; Jodati, A.R.; Yousefi, M. Stem cells as therapy for heart disease: iPSCs, ESCs, CSCs, and skeletal myoblasts. *Biomedicine & Pharmacotherapy* **2019**, *109*, 304–313, doi:<https://doi.org/10.1016/j.biopha.2018.10.065>.
12. Romito, A.; Cobellis, G. Pluripotent Stem Cells: Current Understanding and Future Directions. *Stem cells international* **2016**, *2016*, 9451492–9451492, doi:10.1155/2016/9451492.
13. Shi, Y.; Inoue, H.; Wu, J.C.; Yamanaka, S. Induced pluripotent stem cell technology: a decade of progress. *Nature Reviews Drug Discovery* **2017**, *16*, 115–130, doi:10.1038/nrd.2016.245.
14. Rowe, R.G.; Daley, G.Q. Induced pluripotent stem cells in disease modelling and drug discovery. *Nature Reviews Genetics* **2019**, *20*, 377–388, doi:10.1038/s41576-019-0100-z.
15. Yang, C.; Al-Aama, J.; Stojkovic, M.; Keavney, B.; Trafford, A.; Lako, M.; Armstrong, L. Concise Review: Cardiac Disease Modeling Using Induced Pluripotent Stem Cells. *STEM CELLS* **2015**, *33*, 2643–2651, doi:10.1002/stem.2070.
16. Matsa, E.; Burrridge, P.W.; Wu, J.C. Human stem cells for modeling heart disease and for drug discovery. *Sci Transl Med* **2014**, *6*, 239ps236–239ps236, doi:10.1126/scitranslmed.3008921.
17. Kishino, Y.; Fujita, J.; Tohyama, S.; Okada, M.; Tanosaki, S.; Someya, S.; Fukuda, K. Toward the realization of cardiac regenerative medicine using pluripotent stem cells. *Inflammation and Regeneration* **2020**, *40*, 1, doi:10.1186/s41232-019-0110-4.
18. Christidi, E.; Huang, H.; Brunham, L.R. CRISPR/Cas9-mediated genome editing in human stem cell-derived cardiomyocytes: Applications for cardiovascular disease modelling and cardiotoxicity screening. *Drug Discovery Today: Technologies* **2018**, *28*, 13–21, doi:<https://doi.org/10.1016/j.ddtec.2018.06.002>.
19. Carroll, D. Genome Editing: Past, Present, and Future. *Yale J Biol Med* **2017**, *90*, 653–659.
20. Gaj, T.; Gersbach, C.A.; Barbas, C.F., III. ZFN, TALEN, and CRISPR/Cas-based methods for genome engineering. *Trends in Biotechnology* **2013**, *31*, 397–405, doi:10.1016/j.tibtech.2013.04.004.

21. Ran, F.A.; Hsu, P.D.; Wright, J.; Agarwala, V.; Scott, D.A.; Zhang, F. Genome engineering using the CRISPR-Cas9 system. *Nat Protoc* **2013**, *8*, 2281-2308, doi:10.1038/nprot.2013.143.
22. Amitai, G.; Sorek, R. CRISPR-Cas adaptation: insights into the mechanism of action. *Nature Reviews Microbiology* **2016**, *14*, 67-76, doi:10.1038/nrmicro.2015.14.
23. Makarova, K.S.; Haft, D.H.; Barrangou, R.; Brouns, S.J.J.; Charpentier, E.; Horvath, P.; Moineau, S.; Mojica, F.J.M.; Wolf, Y.I.; Yakunin, A.F.; et al. Evolution and classification of the CRISPR-Cas systems. *Nature Reviews Microbiology* **2011**, *9*, 467-477, doi:10.1038/nrmicro2577.
24. Gleditsch, D.; Pausch, P.; Müller-Esparza, H.; Özcan, A.; Guo, X.; Bange, G.; Randau, L. PAM identification by CRISPR-Cas effector complexes: diversified mechanisms and structures. *RNA Biol* **2019**, *16*, 504-517, doi:10.1080/15476286.2018.1504546.
25. Jinek, M.; Chylinski, K.; Fonfara, I.; Hauer, M.; Doudna, J.A.; Charpentier, E. A Programmable Dual-RNA-Guided DNA Endonuclease in Adaptive Bacterial Immunity. *Science* **2012**, *337*, 816, doi:10.1126/science.1225829.
26. Liu, C.; Zhang, L.; Liu, H.; Cheng, K. Delivery strategies of the CRISPR-Cas9 gene-editing system for therapeutic applications. *J Control Release* **2017**, *266*, 17-26, doi:10.1016/j.jconrel.2017.09.012.
27. Chang, H.H.Y.; Pannunzio, N.R.; Adachi, N.; Lieber, M.R. Non-homologous DNA end joining and alternative pathways to double-strand break repair. *Nature Reviews Molecular Cell Biology* **2017**, *18*, 495-506, doi:10.1038/nrm.2017.48.
28. Mao, Z.; Bozzella, M.; Seluanov, A.; Gorbunova, V. Comparison of nonhomologous end joining and homologous recombination in human cells. *DNA Repair (Amst)* **2008**, *7*, 1765-1771, doi:10.1016/j.dnarep.2008.06.018.
29. Zhu, B.; Cai, G.; Hall, E.O.; Freeman, G.J. In-Fusion™ assembly: seamless engineering of multidomain fusion proteins, modular vectors, and mutations. *BioTechniques* **2007**, *43*, 354-359, doi:10.2144/000112536.
30. In-Fusion® Cloning: Accuracy, Not Background. *BioTechniques* **2018**, *64*, 189-191, doi:10.2144/btn-2016-0120.
31. CRISPR/Cas9: Homology-Directed Repair Available online: <https://sites.tufts.edu/crispr/genome-editing/homology-directed-repair/> (accessed on 06-10-2020).
32. Sadelain, M.; Papapetrou, E.P.; Bushman, F.D. Safe harbours for the integration of new DNA in the human genome. *Nature Reviews Cancer* **2012**, *12*, 51-58, doi:10.1038/nrc3179.
33. Papapetrou, E.P.; Schambach, A. Gene Insertion Into Genomic Safe Harbors for Human Gene Therapy. *Mol Ther* **2016**, *24*, 678-684, doi:10.1038/mt.2016.38.
34. Papapetrou, E.P.; Sadelain, M.; Bushman, F. Genomic Safe Harbors in Human iPS Cells. *Blood* **2011**, *118*, SCI-47-SCI-47, doi:10.1182/blood.V118.21.SCI-47.SCI-47.
35. Ramachandra, C.J.A.; Shahbazi, M.; Kwang, T.W.X.; Choudhury, Y.; Bak, X.Y.; Yang, J.; Wang, S. Efficient recombinase-mediated cassette exchange at the AAVS1 locus in human embryonic stem cells using baculoviral vectors. *Nucleic Acids Res* **2011**, *39*, e107-e107, doi:10.1093/nar/gkr409.
36. Oceguera-Yanez, F.; Kim, S.-I.; Matsumoto, T.; Tan, G.W.; Xiang, L.; Hatani, T.; Kondo, T.; Ikeya, M.; Yoshida, Y.; Inoue, H.; et al. Engineering the AAVS1 locus for consistent and scalable transgene expression in human iPSCs and their differentiated derivatives. *Methods* **2016**, *101*, 43-55, doi:<https://doi.org/10.1016/j.ymeth.2015.12.012>.
37. Smith, J.R.; Maguire, S.; Davis, L.A.; Alexander, M.; Yang, F.; Chandran, S.; French-Constant, C.; Pedersen, R.A. Robust, Persistent Transgene Expression in Human Embryonic Stem Cells Is Achieved with AAVS1-Targeted Integration. *STEM CELLS* **2008**, *26*, 496-504, doi:10.1634/stemcells.2007-0039.
38. Floria, M.; Radu, S.; Gosav, E.M.; Moraru, A.C.; Serban, T.; Carauleanu, A.; Costea, C.F.; Ouatu, A.; Ciocoiu, M.; Tanase, D.M. Cardiac Optogenetics in Atrial Fibrillation: Current Challenges and Future Opportunities. *BioMed Research International* **2020**, *2020*, 8814092, doi:10.1155/2020/8814092.
39. Joshi, J.; Rubart, M.; Zhu, W. Optogenetics: Background, Methodological Advances and Potential Applications for Cardiovascular Research and Medicine. *Frontiers in Bioengineering and Biotechnology* **2020**, *7*, doi:10.3389/fbioe.2019.00466.
40. Williams, J.C.; Entcheva, E. Optogenetic versus Electrical Stimulation of Human Cardiomyocytes: Modeling Insights. *Biophysical Journal* **2015**, *108*, 1934-1945, doi:10.1016/j.bpj.2015.03.032.
41. Ferenczi, E.A.; Tan, X.; Huang, C.L.-H. Principles of Optogenetic Methods and Their Application to Cardiac Experimental Systems. *Frontiers in Physiology* **2019**, *10*, doi:10.3389/fphys.2019.01096.
42. Jia, Z.; Valiunas, V.; Lu, Z.; Bien, H.; Liu, H.; Wang, H.-Z.; Rosati, B.; Brink, P.R.; Cohen, I.S.; Entcheva, E. Stimulating cardiac muscle by light: cardiac optogenetics by cell delivery. *Circ Arrhythm Electrophysiol* **2011**, *4*, 753-760, doi:10.1161/CIRCEP.111.964247.

43. Ambrosi, C.M.; Entcheva, E. Optogenetic control of cardiomyocytes via viral delivery. *Methods in molecular biology (Clifton, N.J.)* **2014**, *1181*, 215-228, doi:10.1007/978-1-4939-1047-2_19.
44. Johnston, C.M.; Rog-Zielinska, E.A.; Wülfers, E.M.; Houwaart, T.; Siedlecka, U.; Naumann, A.; Nitschke, R.; Knöpfel, T.; Kohl, P.; Schneider-Warme, F. Optogenetic targeting of cardiac myocytes and non-myocytes: Tools, challenges and utility. *Progress in Biophysics and Molecular Biology* **2017**, *130*, 140-149, doi:<https://doi.org/10.1016/j.pbiomolbio.2017.09.014>.
45. Boyle, P.M.; Karathanos, T.V.; Trayanova, N.A. Cardiac Optogenetics: 2018. *JACC Clin Electrophysiol* **2018**, *4*, 155-167, doi:10.1016/j.jacep.2017.12.006.
46. Abilez, Oscar J.; Wong, J.; Prakash, R.; Deisseroth, K.; Zarins, Christopher K.; Kuhl, E. Multiscale Computational Models for Optogenetic Control of Cardiac Function. *Biophysical Journal* **2011**, *101*, 1326-1334, doi:10.1016/j.bpj.2011.08.004.
47. Bos, T.R.v.d. *Genomic safe harbor locations AAVS1 and CLYBL for CRISPR-Cas9 genome editing in human pluripotent stem cells*; Saxion University of applied science and University of Twente: 2018.
48. Zeng, G. Sticky-End PCR: New Method for Subcloning. *BioTechniques* **1998**, *25*, 206-208, doi:10.2144/98252bm05.
49. Schwach, V.; Verkerk, A.O.; Mol, M.; Monshouwer-Kloots, J.J.; Devalla, H.D.; Orlova, V.V.; Anastassiadis, K.; Mummery, C.L.; Davis, R.P.; Passier, R. A COUP-TFII Human Embryonic Stem Cell Reporter Line to Identify and Select Atrial Cardiomyocytes. *Stem Cell Reports* **2017**, *9*, 1765-1779, doi:10.1016/j.stemcr.2017.10.024.
50. Nagel, G.; Brauner, M.; Liewald, J.F.; Adeishvili, N.; Bamberg, E.; Gottschalk, A. Light Activation of Channelrhodopsin-2 in Excitable Cells of *Caenorhabditis elegans* Triggers Rapid Behavioral Responses. *Current Biology* **2005**, *15*, 2279-2284, doi:<https://doi.org/10.1016/j.cub.2005.11.032>.
51. Giacomelli, E.; Mummery, C.L.; Bellin, M. Human heart disease: lessons from human pluripotent stem cell-derived cardiomyocytes. *Cellular and Molecular Life Sciences* **2017**, *74*, 3711-3739, doi:10.1007/s00018-017-2546-5.
52. Brandão, K.O.; Tabel, V.A.; Atsma, D.E.; Mummery, C.L.; Davis, R.P. Human pluripotent stem cell models of cardiac disease: from mechanisms to therapies. *Dis Model Mech* **2017**, *10*, 1039-1059, doi:10.1242/dmm.030320.
53. Ding, Q.; Regan, S.N.; Xia, Y.; Oostrom, L.A.; Cowan, C.A.; Musunuru, K. Enhanced efficiency of human pluripotent stem cell genome editing through replacing TALENs with CRISPRs. *Cell stem cell* **2013**, *12*, 393-394, doi:10.1016/j.stem.2013.03.006.
54. Khan, S.H. Genome-Editing Technologies: Concept, Pros, and Cons of Various Genome-Editing Techniques and Bioethical Concerns for Clinical Application. *Molecular Therapy - Nucleic Acids* **2019**, *16*, 326-334, doi:<https://doi.org/10.1016/j.omtn.2019.02.027>.
55. Den Hartogh, S.C.; Passier, R. Concise Review: Fluorescent Reporters in Human Pluripotent Stem Cells: Contributions to Cardiac Differentiation and Their Applications in Cardiac Disease and Toxicity. *STEM CELLS* **2016**, *34*, 13-26, doi:10.1002/stem.2196.
56. Bruegmann, T.; Malan, D.; Hesse, M.; Beiert, T.; Fuegemann, C.; Fleischmann, B.; Sasse, P. Optogenetic control of heart muscle in vitro and in vivo. *Nat Methods* **2010**, *7*, 897-900, doi:10.1038/nmeth.1512.
57. Hoogland, S. *Genetically modified cardiomyocytes to detect heart failure: A mef2c dna binding reporter construct in stem cells using CRISPR-Cas9*; Saxion University of applied science and University of Twente: 2019.
58. Zhou, X.; Vink, M.; Klaver, B.; Berkhout, B.; Das, A.T. Optimization of the Tet-On system for regulated gene expression through viral evolution. *Gene Therapy* **2006**, *13*, 1382-1390, doi:10.1038/sj.gt.3302780.
59. Xu, H.; Yi, B.A.; Wu, H.; Bock, C.; Gu, H.; Lui, K.O.; Park, J.-H.C.; Shao, Y.; Riley, A.K.; Domian, I.J.; et al. Highly efficient derivation of ventricular cardiomyocytes from induced pluripotent stem cells with a distinct epigenetic signature. *Cell Research* **2012**, *22*, 142-154, doi:10.1038/cr.2011.171.
60. Liebau, S.; Tischendorf, M.; Ansoorge, D.; Linta, L.; Stockmann, M.; Weidgang, C.; Iacovino, M.; Boeckers, T.; von Wichert, G.; Kyba, M.; et al. An Inducible Expression System of the Calcium-Activated Potassium Channel 4 to Study the Differential Impact on Embryonic Stem Cells. *Stem Cells International* **2011**, *2011*, 456815, doi:10.4061/2011/456815.
61. Wu, B.; Zhou, B.; Wang, Y.; Cheng, H.-L.; Hang, C.T.; Pu, W.T.; Chang, C.-P.; Zhou, B. Inducible cardiomyocyte-specific gene disruption directed by the rat Tnnt2 promoter in the mouse. *Genesis* **2010**, *48*, 63-72, doi:10.1002/dvg.20573.

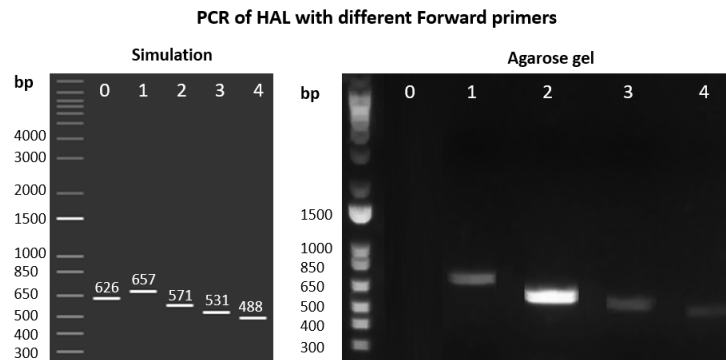
62. Valencia, T.G.; Roberts, L.D.; Zeng, H.; Grant, S.R. Tetracycline-Inducible CaM Kinase II Silences Hypertrophy-Sensitive Gene Expression in Rat Neonate Cardiomyocytes. *Biochemical and Biophysical Research Communications* **2000**, *274*, 803-810, doi:<https://doi.org/10.1006/bbrc.2000.3239>.
63. Suarez, J.; Gloss, B.; Belke, D.D.; Hu, Y.; Scott, B.; Dieterle, T.; Kim, Y.-K.; Valencik, M.L.; McDonald, J.A.; Dillmann, W.H. Doxycycline inducible expression of SERCA2a improves calcium handling and reverts cardiac dysfunction in pressure overload-induced cardiac hypertrophy. *American Journal of Physiology-Heart and Circulatory Physiology* **2004**, *287*, H2164-H2172, doi:10.1152/ajpheart.00428.2004.
64. Wang, B. Improving CRISPR-Cas9's Rate of Homology-Directed Repair. *Genetic Engineering & Biotechnology News* **2018**, *38*, 12-13, doi:10.1089/gen.38.14.06.
65. Paquet, D.; Kwart, D.; Chen, A.; Sproul, A.; Jacob, S.; Teo, S.; Olsen, K.M.; Gregg, A.; Noggle, S.; Tessier-Lavigne, M. Efficient introduction of specific homozygous and heterozygous mutations using CRISPR/Cas9. *Nature* **2016**, *533*, 125-129, doi:10.1038/nature17664.
66. Byrne, S.M.; Ortiz, L.; Mali, P.; Aach, J.; Church, G.M. Multi-kilobase homozygous targeted gene replacement in human induced pluripotent stem cells. *Nucleic Acids Res* **2015**, *43*, e21-e21, doi:10.1093/nar/gku1246.
67. Li, H.; Beckman, K.A.; Pessino, V.; Huang, B.; Weissman, J.S.; Leonetti, M.D. Design and specificity of long ssDNA donors for CRISPR-based knock-in. *bioRxiv* **2019**, 178905, doi:10.1101/178905.
68. Zhang, J.-P.; Li, X.-L.; Li, G.-H.; Chen, W.; Arakaki, C.; Botimer, G.; Baylink, D.; Zhang, L.; Wen, W.; Fu, Y.-W.; et al. Efficient precise knockin with a double cut HDR donor after CRISPR/Cas9-mediated double-stranded DNA cleavage. *Genome Biology* **2017**, *18*, doi:10.1186/s13059-017-1164-8.
69. Petrezselyova, S.; Kinsky, S.; Fricova, D.; Sedlacek, R.; Burtscher, I.; Lickert, H. Homology Arms of Targeting Vectors for Gene Insertions and Crispr/Cas9 Technology: Size Does Not Matter; Quality Control of Targeted Clones Does. *Cellular & molecular biology letters* **2015**, *20*, doi:10.1515/cmble-2015-0047.
70. Guo, Q.; Mintier, G.; Ma-Edmonds, M.; Storton, D.; Wang, X.; Xiao, X.; Kienzle, B.; Zhao, D.; Feder, J.N. 'Cold shock' increases the frequency of homology directed repair gene editing in induced pluripotent stem cells. *Scientific Reports* **2018**, *8*, 2080, doi:10.1038/s41598-018-20358-5.
71. Bencsik, R.; Boto, P.; Szabó, R.N.; Toth, B.M.; Simo, E.; Bálint, B.L.; Szatmari, I. Improved transgene expression in doxycycline-inducible embryonic stem cells by repeated chemical selection or cell sorting. *Stem Cell Research* **2016**, *17*, 228-234, doi:<https://doi.org/10.1016/j.scr.2016.08.014>.
72. Wong, E.T.; Kolman, J.L.; Li, Y.-C.; Mesner, L.D.; Hillen, W.; Berens, C.; Wahl, G.M. Reproducible doxycycline-inducible transgene expression at specific loci generated by Cre-recombinase mediated cassette exchange. *Nucleic Acids Res* **2005**, *33*, e147-e147, doi:10.1093/nar/gni145.
73. Randolph, L.N.; Bao, X.; Zhou, C.; Lian, X. An all-in-one, Tet-On 3G inducible PiggyBac system for human pluripotent stem cells and derivatives. *Scientific Reports* **2017**, *7*, 1549, doi:10.1038/s41598-017-01684-6.
74. Sim, X.; Cardenas-Diaz, F.L.; French, D.L.; Gadue, P. A Doxycycline-Inducible System for Genetic Correction of iPSC Disease Models. *Methods in molecular biology (Clifton, N.J.)* **2016**, *1353*, 13-23, doi:10.1007/7651_2014_179.
75. Ahler, E.; Sullivan, W.J.; Cass, A.; Braas, D.; York, A.G.; Bensinger, S.J.; Graeber, T.G.; Christofk, H.R. Doxycycline alters metabolism and proliferation of human cell lines. *PLoS one* **2013**, *8*, e64561-e64561, doi:10.1371/journal.pone.0064561.
76. Twyman, R. *Gene Transfer to Animal Cells*; Taylor & Francis: 2004.
77. Munroe, D.; Jacobson, A. mRNA poly(A) tail, a 3' enhancer of translational initiation. *Mol Cell Biol* **1990**, *10*, 3441-3455, doi:10.1128/mcb.10.7.3441-3455.1990.
78. Azzoni, A.R.; Ribeiro, S.C.; Monteiro, G.A.; Prazeres, D.M.F. The impact of polyadenylation signals on plasmid nuclease-resistance and transgene expression. *The Journal of Gene Medicine* **2007**, *9*, 392-402, doi:<https://doi.org/10.1002/jgm.1031>.
79. Regot, S.; Hughey, J.J.; Bajar, B.T.; Carrasco, S.; Covert, M.W. High-sensitivity measurements of multiple kinase activities in live single cells. *Cell* **2014**, *157*, 1724-1734, doi:10.1016/j.cell.2014.04.039.
80. Qian, K.; Huang, C.-L.; Chen, H.; Blackburn IV, L.W.; Chen, Y.; Cao, J.; Yao, L.; Sauvey, C.; Du, Z.; Zhang, S.-C. A Simple and Efficient System for Regulating Gene Expression in Human Pluripotent Stem Cells and Derivatives. *STEM CELLS* **2014**, *32*, 1230-1238, doi:<https://doi.org/10.1002/stem.1653>.
81. Faedo, A.; Laporta, A.; Segnali, A.; Galimberti, M.; Besusso, D.; Cesana, E.; Belloli, S.; Moresco, R.M.; Tropiano, M.; Fucà, E.; et al. Differentiation of human telencephalic progenitor cells into MSNs by

- inducible expression of Gsx2 and Ebf1. *Proceedings of the National Academy of Sciences* **2017**, *114*, E1234, doi:10.1073/pnas.1611473114.
82. Abilez, O.; Prakash, R.; Wong, J.; Kuhl, E.; Deisseroth, K.; Zarins, C. In vitro and In silico Optogenetic Control of Differentiated Human Pluripotent Stem Cells. *Biophysical Journal* **2011**, *100*, 368a, doi:<https://doi.org/10.1016/j.bpj.2010.12.2197>.
 83. Zhuge, Y.; Patlolla, B.; Ramakrishnan, C.; Beygui, R.; Zarins, C.; Deisseroth, K.; Kuhl, E.; Abilez, O. Human pluripotent stem cell tools for cardiac optogenetics. *2014 36th Annual International Conference of the IEEE Engineering in Medicine and Biology Society, EMBC 2014* **2014**, *2014*, 6171-6174, doi:10.1109/EMBC.2014.6945038.
 84. Lou, Y.-j.; Jin, J. Insert restriction enzyme cutting-free cloning strategy for expression plasmid construction. *Biotechnology & Biotechnological Equipment* **2017**, *31*, 1033-1039, doi:10.1080/13102818.2017.1351310.
 85. Yu, Y.; Qin, N.; Lu, X.-A.; Li, J.; Han, X.; Ni, X.; Ye, L.; Shen, Z.; Chen, W.; Zhao, Z.-A.; et al. Human embryonic stem cell-derived cardiomyocyte therapy in mouse permanent ischemia and ischemia-reperfusion models. *Stem Cell Research & Therapy* **2019**, *10*, 167, doi:10.1186/s13287-019-1271-4.
 86. Ordovás, L.; Boon, R.; Pistoni, M.; Chen, Y.; Wolfs, E.; Guo, W.; Sambathkumar, R.; Bobis-Wozowicz, S.; Helsen, N.; Vanhove, J.; et al. Efficient Recombinase-Mediated Cassette Exchange in hPSCs to Study the Hepatocyte Lineage Reveals AAVS1 Locus-Mediated Transgene Inhibition. *Stem Cell Reports* **2015**, *5*, 918-931, doi:10.1016/j.stemcr.2015.09.004.
 87. Bhagwan, J.; Collins, E.; Mosqueira, D.; Bakar, M.; Johnson, B.; Thompson, A.; Smith, J.; Denning, C. Variable expression and silencing of CRISPR-Cas9 targeted transgenes identifies the AAVS1 locus as not an entirely safe harbour. *F1000Res* **2019**, *8*, 1911, doi:10.12688/f1000research.19894.1.
 88. Cerbini, T.; Funahashi, R.; Luo, Y.; Liu, C.; Park, K.; Rao, M.; Malik, N.; Zou, J. Transcription activator-like effector nuclease (TALEN)-mediated CLYBL targeting enables enhanced transgene expression and one-step generation of dual reporter human induced pluripotent stem cell (iPSC) and neural stem cell (NSC) lines. *PLoS one* **2015**, *10*, e0116032-e0116032, doi:10.1371/journal.pone.0116032.
 89. Thyagarajan, B.; Liu, Y.; Shin, S.; Lakshminpathy, U.; Scheyhing, K.; Xue, H.; Ellerström, C.; Strehl, R.; Hyllner, J.; Rao, M.S.; et al. Creation of Engineered Human Embryonic Stem Cell Lines Using phiC31 Integrase. *STEM CELLS* **2008**, *26*, 119-126, doi:10.1634/stemcells.2007-0283.
 90. Strittmatter, L.; Li, Y.; Nakatsuka, N.J.; Calvo, S.E.; Grabarek, Z.; Mootha, V.K. CLYBL is a polymorphic human enzyme with malate synthase and β -methylmalate synthase activity. *Hum Mol Genet* **2014**, *23*, 2313-2323, doi:10.1093/hmg/ddt624.
 91. Chan, K.Y.; Jang, M.J.; Yoo, B.B.; Greenbaum, A.; Ravi, N.; Wu, W.-L.; Sánchez-Guardado, L.; Lois, C.; Mazmanian, S.K.; Deverman, B.E.; et al. Engineered AAVs for efficient noninvasive gene delivery to the central and peripheral nervous systems. *Nature Neuroscience* **2017**, *20*, 1172-1179, doi:10.1038/nn.4593.
 92. Bischoff, N.; Wimberger, S.; Maresca, M.; Brakebusch, C. Improving Precise CRISPR Genome Editing by Small Molecules: Is there a Magic Potion? *Cells* **2020**, *9*, 1318, doi:10.3390/cells9051318.
 93. Di Stazio, M.; Foschi, N.; Athanasakis, E.; Gasparini, P.; d'Adamo, A.P. Systematic analysis of factors that improve homologous direct repair (HDR) efficiency in CRISPR/Cas9 technique. *PLOS ONE* **2021**, *16*, e0247603, doi:10.1371/journal.pone.0247603.
 94. Yang, H.; Ren, S.; Yu, S.; Pan, H.; Li, T.; Ge, S.; Zhang, J.; Xia, N. Methods Favoring Homology-Directed Repair Choice in Response to CRISPR/Cas9 Induced-Double Strand Breaks. *Int J Mol Sci* **2020**, *21*, 6461, doi:10.3390/ijms21186461.
 95. Liu, M.; Rehman, S.; Tang, X.; Gu, K.; Fan, Q.; Chen, D.; Ma, W. Methodologies for Improving HDR Efficiency. *Front Genet* **2019**, *9*, doi:10.3389/fgene.2018.00691.
 96. Tálás, A.; Kulcsár, P.I.; Weinhardt, N.; Borsy, A.; Tóth, E.; Szebényi, K.; Krausz, S.L.; Huszár, K.; Vida, I.; Sturm, Á.; et al. A convenient method to pre-screen candidate guide RNAs for CRISPR/Cas9 gene editing by NHEJ-mediated integration of a 'self-cleaving' GFP-expression plasmid. *DNA Research* **2017**, *24*, 609-621, doi:10.1093/dnares/dsx029.
 97. Song, F.; Stieger, K. Optimizing the DNA Donor Template for Homology-Directed Repair of Double-Strand Breaks. *Mol Ther Nucleic Acids* **2017**, *7*, 53-60, doi:10.1016/j.omtn.2017.02.006.
 98. Kanca, O.; Zirin, J.; Garcia-Marques, J.; Knight, S.M.; Yang-Zhou, D.; Amador, G.; Chung, H.; Zuo, Z.; Ma, L.; He, Y.; et al. An efficient CRISPR-based strategy to insert small and large fragments of DNA using short homology arms. *eLife* **2019**, *8*, e51539, doi:10.7554/eLife.51539.
 99. Li, K.; Wang, G.; Andersen, T.; Zhou, P.; Pu, W.T. Optimization of genome engineering approaches with the CRISPR/Cas9 system. *PLoS one* **2014**, *9*, e105779-e105779, doi:10.1371/journal.pone.0105779.

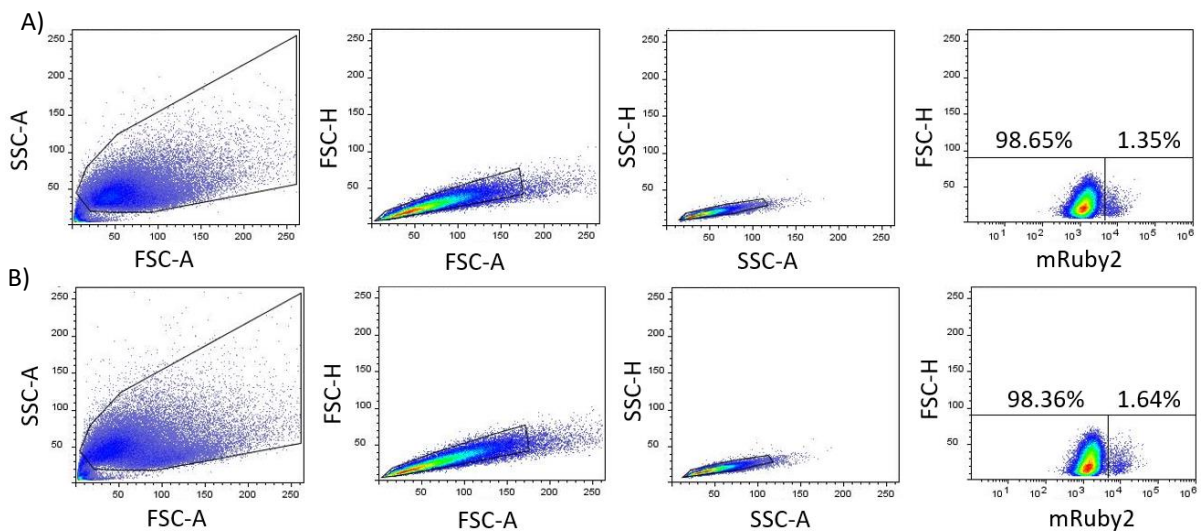
100. Ishii, A.; Kurosawa, A.; Saito, S.; Adachi, N. Analysis of the role of homology arms in gene-targeting vectors in human cells. *PLoS one* **2014**, *9*, e108236–e108236, doi:10.1371/journal.pone.0108236.
101. Campostrini, G.; Windt, L.M.; van Meer, B.J.; Bellin, M.; Mummery, C.L. Cardiac Tissues From Stem Cells. *Circulation Research* **2021**, *128*, 775–801, doi:10.1161/CIRCRESAHA.121.318183.
102. Goldfracht, I.; Protze, S.; Shiti, A.; Setter, N.; Gruber, A.; Shaheen, N.; Nartiss, Y.; Keller, G.; Gepstein, L. Generating ring-shaped engineered heart tissues from ventricular and atrial human pluripotent stem cell-derived cardiomyocytes. *Nature Communications* **2020**, *11*, 75, doi:10.1038/s41467-019-13868-x.
103. Schaaf, S.; Shibamiya, A.; Mewe, M.; Eder, A.; Stöhr, A.; Hirt, M.N.; Rau, T.; Zimmermann, W.-H.; Conradi, L.; Eschenhagen, T.; et al. Human Engineered Heart Tissue as a Versatile Tool in Basic Research and Preclinical Toxicology. *PLOS ONE* **2011**, *6*, e26397, doi:10.1371/journal.pone.0026397.
104. Goldfracht, I.; Efrain, Y.; Shinnawi, R.; Kovalev, E.; Huber, I.; Gepstein, A.; Arbel, G.; Shaheen, N.; Tiburcy, M.; Zimmermann, W.H.; et al. Engineered heart tissue models from hiPSC-derived cardiomyocytes and cardiac ECM for disease modeling and drug testing applications. *Acta Biomaterialia* **2019**, *92*, 145–159, doi:<https://doi.org/10.1016/j.actbio.2019.05.016>.
105. Tzatzalos, E.; Abilez, O.J.; Shukla, P.; Wu, J.C. Engineered heart tissues and induced pluripotent stem cells: Macro- and microstructures for disease modeling, drug screening, and translational studies. *Adv Drug Deliv Rev* **2016**, *96*, 234–244, doi:10.1016/j.addr.2015.09.010.
106. Schwach, V.; Slaats, R.H.; Passier, R. Human Pluripotent Stem Cell-Derived Cardiomyocytes for Assessment of Anticancer Drug-Induced Cardiotoxicity. *Frontiers in Cardiovascular Medicine* **2020**, *7*, doi:10.3389/fcvm.2020.00050.
107. Passier, R.; Orlova, V.; Mummery, C. Complex Tissue and Disease Modeling using hiPSCs. *Cell Stem Cell* **2016**, *18*, 309–321, doi:10.1016/j.stem.2016.02.011.
108. Dwenger, M.; Kowalski, W.J.; Masumoto, H.; Nakane, T.; Keller, B.B. Chronic Optogenetic Pacing of Human-Induced Pluripotent Stem Cell-Derived Engineered Cardiac Tissues. *Methods in molecular biology (Clifton, N.J.)* **2021**, *2191*, 151–169, doi:10.1007/978-1-0716-0830-2_10.
109. Lemme, M.; Braren, I.; Prondzynski, M.; Aksehirlioglu, B.; Ulmer, B.M.; Schulze, M.L.; Ismaili, D.; Meyer, C.; Hansen, A.; Christ, T.; et al. Chronic intermittent tachypacing by an optogenetic approach induces arrhythmia vulnerability in human engineered heart tissue. *Cardiovascular Research* **2020**, *116*, 1487–1499, doi:10.1093/cvr/cvz245.
110. Desjardins, C.A.; Naya, F.J. The Function of the MEF2 Family of Transcription Factors in Cardiac Development, Cardiogenomics, and Direct Reprogramming. *Journal of Cardiovascular Development and Disease* **2016**, *3*, 26.
111. Materna, S.C.; Sinha, T.; Barnes, R.M.; Lammerts van Bueren, K.; Black, B.L. Cardiovascular development and survival require Mef2c function in the myocardial but not the endothelial lineage. *Developmental Biology* **2019**, *445*, 170–177, doi:<https://doi.org/10.1016/j.ydbio.2018.12.002>.
112. Muñoz, J.P.; Collao, A.; Chiong, M.; Maldonado, C.; Adasme, T.; Carrasco, L.; Ocaranza, P.; Bravo, R.; Gonzalez, L.; Díaz-Araya, G.; et al. The transcription factor MEF2C mediates cardiomyocyte hypertrophy induced by IGF-1 signaling. *Biochemical and Biophysical Research Communications* **2009**, *388*, 155–160, doi:<https://doi.org/10.1016/j.bbrc.2009.07.147>.
113. Filomena, M.C.; Bang, M.-L. In the heart of the MEF2 transcription network: novel downstream effectors as potential targets for the treatment of cardiovascular disease. *Cardiovascular Research* **2018**, *114*, 1425–1427, doi:10.1093/cvr/cvy123.
114. Cardoso, A.; Pereira, A.H.; Ambrosio, Andre Luis B.; Consonni, S.; Rocha de Oliveira, R.; Bajgelman, M.; Dias, Sandra Martha G.; Franchini, Kleber G. FAK Forms a Complex with MEF2 to Couple Biomechanical Signaling to Transcription in Cardiomyocytes. *Structure* **2016**, *24*, doi:10.1016/j.str.2016.06.003.
115. Gárate, J.; Lagos, D.; Pavez Giani, M.; Troncoso, M.; Ramos, S.; Barrientos, G.; Ibarra, C.; Lavandero, S.; Estrada, M. Ca²⁺/Calmodulin-Dependent Protein Kinase II and Androgen Signaling Pathways Modulate MEF2 Activity in Testosterone-Induced Cardiac Myocyte Hypertrophy. *Frontiers in Pharmacology* **2017**, *8*, 604, doi:10.3389/fphar.2017.00604.
116. Hashemi, S.; Salma, J.; Wales, S.; McDermott, J.C. Pro-survival function of MEF2 in cardiomyocytes is enhanced by β -blockers. *Cell Death Discov* **2015**, *1*, 15019–15019, doi:10.1038/cddiscovery.2015.19.
117. Naya, F.J.; Wu, C.Z.; Richardson, J.A.; Overbeek, P.; Olson, E. Transcriptional activity of MEF2 during mouse embryogenesis monitored with a MEF2-dependent transgene. *Development (Cambridge, England)* **1999**, *126*, 2045–2052.

Supplemental information

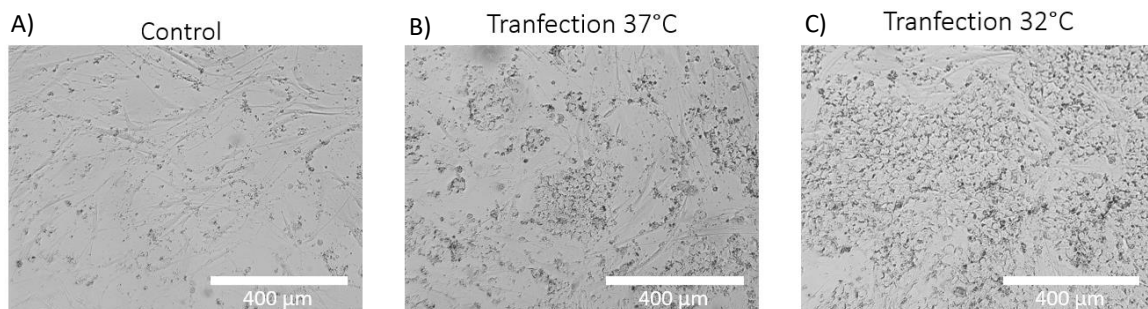
Supplementary figures



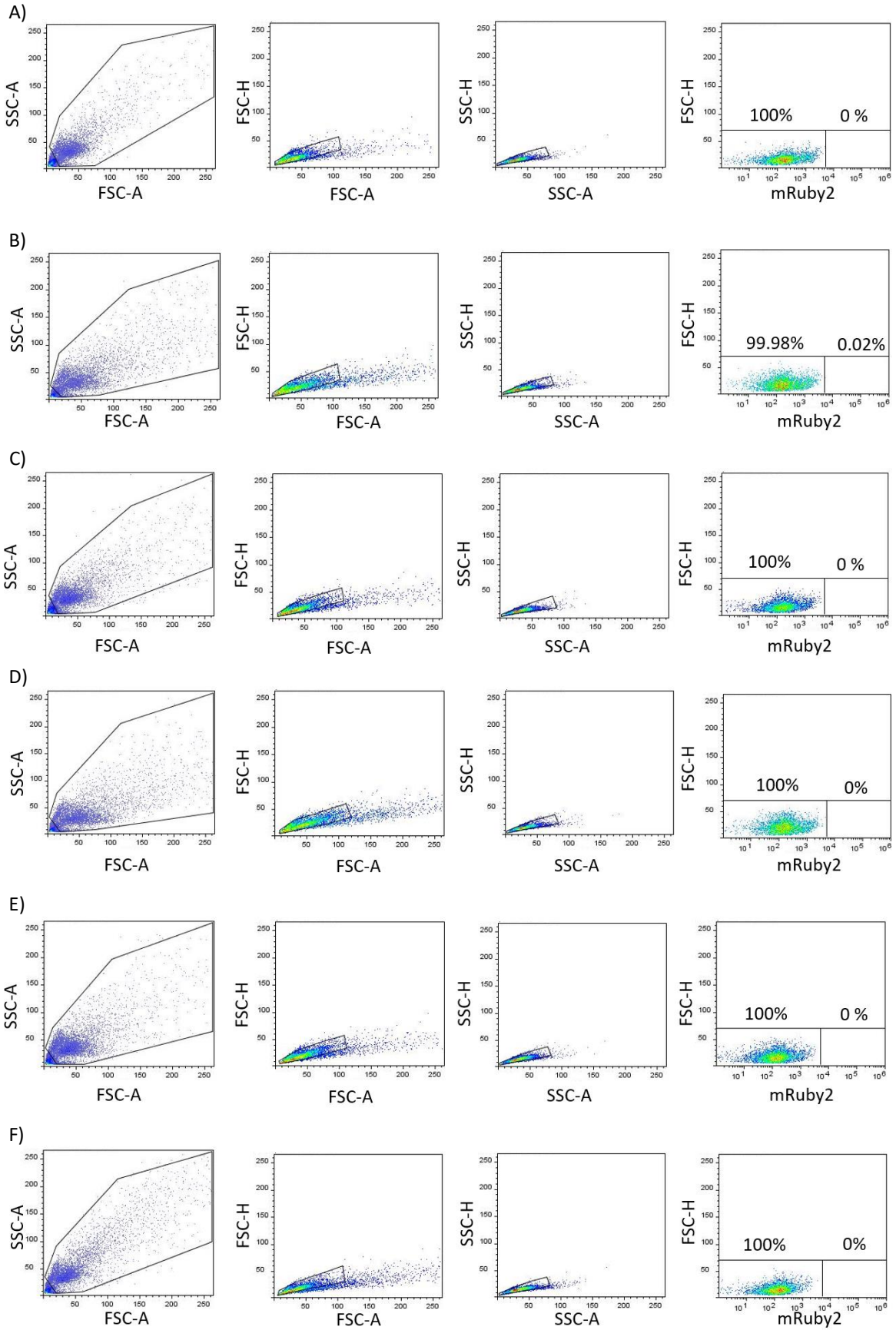
Supplementary figure 1: PCR reaction of the HAL fragment with the originally designed primers (number 0) did not result in a product. Four new In-Fusion® cloning forward primers were designed and tested (number 1 – 4). Those primers were located on a slightly different location on the AAVS1 GSH locus. The PCR product with the brightest band (nr. 2) was used in the In-Fusion® cloning reaction.

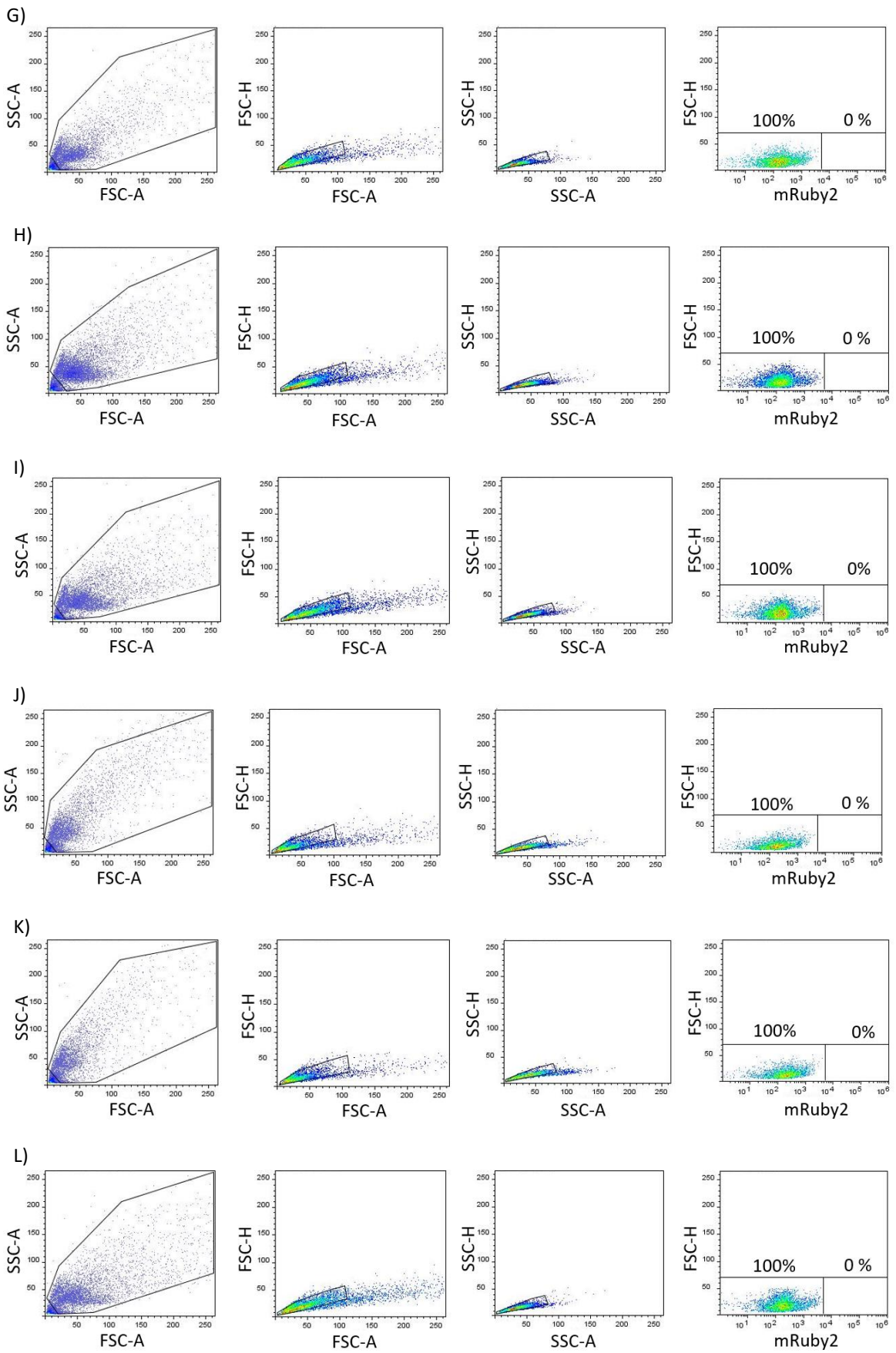


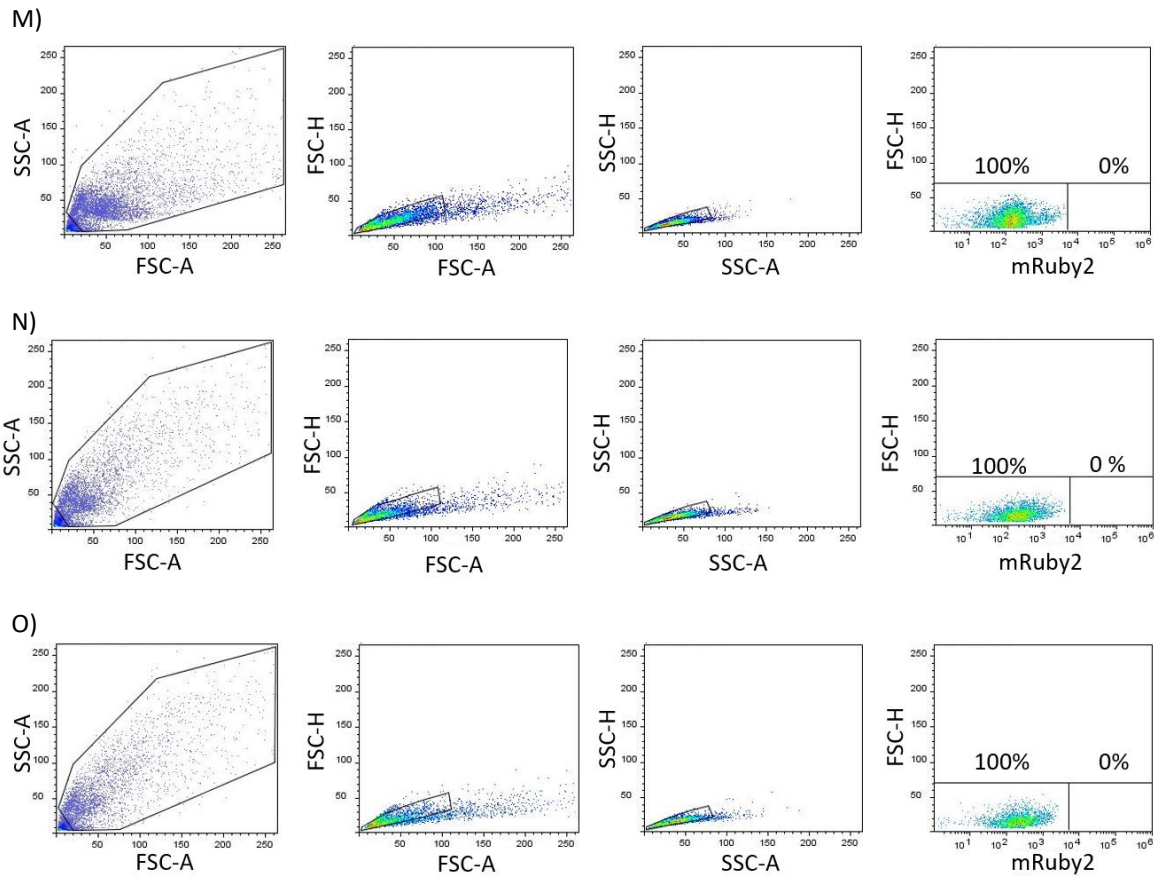
Supplementary figure 2: Flow cytometry plots with gates showing the mRuby2 positive hiPSC cells after doxycycline stimulation (2 µg/ml for 24h) of targeted cells with sgRNA3 and **A)** low HDR (3.0 µg) or **B)** high HDR (4.5 µg) template.



Supplementary figure 3: Comparison of hESC survival between transection at 37 °C with “cold shock” transfection after puromycin selection. **A)** In the control condition, all the hESC cells died. **B-C)** Cell survival at “cold shock” was superior to transection at 37 °C. Large hESC colonies can be seen in the “cold shock” condition.







Supplementary figure 4: Flow cytometry plots with gates showing the mRuby2 positive hESC cells after doxycycline stimulation of CRISPR-Cas9-mediated targeting of doxycycline inducible mRuby2. Conditions:

A) Control without doxycycline stimulation

B) sgRNA1 – 3.0 μg HDR template stimulated with 1 $\mu\text{g}/\text{ml}$ doxycycline for 24h.

C) sgRNA1 – 4.5 μg HDR template stimulated with 1 $\mu\text{g}/\text{ml}$ doxycycline for 24h.

D) sgRNA2 – 4.5 μg HDR template stimulated with 1 $\mu\text{g}/\text{ml}$ doxycycline for 24h.

E) sgRNA1 – 3.0 μg HDR template (“cold shock” transfection) stimulated with 1 $\mu\text{g}/\text{ml}$ doxycycline for 24h.

F) sgRNA3 – 3.0 μg HDR template (“cold shock” transfection) stimulated with 1 $\mu\text{g}/\text{ml}$ doxycycline for 24h.

G) sgRNA3 – 4.5 μg HDR template (“cold shock” transfection) stimulated with 1 $\mu\text{g}/\text{ml}$ doxycycline for 24h.

H) sgRNA3 – 4.5 μg HDR template stimulated with 100 ng/ml doxycycline for 48h.

I) sgRNA3 – 4.5 μg HDR template stimulated with 1 $\mu\text{g}/\text{ml}$ doxycycline for 48h.

J) sgRNA1 – 3.0 μg HDR template (“cold shock” transfection) stimulated with 1 $\mu\text{g}/\text{ml}$ doxycycline for 48h.

K) sgRNA1 – 3.0 μg HDR template (“cold shock” transfection) stimulated with 2 $\mu\text{g}/\text{ml}$ doxycycline for 48h.

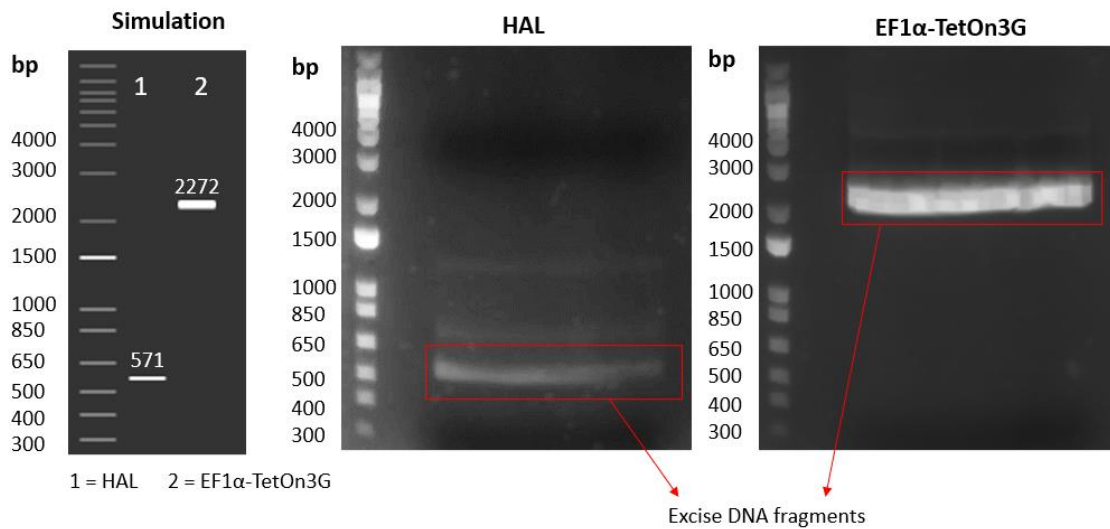
L) sgRNA2 – 3.0 μg HDR template (“cold shock” transfection) stimulated with 100 ng/ml doxycycline for 48h.

M) sgRNA2 – 3.0 μg HDR template (“cold shock” transfection) stimulated with 1 $\mu\text{g}/\text{ml}$ doxycycline for 48h.

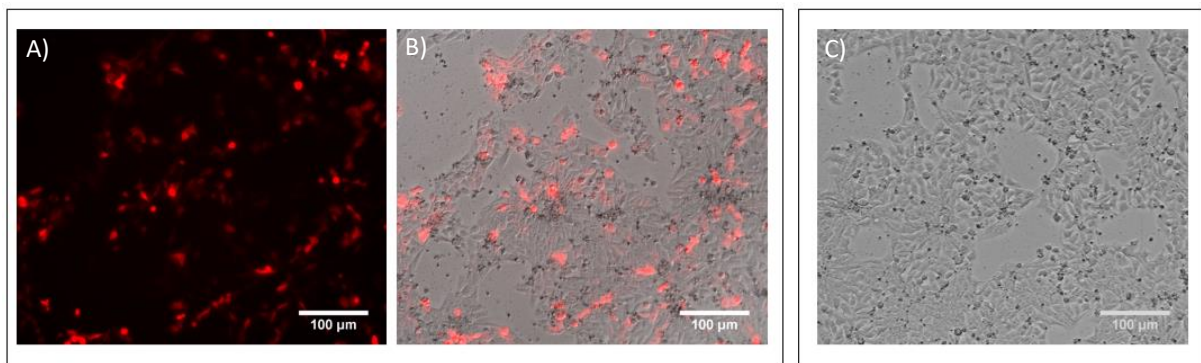
N) sgRNA3 – 4.5 μg HDR template (“cold shock” transfection) stimulated with 1 $\mu\text{g}/\text{ml}$ doxycycline for 48h.

O) sgRNA3 – 4.5 μg HDR template (“cold shock” transfection) stimulated with 2 $\mu\text{g}/\text{ml}$ doxycycline for 48h.

PCR of HAL and EF1 α -TetOn3G for HDR template 2.0



Supplementary figure 5: New *In-Fusion*[®] cloning primers were designed to amplify the HAL and the EF1 α -TetOn3G fragment with poly(A) tail after the TetOn3G gene. The HAL (571 bp) and EF1 α -TetOn3G (2272 bp) were successfully amplified. The fragments were extracted from the agarose gel and used for *Fusion*[®] cloning reaction.



Supplementary figure 6: Fluorescent mRuby2 expression in hESCs 48h after transfection. **A)** Fluorescence and **B)** merged image (fluorescence and brightfield) of cells transfected with mRubyII-N1 plasmid (as positive control). **C)** Merged image (fluorescence and brightfield) of doxycycline inducible HDR template 2.0. The HDR template was stimulated with 1000 ng/ml doxycycline for 48 h. The settings (exposure time and light intensity) were the same used to image mRubyII-N1 plasmid expression. There are no fluorescent cells visible.

Supplementary experimental procedures

sgRNA-Cas9 plasmid

The sgRNA-Cas9 plasmids were designed and produced by Van den Bos [1]. In short, Van den Bos designed partially complementary oligonucleotides (encoding the 20-nucleotide guide sequence) targeting the AAVS1 GSH location using the CRISPR Design tool [2]. The oligonucleotides were ligated into the Bpil (BbsI) restriction sites in the pSp-Cas9(BB)-2A-puro plasmid as described by Ran et al. [2]. There were three different guide sequences produced for the AAVS1 region, based on the article of Smith et al. [3]. Sanger sequencing (Eurofins Genomics) with the U6 forward primer was performed to confirm the presence of the 20-nucleotide guide sequence within the pSp-Cas9(BB)-2A-puro plasmid (**Supplementary table 1**).

Supplementary table 1: Sequencing primer sgRNA-Cas9 plasmid

Fragment	Primer names	Sequence 5'-3'
sgRNA-Cas9	U6 Forward	GAGGGCCTATTTCCCATGATTCC

Generation of the HDR template fragments

The HDR template and primers were designed with the In-Fusion® cloning tool in SnapGene (SnapGene® software from GSL Biotech; available at snapgene.com). The HDR template contains five DNA fragments: The red fluorescent protein mRuby2 ($\lambda_{ex} = 559$ nm, $\lambda_{em} = 600$ nm), the minimal promoter TRE3G, the constitutively active promoter EF1 α before the gene encoding for the TetOn3G transactivator protein and two homology arms, which allows integration in the genomic AAVS1 locus. The designed primers contain homologous overlapping ends between adjacent DNA fragments, which allows the In-Fusion® cloning reaction in the pENTR1A backbone vector (**Supplementary table 2-3**). The PAM sequence was mutated to prevent Cas9 from cutting the HDR template during transfection (**Supplementary table 3**, nucleobases marked in red)

Genomic DNA of hiPSCs (LUMC0020iCTRL-06) was used to amplify the homology arms, HAR and HAL. First, genomic DNA was isolated with the QuickExtract™ DNA Extraction Solution (Lucigen). The cells were resuspended in PBS with a density of 600 cells/ μ L and 30 μ L was spun down for 5 min in a PCR tube mini centrifuge. The PBS (circa 28 μ L) was removed from the cell pellet and 30 μ L QuickExtract™ DNA Extraction Solution was used to dissolve the cell pellet. The tube was heated to 65 °C for 15 min, 68 °C for 15 min and 98 °C for 10 min. Subsequently, the isolated DNA was used to amplify the HAR and HAL. The fragments mRuby2, TRE3G promoter and EF1 α -TetOn3G were amplified from the plasmids mRubyII-N1 (Addgene #54614), pTRE3G-GSX2 (Addgene #96964) and PB-EF1 α -TetOn3G (Addgene #104543), respectively. The plasmids are available in **Supplementary experimental procedures, "Vector maps"**. The Phusion High-Fidelity PCR Kit (Thermo Fisher Scientific™) was used to

amplify the 5 fragments (HAR, HAL, mRuby2, TRE3G promotor and EF1 α -TetOn3G). PCR amplifications were carried out using the T100™ Thermal Cycler (Bio-Rad) in a 20 μ L mixture containing 5X Phusion GC buffer, 200 μ M of each dNTPs, 0.5 μ M forward primer, 0.5 μ M reverse primer, 3% DMSO and 0.02 U/ μ L Phusion DNA polymerase. In case of the HAL and HAR, 1 μ L of isolated DNA was used, whereas the plasmid concentration was in the range of 0.5 pg to 10 ng. A 2-step PCR protocol was used, with initial denaturation at 98 °C for 30 seconds followed by 29 cycles of denaturation at 98 °C for 10 seconds and annealing/extension at 72 °C for 30 seconds. Then the final extension was done at 72 °C for 10 minutes. In case of the HAL and HAR the number of cycles was increased to 35 and 40 cycles, respectively. The annealing/extension step was increased to 1 minute instead of 30 seconds in case of EF1 α -TetOn3G. The pENTR1A plasmid (Addgene #2525) was used as backbone vector to insert the 5 fragments. The pENTR1A plasmid was linearized with the AjiI (BmgBI) restriction enzyme (Thermo Fisher Scientific™) at 37 °C for 45 minutes.

The PCR products and linearized plasmids were mixed with 6X DNA Gel Loading Dye (Thermo Fisher Scientific™) and were loaded on a 1% agarose gel consisting of UltraPure™ Agarose-1000 (Invitrogen™), 1X Tris-acetate-EDTA (TAE) Buffer and 1:10000 diluted SYBR™ Safe DNA Gel Stain (Invitrogen™). As reference, the 1 Kb Plus DNA Ladder (Invitrogen™) was used. The running time was 90 minutes at 90 volts and the gel was visualized with FluorChem™ M imaging system (ProteinSimple). After confirmation of the correct DNA fragment on the gel, the PCR reaction was repeated in large volumes (100 – 200 μ L) and the desired DNA fragments were isolated and purified with the NucleoSpin Gel and PCR Clean-up kit (Macherey-Nagel). After DNA isolation, the concentration was measured with the NanoDrop™ 1000 Spectrophotometer (Thermo Fisher Scientific™) and 200-400 ng of the extracted DNA was loaded on an agarose gel to confirm successful isolation of the HDR template fragments.

Supplementary table 2: HAL In-Fusion® cloning forward primers

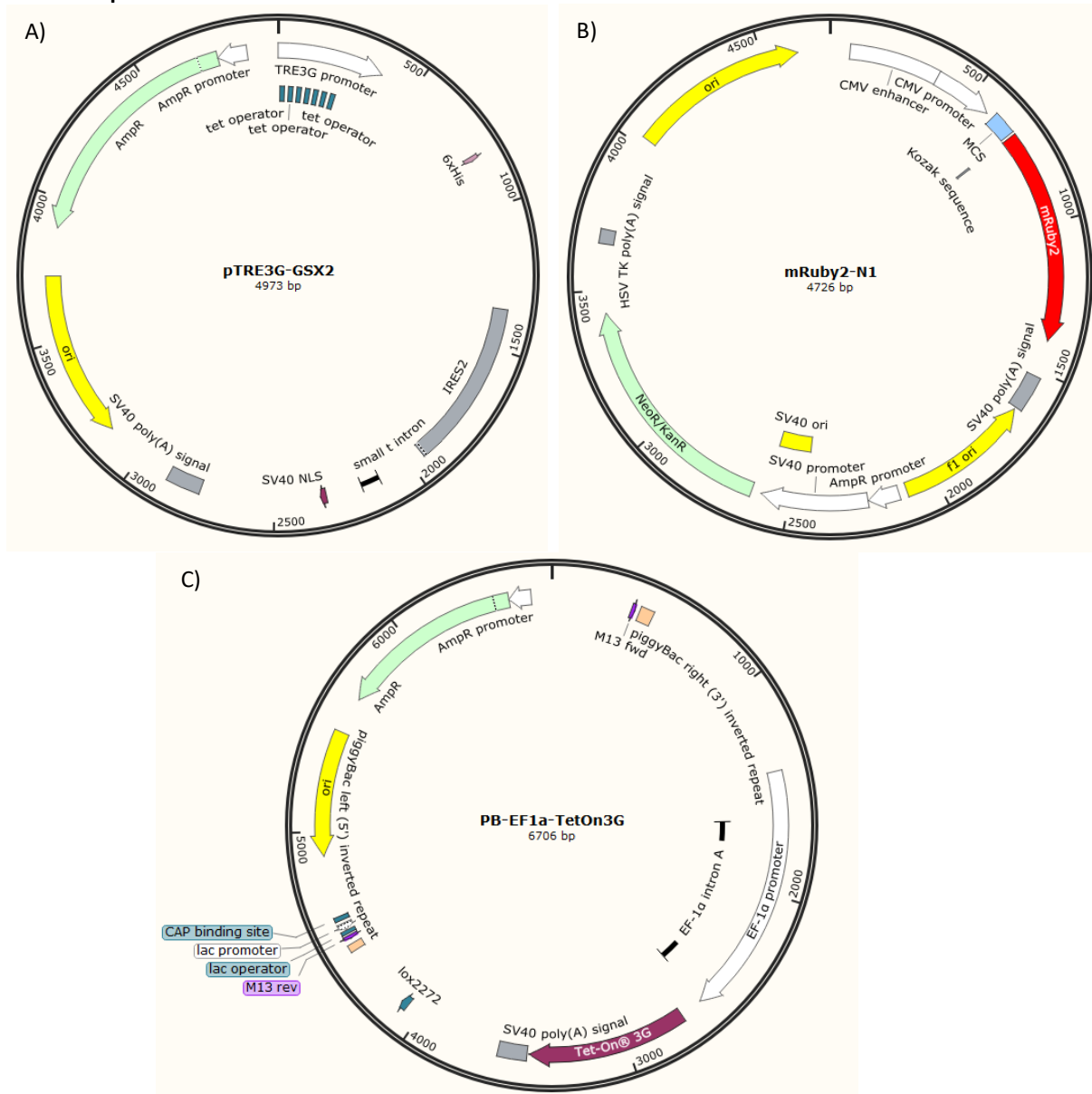
Nr.	Primer names	Sequence 5'-3'
0	HAL_pENTR1A_RS	CCCTGGCCAGTGCCTAGGCCGCCGCCCGC
1	HAL Fwd GH1	TGGCCAGTGCCTAGGCCGTCTGATGCTGCGC
2	HAL Fwd GH2	TGGCCAGTGCCTAGCTGCACCAGGTCAGCGC
3	HAL Fwd GH3	TGGCCAGTGCCTAGCAGGTCCACCCTCTGCG
4	HAL Fwd GH4	TGGCCAGTGCCTAGCCGTTGCCAGTCTCGATCC

Supplementary table 3: In-Fusion® cloning primers of the HDR template

Fragment	Primer names	Sequence 5'-3'	Length (bp)
HAR primers	RobustHAR-Prom-Fw	TAAACTCGCCGGAAGCTGTCTCTCTAAC	532
	RobustHAR-pENTR1A-Rv	TATCTGACAGCAGACAGGGGAGGCGGGACG	
TRE3G primers	Prom-robustHAR-Fw	GTTCCGGCGAGTTTACTCCCTATCAGTGATAGAGAACGTATGAA	400
	Prom-mRuby2-Rv	GGTGGCGGTCTGACTTTACGAGGGTAGGAAGT	

mRuby2 primers	Fw-mRuby2-promotor-Xmil	AAGTCGACCGCCACCGCCTAGG CGCCACCATGGTGTCTAAGGGC G	760
	mRuby2-pENTR1A Ajil Rv	CCCTGGCCAGTGCCTAGTACTT GTACAGCTCGTC	
EF1 α -TetOn3G primers	Teton-RobustHAL-Rv	CTGTGCCCTTAGTTACCCGGGGA GCATGTCA	2146
	Fragment 2.FOR-Fw	GACGAGCTGTACAAGTACTAGT AAGCGGATTACATCCCTGGGGG CTTTGGGG	
HAL primers	AAVS1-HAL-FWD-GH2	TGCCAGTGCCTAGCTGCACC AGGTCAGCGC	571
	RobustHAL-TetOn-Rv	TAACTAAGGGCACAGCAAGGGC ACTCG	

Vector maps



A) pTRE3G-GSX2 plasmid (Addgene #96964), **B)** mRuby2-N1 plasmid (Addgene #54614) and **C)** PB-EF1a-TetOn3G plasmid (Addgene #104543)

In-Fusion cloning and transformation

The different fragments of the HDR template were inserted in the linearized pENTR1A by a two-step In-Fusion® cloning mechanism. In the first step, mRuby2, the TRE3G promoter and HAR were inserted in the linearized pENTR1A plasmid using the In-Fusion® HD Cloning Kit (Takara Bio). The 10 µl reaction mixture contains 60 ng linearized pENTR1A, 90 ng mRuby2, 90 ng TRE3G, 50 ng HAR and 2 µl of the 5X In-Fusion HD enzyme premix. The reaction mixture was incubated at 50 °C for 15 minutes. Thereafter, the reaction mixture was transformed into One Shot® TOP10 Competent *E. coli* Cells (Invitrogen™). The cells (50 µl) were thawed on ice for 20 minutes and 5 µl of the In-Fusion reaction mixture was added to the cells. After 30 minutes incubation on ice, the cells were heat-shocked at 42°C for 30 seconds followed by 2 minutes incubation on ice. Thereafter, 250 µl of S.O.C. Medium (Invitrogen™) was added and the cells were incubated at 37 °C at a shaker for 1 hour. The cells were divided and plated on three LB agar (Miller, Fisher BioReagents™) plates containing 50 µg/ml Kanamycin for selection. The pENTR1A vector contains a kanamycin resistance gene and a cell division B gene (*ccdB*) gene to select the successfully transformed bacteria. The *ccdB* gene, encoding for a lethal protein, is present in the cloning region of the vector. If the *ccdB* gene is not disturbed or removed, a toxic protein is produced causing chromosomal damage to the bacterial cell and eventually cell death [4]. The LB agar plates were incubated overnight at 37 °C. The next day ten colonies were picked and each colony was grown in 3 ml LB broth (Miller, Fisher BioReagents™) overnight at 37 °C. Half of the bacterial cell suspension was used for plasmid isolation. The plasmids were isolated and purified with the PureLink™ Quick Plasmid Miniprep Kit (Invitrogen™) according to the manufacturer's protocol. The isolated plasmids were analysed by digestion with the restriction enzyme Bpil (BbsI) (Thermo Fisher Scientific™). Three plasmids were selected and the corresponding bacterial clone was grown in 150 ml LB broth overnight at 37 °C. The plasmids were isolated and purified with the PureYield™ Plasmid Midiprep System (Promega Corporation) according to the manufacturer's protocol. The isolated plasmids were analysed by restriction digestions with the enzymes Bpil (BbsI), XmaJI (AvrII) and Bcul (SpeI) (Thermo Fisher Scientific™). Finally, the sequences were checked by Sanger sequencing (Eurofins Genomics). The sequencing primers of the HDR template step 1 are shown in **Supplementary table 4**.

After confirmation of the insertion of mRuby2, TRE3G and HAR into the pENTR1A plasmid, the plasmid was opened at the Bcul (SpeI) (Thermo Fisher Scientific™) restriction site present between mRuby2 and pENTR1A. The HAL and EF1α-TetOn3G fragments were inserted in the linearized pENTR1A plasmid using In-Fusion® HD Cloning kit as described earlier. The 10 µl reaction mixture contains 60 ng linearized pENTR1A, 50 ng HAL and 90 ng EF1α-TetOn3G. Bacterial transformation, plasmid isolation and plasmid analysis were performed in the same way as described in the first step. The sequencing primers of the HDR template step 2 are shown in **Supplementary table 5**.

Supplementary table 4: Sequencing primers HDR template step 1

Nr	Primer names	Sequence 5'-3'
1	SeqpENTR1A Fwd	CCGGTACCGAATTTCGCTTA
2	Seq Ruby mRev	CTTGGACGTGGTAAACGAG
3	Seq Ruby mFwd	CTCGTTTACCACGTCCAAG
4	Teton3G-seq-1	GAGAGCTCGTTTAGTGAACC
5	AAVS1-seq-5	AGTAGAGCTCAAAGTGGTCCG
6	SeqpENTR1A Rev	GCTGGGTCTAGATATCTCG

Supplementary table 5: Sequencing primers HDR template step 2

Nr	Primer names	Sequence 5'-3'
1	SeqpENTR1A Fwd	CCGGTACCGAATTTCGCTTA
2	Seq Teton Fwd	CTGTTCCCTCCAATACGCAG
3	Seq Teton Rev	AAGTCATACCGCTGTGCTC
4	Seq EF1a Rev	GTGAGTCACCCACACAAAG
5	Teton3G-seq-2	ACAGTCCCCGAGAAGTTGG
6	Seq Ruby mRev	CTTGGACGTGGTAAACGAG
7	Seq Ruby mFwd	CTCGTTTACCACGTCCAAG
8	AAVS1-seq-5	AGTAGAGCTCAAAGTGGTCCG
9	SeqpENTR1A Rev	GCTGGGTCTAGATATCTCG

Stem cell culture

Stem cells (hESCs and hiPSCs) were maintained in Essential 8™ medium on 0.5 µg/cm² vitronectin (Gibco™, Thermo Fisher Scientific™) at 37°C, 5% CO₂ and were passaged twice a week. Passaging of hESCs and hiPSCs on vitronectin was done using 0.5 mM EDTA (Invitrogen™, Thermo Fisher Scientific™) until the cells were loosely adherent to the culture plate. The EDTA was aspirated and the cells were detached by gentle washing with Essential 8™ medium. After counting, the cells were seeded to wells coated with vitronectin.

Stem cell transfection, selection and sorting

HiPSCs and hESCs were seeded in a 6-well one day before transfection at a density of 40 K per cm² on 30 K per cm² irradiated mouse embryonic fibroblasts (MEF feeder cells) in hESC medium (DMEM/F12-based medium containing 20% knockout serum replacement (Thermo Fisher Scientific™) and 10 ng/mL basic fibroblast growth factor (bFGF) (Miltenyi Biotech)). The stem cells were transfected with 4 µg sgRNA-Cas9 plasmid and 3 – 4.5 µg of HDR plasmid using 10 µl Lipofectamine™ Stem Transfection Reagent (Invitrogen™, Thermo Fisher Scientific™) according to manufacturer's instructions. The cells were incubated in 37 °C and 5% CO₂ or 32 °C and 5% CO₂ for 24 h. The presence of the puromycin resistance gene in the sgRNA-Cas9 plasmid allowed selection of the transfected cells. After 24 h of 0.5 µg/ml puromycin exposure, the cells were recovered for several days on MEFs in hESC medium. The cells transfected at 32 °C were incubated for 3 days at 32 °C, including puromycin selection. Passaging of hESCs and hiPSCs on MEFs was done by dissociation using 1xTriplE Select (Thermo Fisher Scientific™). The TripLE Select was inactivated by dilution in hESC medium and the cells were

centrifuged at 240*g for three minutes. The cell pellet was resuspended in Essential 8™ medium and seeded to vitronectin coated plates without feeder cells. The cells were grown for several days and treated with doxycycline (Doxycycline Hydrochloride, Ready Made Solution, Sigma-Aldrich) 24 h or 48 h before fluorescence-activated cell sorting (FACS). Different doxycycline concentrations (ranging from 10 ng/ml to 10 µg/ml) were tested. The stem cells on vitronectin were treated with 0.5 mM EDTA until the cells were loosely adherent and the cells were dissociated with FACS buffer (PBS, 0.5% BSA and 2 mM EDTA). The cell suspension was added into a Falcon™ Round-Bottom Polystyrene Test Tubes with Cell Strainer Snap Cap. The mRuby2 positive cells were sorted with a 488 nm laser and 600/60 nm emission filter using the SH800S Cell Sorter (Sony Biotechnology) after exclusion of dead cells and debris according to side and forward scatter. Subsequent data analysis was performed with the FlowLogic Software.

The positive cells were collected into tube containing a small amount of culture medium and the cell suspension were centrifuged at 240*g for three minutes. The cell pellet was resuspended in Essential 8 medium plus 100 µg/ml Primocin™ (InvivoGen) and seeded on vitronectin coated wells. Insertion of the HDR template into the AAVS1 locus was validated by PCR and subsequent agarose gel electrophoresis. The primer used for sequencing of the AAVS1 DSB region is shown in **Supplementary table 6**, whereas the primers used for screening of the insertion of EF1α-TetOn3G, mRuby2 and TRE3G in the AAVS1 locus are the same primers used for In-Fusion® cloning (**Supplementary table 4**). The procedure of genomic DNA isolation and PCR reactions volumes and settings were the same as described in Supplementary experimental procedures “Generation of the HDR template fragments”. The only difference is that the number of PCR cycles was increased to 40.

Supplementary table 6: Sequencing DSB region (AAVS1) of sorted cells

Nr	Primer names	Sequence 5'-3'
1	Seq HAL1	CTCTCTCCGCATTGGAGTC

Transient transfection HDR plasmid

HESCs were seeded at a density of 40 K per cm² on vitronectin coated plates (24-well plate) one day before transfection. The stem cells were transfected with 250 – 500 ng plasmid using 2 µl Lipofectamine™ Stem Transfection Reagent for 48 h at 30 °C and 5% CO₂. The plasmids that were used for transient transfection were mRubyII-N1 (Addgene #54614) and the HDR plasmid. After 24 h, an additional 0.5 ml of Essential 8™ medium was added to the transfected hESCs. The cells that were transfected with HDR template were treated with doxycycline (concentrations ranging from 10 ng/ml to 1000 ng/ml) 24 h after transfection. Medium was refreshed after 48h. Cells were observed 24 h and 54 h post transfection using λ_{ex} = 540 nm with the Nikon Eclipse Ti2 Inverted Microscope.

HDR template 2.0

The HDR template with poly(A) tail after the TetOn3G fragment, called “HDR template 2.0”, was generated as described in Supplementary experimental procedures “Generation of the HDR template fragments”. The pENTR1A plasmid with mRuby2, TRE3G and HAR was used to insert the HAL and EF1 α -TetOn3G. The new In-Fusion[®] cloning primers connecting the HAL with the EF1 α -TetOn3G fragments are shown in **Supplementary table 7**. The PAM sequence was mutated in the HAL Rev1 primer (nucleobase marked in red). In-Fusion[®] cloning, bacterial transformation, plasmid isolation and plasmid analysis were performed in the same way as described in Supplementary experimental procedures “In-Fusion cloning and transformation”.

Supplementary table 7: EF1 α -TetOn3G and HAL In-Fusion[®] cloning primers HDR template 2.0

Fragment	Primer names	Sequence 5'-3'	Length (bp)
EF1 α -TetOn3G primers	EF1a-Teton3G Fwd1	CTGTGCCAACTTGTTTATTGCAG CTTATAATGGTTACAAA	2272
	EF1A-Teton3G Rev	CTGTACAAGTACTAGATTACATC CCTGGGGGGCTTTG	
HAL primers	AAVS1-HAL-FWD-GH2	TGGCCAGTGCACTAGCTGCACC AGGTCAGCGC	571
	HAL Rev1	AACAAGTTGGCACAGCAAGCGC ACTCG	

Chr2 cloning

The mRuby2 gene in the HDR template was replaced with human Chr2 coupled to EYFP (λ_{ex} = 513 nm, λ_{em} = 527 nm). The mRuby2 gene was removed from the HDR template by restriction enzyme digestion using the restriction sites FastDigest SgsI and FastDigest XmaJI (Thermo Fisher Scientific™) at 37 °C for 20h. The digested plasmid was loaded on a 1% agarose gel and the HDR template without mRuby2 was isolated and purified from the agarose gel as described in Supplementary experimental procedures “Generation of the HDR template fragments”. The concentration was measured and 200 ng of the isolated fragment was loaded on an agarose gel to confirm successful isolation.

The Chr2-EYFP gene was amplified from the plasmid tol2-CAG::Chr2-YFP (Addgene #59740). The plasmid was delivered in bacteria as agar stab. The bacteria were streaked on LB agar plates containing 50 μ g/ml Kanamycin and incubated overnight at 37 °C. The next day 2 different colonies were picked and each colony was grown in 3 ml LB broth at 37 °C. After 8 hours, the 3 ml culture was added to 150 ml LB broth and the bacteria were grown overnight at 37 °C. Glycerol stocks were made from the bacterial culture and the plasmids were isolated and purified using the PureYield™ Plasmid Midiprep System according to the manufacturer’s protocol. The Chr2-EYFP sequence was determined with Sanger sequencing. The sequencing primers of the tol2-CAG::Chr2-YFP plasmid are shown in **Supplementary table 8**.

Subsequently, three different sets of “sticky-end PCR” primers were developed, based on the article of Zeng [5]. The primers contain overhangs corresponding to the Sgsl (Ascl) and XmaII (AvrII) restriction sites (**Supplementary table 9**, overhangs marked in red). Each primer set consists of four PCR primers and PCR reactions were performed in two separated tubes using primers 1 and 3, and primers 2 and 4, respectively. Reaction volumes of the PCR amplifications were the same as described in Supplementary experimental procedures “Generation of the HDR template fragments”. A 2-step PCR protocol was used, with initial denaturation at 98 °C for 30 seconds followed by 35 cycles of denaturation at 98 °C for 10 seconds and annealing/extension at 72 °C for 60 seconds. The final extension was done at 72 °C for 10 minutes. The PCR products were loaded on a 1% agarose gel and the desired DNA fragments were isolated and purified (as described in Supplementary experimental procedures “Generation of the HDR template fragments”). The isolated DNA fragments (obtained after PCR amplification with primers 1 and 3 and primers 2 and 4) were mixed, denatured for 4 minutes at 94 °C and annealed for 1 minute at 65 °C and 15 minutes at 21°C.

The Chr2-EYFP fragment was ligated into the HDR template without mRuby using the T4 DNA Ligase kit (Promega Corporation) according to the manufacturer’s protocol. There was 100 ng of vector used and the molar ratio vector: insert was 1:12. (The chosen ratio vector: insert was 1:3 and because the Chr2-EYFP PCR mixture contains 25% of the desired product, the final ratio vector: insert was 1:12) The ligation reaction mixture was incubated at room temperature for 3 hours. Thereafter, 5 µl of the reaction mixture was transformed into TOP10 Competent *E. coli* cell. Bacterial transformation, bacterial growth and plasmid isolation were performed in the same way as described in Supplementary experimental procedures “In-Fusion cloning and transformation”. The isolated plasmids were analysed by restriction digestion with the enzyme Bpil (BbsI) and PCR of Chr2-EYFP using the sticky-end primers 1 and 4. Finally, the insertion of the Chr2-EYFP fragment were checked by Sanger sequencing. The sequencing primers of the HDR (Chr2-EYFP) are shown in **Supplementary table 10**.

Supplementary table 8: Sequencing primers tol2-CAG::Chr2-YFP plasmid

Nr	Primer names	Sequence 5'-3'
1	Seq EYFP Rev	CAATGCGATGCAATTCCTC
2	Seq EYFP-ChR2 Rev	CAGATGAACTTCAGGGTCAG
3	Seq EYFP Fwd	CTGACCCTGAAGTTCATCTG
4	Seq Chr2 Rev	CAGTAACATTGATCCTCAGG
5	Seq Chr2 Fwd	GCAAAGAATTCCTCGAGTC
6	pCAGGS-5	GGTTCGGCTTCTGGCGTGTGACC

Supplementary table 9: Sticky-end PCR primers HDR (Chr2-EYFP) plasmid

Fragment	Primer names	Sequence 5'-3'	Length (bp)
Sticky-end primers 1 and 3	Chr2 StE3 Rev1:	CGCGCCGCAGGAATTCTTACTTG TACA	1712
	Chr2 StE3 Fwd2:	GTCCTCGAGTCTAGCTGGATCCC	
Sticky-end primers 2 and 4	Chr2 StE3 Fwd1:	CTAGGTCCTCGAGTCTAGCTGG ATCC	1712
	Chr2 StE3 Rev2:	CCGCAGGAATTCTTACTTGTACA GCTCG	

Supplementary table 10: Sequencing primers HDR (Chr2-EYFP) plasmid

Nr	Primer names	Sequence 5'-3'
1	SeqENTR1A Fwd	CCGGTACCGAATTCGCTTA
2	Seq Teton Fwd	CTGTTCTCCAATACGCAG
3	Seq Teton Rev	AAGTCATACCGCTGTGCTC
4	Seq EF1a Rev	GTGAGTCACCCACACAAAG
5	Teton3G-seq-2	ACAGTCCCCGAGAAGTTGG
6	Seq EYFP-ChR2 Rev	CTGACCCTGAAGTTCATCTG
7	Seq EYFP Fwd	CAGATGAACTTCAGGGTCAG
8	Seq ChR2 Rev	CAGTAACATTGATCCTCAGG
9	AAVS1-seq-5	AGTAGAGCTCAAAGTGGTCCG
10	SeqENTR1A Rev	GCTGGGTCTAGATATCTCG

Transient transfection HDR (Chr2-EYFP) plasmid

HESCs were seeded at a density of 40 K per cm² on vitronectin coated plates (24-well plate) one day before transfection. The stem cells were transfected with 250 – 500 ng plasmid using 2 µl Lipofectamine™ Stem Transfection Reagent for 48 h at 30 °C and 5% CO₂. The plasmids that were used for transient transfection were tol2-CAG::Chr2-YFP (Addgene #59740) and the HDR (Chr2-EYFP) plasmid. After 24 h, an additional 0.5 ml of Essential 8™ medium was added to the transfected hESCs. The cells that were transfected with HDR (Chr2-EYFP) plasmid were treated with doxycycline (concentrations ranging from 10 ng/ml to 1000 ng/ml) 24 h after transfection. Medium was refreshed after 48h. Cells were observed 24 h and 54 h post transfection using λ_{ex} = 470 nm with the Nikon Eclipse Ti2 Inverted Microscope.

HDR (Chr2-EYFP) template 2.0

The HDR (Chr2-EYFP) template with bGH poly(A) tail behind the EYFP with poly(A) tail was designed and two sets of new sticky-end PCR primers for amplification of Chr2-EYFP with poly(A) after EYFP were designed and ordered (**Supplementary table 11**, overhangs marked in red). The PCR primers Chr2 StE3 Fwd 1 and Fwd 2 are the same primers as depicted in **Supplementary table 9**.

Supplementary table 11: Sticky-end PCR primers HDR (Chr2-EYFP) plasmid with poly(A) tail after EYFP

Fragment	Primer names	Sequence 5'-3'	Length (bp)
Sticky-end primers 1 and 3	ChR2 StE PolyA1:	CGCGCCTCAGAAGCCATAGAGC	2012
	ChR2 StE3 Fwd2:	GTCCTCGAGTCTAGCTGGATCCC	
Sticky-end primers 2 and 4	ChR2 StE3 Fwd1:	CTAGGTCCTCGAGTCTAGCTGG ATCC	2012
	ChR2 StE PolyA2:	CCTCAGAAGCCATAGAGCCCAC CG	
Fragment	Primer names	Sequence 5'-3'	Length (bp)
Sticky-end primers 1 and 3	ChR2 StE PolyA3:	CGCGCCGGTTCCTTCCGCCTCAG AAG	2025
	ChR2 StE3 Fwd2:	GTCCTCGAGTCTAGCTGGATCCC	
Sticky-end primers 2 and 4	ChR2 StE3 Fwd1:	CTAGGTCCTCGAGTCTAGCTGG ATCC	2025
	ChR2 StE PolyA4:	CCGGTTCCTTCCGCCTCAGAAGC CA	

Supplementary references

1. Bos, T.R.v.d. *Genomic safe harbor locations AAVS1 and CLYBL for CRISPR-Cas9 genome editing in human pluripotent stem cells*; Saxion University of applied science and University of Twente: 2018.
2. Ran, F.A.; Hsu, P.D.; Wright, J.; Agarwala, V.; Scott, D.A.; Zhang, F. Genome engineering using the CRISPR-Cas9 system. *Nat Protoc* **2013**, *8*, 2281-2308, doi:10.1038/nprot.2013.143.
3. Smith, J.R.; Maguire, S.; Davis, L.A.; Alexander, M.; Yang, F.; Chandran, S.; French-Constant, C.; Pedersen, R.A. Robust, Persistent Transgene Expression in Human Embryonic Stem Cells Is Achieved with AAVS1-Targeted Integration. *STEM CELLS* **2008**, *26*, 496-504, doi:10.1634/stemcells.2007-0039.
4. Lund, B.A.; Leiros, H.-K.S.; Bjerga, G.E.K. A high-throughput, restriction-free cloning and screening strategy based on ccdB-gene replacement. *Microb Cell Fact* **2014**, *13*, 38-38, doi:10.1186/1475-2859-13-38.
5. Zeng, G. Sticky-End PCR: New Method for Subcloning. *BioTechniques* **1998**, *25*, 206-208, doi:10.2144/98252bm05.